JET ATTACHMENT TO COANDA WALLS IN BISTABLE AMPLIFIERS

by

Daniel Charles Richardson

United States
Naval Postgraduate School

THESIS

JET ATTACHMENT TO COANDA WALLS

IN BISTABLE AMPLIFIERS

by

Daniel Charles Richardson

April 1969

JET ATTACHMENT TO COANDA WALLS IN BISTABLE AMPLIFIERS

by

Daniel Charles Richardson
Lieutenant Commander, United States Navy
B. S., Naval Academy, 1959

Submitted in partial fulfillment of the
requirements for the degree of

MASTER OF SCIENCE IN MECHANICAL ENGINEERING

from the

NAVAL POSTGRADUATE SCHOOL
April 1969

ABSTRACT

The flow in a two-dimensional plane wall jet with a control port and setback between the nozzle exit and the leading edge of the wall was probed at various stations along the jet. The nozzle dimensions, the width of the control port, the slope of the side wall, and the setback were kept constant. The Reynolds number, defined in terms of the nozzle width, was varied from 20,000 to 141,000. It was found that the region close to the leading edge of the wall behaved like a transition region where the characteristics of flow changed from those of a free jet to those of a wall jet. In addition, it was found that while the outer region of the velocity profile obeyed a similarity law beyond the transition region, the inner region of the profile followed neither the classic one-seventh power law nor any other power law with a constant exponent. In fact the results have shown that the exponent in the power-law model has to be varied from one-seventh to one-fifteenth to represent the majority of the inner velocity profiles for the range of Reynolds numbers tested. The reasons leading to this result are discussed in terms of the equation of momentum and of the pressure distribution along the wall.

TABLE OF CONTENTS

Section	Title	Page
1.	Introduction	13
2.	Theoretical Considerations	19
3.	Experimental Equipment and Procedure	28
4.	Discussion of Results	34
5.	Recommendations for Further Work	42
	References	43
	Bibliography	45
	Figures	48
	Appendix I (Tabulated Data)	91

LIST OF ILLUSTRATIONS

Figure	Title	Page
1.	Test Assembly and Instrumentation	48
2.	Schematic of Test Section	49
3.	Normalized Velocity Profiles - Station 1 (Four Reynolds numbers; Control Port Open)	50
4.	Normalized Velocity Profiles - Station 2 (Four Reynolds numbers; Control Port Open)	51
5.	Normalized Velocity Profiles - Station 3 (Four Reynolds numbers; Control Port Open)	52
6.	Normalized Velocity Profiles - Station 4 (Four Reynolds numbers; Control Port Open)	53
7.	Normalized Velocity Profiles - Station 5 (Four Reynolds numbers; Control Port Open)	54
8.	Normalized Velocity Profiles - Station 6 (Four Reynolds numbers; Control Port Open)	55
9.	Normalized Velocity Profiles - Station 7 (Four Reynolds numbers; Control Port Open)	56
10.	Normalized Velocity Profiles - Station 1 (Four Reynolds numbers; Control Port Closed)	57
11.	Normalized Velocity Profiles - Station 2 (Four Reynolds numbers; Control Port Closed)	58
12.	Normalized Velocity Profiles - Station 3 (Four Reynolds numbers; Control Port Closed)	59
13.	Normalized Velocity Profiles - Station 4 (Four Reynolds numbers; Control Port Closed)	60
14.	Normalized Velocity Profiles - Station 5 (Four Reynolds numbers; Control Port Closed)	61
15.	Normalized Velocity Profiles - Station 6 (Four Reynolds numbers; Control Port Closed)	62
16.	Normalized Velocity Profiles - Station 7 (Four Reynolds numbers; Control Port Closed)	63
17.	Normalized Inner Velocity Profile - Station 4 (Rew = 20,000; Control Port Open)	64
18.	Normalized Inner Velocity Profile - Station 5 (Rew = 20,000; Control Port Open)	65

Figure	Title	Page
19.	Normalized Inner Velocity Profile - Station 7 (Rew = 20,000; Control Port Open)	66
20.	Normalized Inner Velocity Profile - Station 4 (Rew = 37,000; Control Port Open)	67
21.	Normalized Inner Velocity Profile - Station 5 (Rew = 37,000; Control Port Open)	68
22.	Normalized Inner Velocity Profile - Station 7 (Rew = 37,000; Control Port Open)	69
23.	Normalized Inner Velocity Profile - Station 4 (Rew = 69,000; Control Port Open)	70
24.	Normalized Inner Velocity Profile - Station 5 (Rew = 69,000; Control Port Open)	71
25.	Normalized Inner Velocity Profile - Station 7 (Rew = 69,000; Control Port Open)	72
26.	Normalized Inner Velocity Profile - Station 4 (Rew = 100,000; Control Port Open)	73
27.	Normalized Inner Velocity Profile - Station 5 (Rew = 100,000; Control Port Open)	74
28.	Normalized Inner Velocity Profile - Station 7 (Rew = 100,000; Control Port Open)	75
29.	Normalized Inner Velocity Profile - Station 4 (Rew = 141,000; Control Port Open)	76
30.	Normalized Inner Velocity Profile - Station 5 (Rew = 141,000; Control Port Open)	77
31.	Normalized Inner Velocity Profile - Station 7 (Rew = 141,000; Control Port Open)	78
32.	Normalized Outer Velocity Profiles (Stations 3 through 7; Four Reynolds numbers; Control Port Open and Closed)	79
33.	Plot of Equation 24	80
34.	Inner Velocity Profiles (According to the power law with an exponent of: 1/7, 1/12, and 1/15)	81
35.	Normalized Pressure Profile (Rew = 20,000; Control Port Open)	82

Figure	Title	Page
36.	Normalized Pressure Profile (Rew = 20,000; Control Port Closed)	83
37.	Normalized Pressure Profile (Rew = 37,000; Control Port Open)	84
38.	Normalized Pressure Profile (Rew = 37,000; Control Port Closed)	85
39.	Normalized Pressure Profile (Rew = 69,000; Control Port Open)	86
40.	Normalized Pressure Profile (Rew = 69,000; Control Port Closed)	87
41.	Normalized Pressure Profile (Rew = 100,000; Control Port Open)	88
42.	Normalized Pressure Profile (Rew = 141,000; Control Port Open)	89
43.	Normalized Pressure Profile (Rew = 141,000; Control Port Closed)	90

LIST OF SYMBOLS

A_c	cross sectional area of the power jet
CF(P)	pressure correction factor
CF(T)	temperature correction factor
CFP	dimensionless pressure
P	pressure
P_d	differential pressure sensed by the Pitot tube, $\frac{\rho U^2}{2}$
P_t	pressure as defined by Eq. (6)
P_w	wall pressure
Q	volumetric flow rate
Rew	Reynolds number based on width of the power jet
R	radius of curvature of the side wall for a curved wall
U_m	maximum fluid velocity in a given profile
$U_{m/2}$	one-half the maximum fluid velocity in a given profile
U_o	average velocity in the power jet
U	local velocity as measured by the Pitot tube
u	local velocity component
u'	turbulent velocity component
v	local velocity component
v'	turbulent velocity component
w	power jet width
x	downstream distance measured from the origin of the jet
y	distance from the flat plate to the local velocity
y_m	distance from the plate to the maximum local velocity
$y_{m/2}$	distance from the plate to the point where the local velocity outside the boundary layer is $U_{m/2}$
μ	dynamic viscosity

ν	kinematic viscosity
ρ	fluid density
τ	shear stress

ACKNOWLEDGEMENT

The work described herein was made possible through the sponsorship of the Harry Diamond Laboratories of the United States Army Materiel Command, Washington, D. C. The author wishes to express his appreciation to Dr. T. Sarpkaya for his guidance and advice during the course of the investigation. A special note of appreciation is also extended to Messrs. K. Mothersell, J. Beck, and J. McKay, of the Mechanical Engineering Machine Shop, for their efforts in the construction of the experimental apparatus.

1. Introduction.

All jets in general, and plane, two-dimensional jets, in particular, attach to and flow around nearby solid surfaces. This phenomenon is known today as the "Coanda Effect." Historically, the Coanda effect was first observed by Young [1] in 1800 and described by Reynolds [2] in 1870, but it was not until about 1910 that Coanda [3] realized its importance and undertook detailed investigations which were later described in his various patents.

The Coanda effect could readily be observed either by holding one's finger close to a thin stream of water coming from a tap, or by slowly pouring a liquid from a glass. In either case, the direction of motion of the liquid quickly deviates from its anticipated direction and the liquid adheres to the finger or to the outside of the glass.

In 1960, the consequences of the Coanda effect and its potential application to pneumatic control devices were realized by the researchers of the Harry Diamond Laboratories and a very extensive series of studies were undertaken. The results of these studies gave birth to a new technology known as "Fluidics." It may be defined as a system in which sensing, amplification, control, information processing and/or actuation are performed by devices that have no moving parts other than the fluid flowing in them. Fluidic devices have a number of advantages. Reliability is a major advantage since, by definition, fluidic devices contain no moving parts. In addition, they are immune to environmental conditions such as high or low temperatures, nuclear radiation effects, shock and vibration, etc. Absence of electrical wiring precludes short circuits. Fluidic units can be made of a variety of materials, including

various plastics or glass. Current manufacturing techniques permit low-cost fabrication within the required degree of accuracy, in large production runs.

Fluidic devices are customarily classified in four categories, depending on the type of fluid-flow interaction that takes place within them. These categories are: (1) wall attachment; (2) momentum exchange; (3) turbulence amplifier; and (4) vortex amplifier.

Wall attachment or bistable devices form the largest group of fluidic components. In these devices, a high-velocity jet of fluid, emitted between two walls, attaches itself to one of them, attracted there by an area of lower pressure next to the wall caused by air entrainment. The jet remains stable in this one position (bistable) unless it is disturbed by a pressure pulse, or by continuous pressure from a control port. Such a device can perform a number of digital logic functions. The present investigation deals, as will be described later, with the understanding of the characteristics of this type of device.

The second category, momentum exchange devices, do not depend on the wall effect for their function - indeed they are so designed that wall attachment cannot take place. These devices depend on direct interaction between the control jets and power jets to deflect the power stream. Application of control pressure deflects the output proportionately toward the opposing port. The device is therefore an analog unit.

The impact modulator, another type of momentum exchange device, uses the collision of two submerged fluid jets originating from opposing directions. The location of the plane of impact depends on the relative

initial momentum of the two streams, which, in turn, depends on the pressure in the respective reservoirs. Thus pressure changes shift the position of impact.

The turbulence amplifier depends on the change in flow conditions that accompany a change from laminar to turbulent flow in a fluid stream. When a laminar flowing fluid leaves a tube, it remains laminar for distances as great as one hundred times the tube diameter. The point at which the flow becomes turbulent depends on the velocity of the stream, or the presence of an external disturbance. A collector tube placed in the path of the stream measures output in terms of static pressure. One or more control jets are placed at right angles to the power jet. Small disturbances, created by control pressure, cause the stream's point of turbulence to shift drastically toward the supply tube, with a consequent sudden fall in output pressure.

Vortex amplifiers operate on the principle of momentum conservation, as opposed to the momentum exchange devices previously described. These devices normally consist of a hollow cylinder with a hole in the center. If flow is introduced into the input port, without any control flow, then this power flow encounters little impedance before exiting through the output orifice. When control flow is applied, a vortex forms because of the tangential application of the control flow. The input now no longer follows a direct radial path but is caught by the vortex and spirals inward. As the power flow comes closer to the center, the radius decreases with a corresponding increase in tangential velocity. This increases the pressure drop and reduces the output flow.

As cited above, the present study deals with the first category of fluidic devices: Wall attachment amplifiers. In order to understand

the fundamental characteristics of flow, and the reasons for the Coanda effect, extensive studies were undertaken on jet flows in general and on jet attachment to plane and curved walls in particular (See Bibliography). Previous investigations by Sarpkaya and Kirschner [4] have shown that a vented convex-walled bistable amplifier exhibits performance characteristics superior to those of a straight-walled amplifier. In an effort to discover the underlying reasons, extensive studies were carried out by Kesler [5] and Johnson [6] on the attachment of turbulent jets to convex walls. Since only a comparison of the characteristics of flows along a convex and a straight side wall could reveal the reasons leading to the better performance of the convex-walled amplifiers, it was necessary to investigate the evolution of a jet along a straight wall set back relative to the nozzle and at an angle to the initial direction of the power jet. It is for this purpose that the work described herein was undertaken.

The velocity distributions for a two-dimensional plane wall jet have been analyzed by Gőrtler [7] in 1942 and Glauert [8] in 1956. Newman [9] in 1961 discussed these analyses and the underlying assumptions made in their derivation. It appears that there is no theoretical work on the characteristics of the confined jet flow as it takes place in a straight-walled bistable amplifier. However, extensive measurements of either the velocity and/or pressure profiles were made by various investigators. Noteworthy among these are those made by Fő rthmann [10], Reichardt [11], Sigalla [12], Bourque and Newman [13], Schwarz and Cosart [14], Sawyer [15,16], Kadosch [17], McGlaughlin and Taft [18], and McGlaughlin and Greber [19]. None of these measurements included a wall setback or control port. Investigations by Sridhar and Tu [20], Kesler [5], Johnson [6], Paranjpe and Sridhar [21], Korbacher [22], and by the Institute of

for Aerospace Studies of the University of Toronto [23] included various sizes of setbacks and control port openings. The difficulty with most of the studies cited above arises from the limitations imposed on the parameters selected by each investigator. This makes it not only impossible to compare and correlate a given set of data with those obtained by others, but also prevents any one investigator from drawing basic conclusions regarding the fundamental characteristics of flow such as the similarity or dissimilarity of the velocity profiles in a given region of flow and the variation of the pressure both along the side-wall and across the boundary layer. The works of Sridhar and Tu [20] and Paranjpe and Sridhar [21] are based on a single Reynolds number. The works of Kobacher [22] and the Institute of Aerospace Studies of Toronto [23] dealt only with the determination of the pressure distribution and the size of the control port gap which the jet can bridge between the nozzle and the side-wall. No velocity profiles were taken and no attempt was made to compare the results with exact or approximate theoretical predictions. It is of course realized that the number of the geometrical and flow parameters are extremely large and that it is all but impossible for any one investigator to cover the entire range. Thus it is extremely important to state all of the flow and test conditions and the limitations imposed on the measurements so that the work of one investigator can be tied to the works of others.

The present investigation is part of a systematic evaluation of the velocity and pressure distributions about straight and curved side-walls set back relative to the power nozzle. More specifically, the work reported herein deals with the investigation of the velocity and pressure characteristics of a two-dimensional plane-wall jet as it progresses along a straight-wall. The nozzle dimensions, the width of the control

port, the slope of the side wall, and the setback were kept constant as shown in Figs. 1 and 2. The Reynolds number, defined in terms of the nozzle width, was varied from 20,000 to 141,000.

2. Theoretical Considerations.

The theoretical analysis of laminar and turbulent jets over straight and curved walls is quite limited partly because of mathematical difficulties and partly because of the lack of information regarding turbulent eddy viscosity. Glauert [8] studied the flow of a jet along a straight-wall when the pressure everywhere equals that of the surrounding fluid which is at rest. Experiments described herein show that the pressure is not everywhere equal to that of the surrounding medium (particularly near the wall) and that the predicted velocity distribution near the wall deviates considerably from that predicted by Glauert. The analysis further assumes the existence of similarity between the velocity profiles. It has been recognized by Glauert that such a similarity can only be approximate since the inner part of the flow depends on the fluid viscosity while the outer part is very nearly independent of the viscosity. Nevertheless, Glauert obtained an approximate solution by matching the inner boundary layer flow for which the eddy viscosity varies with y to the outer flow for which the eddy viscosity is assumed constant. This analysis will be referred to later.

The equations of motion and continuity for a two-dimensional incompressible, steady, and turbulent flow over a curved wall may be written [11, pg. 112, 4th Ed.] as (the terms in the order of $(y_m/R)^2$ and higher are neglected),

$$u\frac{\partial u}{\partial x}+\left(1+\frac{y}{R}\right)v\frac{\partial u}{\partial y}+\frac{uv}{R}=-\frac{1}{\rho}\frac{\partial}{\partial x}\left(p+\rho\overline{v'^2}\right)$$

$$-\left(1+\frac{y}{R}\right)\frac{\partial}{\partial y}\left(\overline{u'v'}\right)-\frac{2}{R}\overline{u'v'}+\nu\left[\left(1+\frac{y}{R}\right)\frac{\partial^2 u}{\partial y^2}+\frac{1}{R}\frac{\partial u}{\partial y}\right] \quad (1)$$

$$\frac{u^2}{R} = \left(1+\frac{y}{R}\right)\frac{1}{\rho}\frac{\partial}{\partial y}\left(P+\rho\overline{v'^2}\right) \tag{2}$$

$$\frac{\partial u}{\partial x} + \frac{\partial}{\partial y}\left[\left(1+\frac{y}{R}\right)v\right] = 0 \tag{3}$$

The shear stress may be written as

$$\tau = \mu\left(1+\frac{y}{R}\right)\frac{\partial}{\partial y}\left(\frac{u}{1+\frac{y}{R}}\right) - \rho\,\overline{u'v'} \tag{4}$$

Introducing Eq. (4) into Eq. (1) and simplifying, one has

$$u\frac{\partial u}{\partial x} + \left(1+\frac{y}{R}\right)v\frac{\partial u}{\partial y} + \frac{uv}{R} = -\frac{1}{\rho}\frac{\partial}{\partial x}\left(P+\rho\overline{v'^2}\right)$$

$$+\frac{1}{\rho}\left[\left(1+\frac{y}{R}\right)\frac{\partial \tau}{\partial y} + \frac{2}{R}\tau\right] \tag{5}$$

It is apparent from Eq. (2) that as $R \to \infty$,

$$P_t = P + \rho\overline{v'^2} = \left[P+\rho\overline{v'^2}\right]_{R\to\infty} \tag{6}$$

Thus it is not the static pressure P, but rather the sum given by Eq. (6) that remains constant across the boundary layer. Then the equation of Bernoulli along a streamline reduces to

$$\rho\frac{\bar{u}^2+\bar{v}^2}{2} + P + \rho\overline{v'^2} = \text{constant} \tag{7}$$

The foregoing is clear evidence of the fact that only in laminar jets flowing along straight walls one can assume the pressure to be equal to that of the surroundings. In turbulent jets, the assumption of constant pressure leads to velocity profiles which are not sufficiently accurate particularly near the wall where the local static pressure is considerably below that of the surroundings.

Integrating Eq. (5) from y to ∞ (see the accompanying figure) where $u(y \longrightarrow \infty) = 0$ and $u(0) = v(0) = 0$,

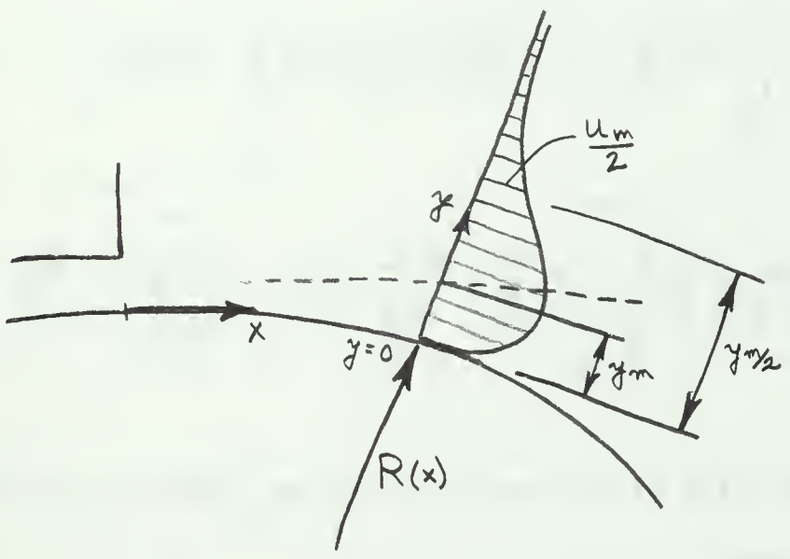

$$\frac{\partial}{\partial x}\int_y^\infty \frac{u^2}{2}\,dy + \int_y^\infty \left(1+\frac{y}{R}\right) v\,\frac{\partial u}{\partial y}\,dy + \frac{1}{R}\int_y^\infty uv\,dy =$$

$$-\int_y^\infty \left(\frac{1}{\rho}\,\frac{\partial P_t}{\partial x}\right) dy + \frac{1}{\rho}\int_y^\infty \left(1+\frac{y}{R}\right)\frac{\partial \tau}{\partial y}\,dy + \frac{1}{\rho}\int_y^\infty \frac{2}{R}\,\tau\,dy \qquad (8)$$

Noting that

$\lim_{y\to\infty} \left(1 + \frac{y}{R}\right) vu = 0$ and $\lim_{y\to\infty} \left(1 + \frac{y}{R}\right)\frac{\partial u}{\partial y} = 0$, one has for the second term in Eq. (8),

$$\int_y^\infty \left(1+\frac{y}{R}\right) v \frac{\partial u}{\partial y}\, dy = \left(1+\frac{y}{R}\right) vu \Big|_y^\infty - \int_y^\infty u\left(-\frac{\partial u}{\partial x}\right) dy$$

$$= -\left(1+\frac{y}{R}\right) vu + \frac{\partial}{\partial x}\int_y^\infty \frac{u^2}{2}\, dy \qquad (9)$$

The combining of Eqs. (8) and (9), yields

$$\frac{\partial}{\partial x}\int_y^\infty u^2\, dy - \left(1+\frac{y}{R}\right) vu + \frac{1}{R}\int_y^\infty uv\, dy =$$

$$\int_y^\infty \left(-\frac{1}{\rho}\frac{\partial P_t}{\partial x}\right) dy + \frac{1}{\rho}\int_y^\infty \left(1+\frac{y}{R}\right)\frac{\partial \tau}{\partial y}\, dy + \frac{1}{\rho}\int_y^\infty \frac{2}{R}\tau\, dy \qquad (10)$$

Multiplying Eq. (10) with u and integrating, this time from y = 0 to $y = \infty$, one has

$$\int_0^\infty u\left\{\frac{\partial}{\partial x}\int_y^\infty u^2 dy\right\} dy - \int_0^\infty \left(1+\frac{y}{R}\right) vu^2\, dy + \frac{1}{R}\int_0^\infty u\left\{\int_y^\infty uv\, dy\right\} dy =$$

$$\int_0^\infty u\left\{\int_y^\infty \left(-\frac{1}{\rho}\frac{\partial P_t}{\partial x}\right) dy\right\} dy + \frac{1}{\rho}\int_0^\infty u\left\{\int_y^\infty \left(1+\frac{y}{R}\right)\frac{\partial \tau}{\partial y}\, dy\right\} dy +$$

$$\frac{1}{\rho}\int_0^\infty u\left\{\int_y^\infty \frac{2}{R}\tau\, dy\right\} dy \qquad (11)$$

Each term in Eq. (11) may be evaluated and reduced to simpler forms. The general procedure is demonstrated for the first term as follows:

$$M_1=\int_0^\infty u\frac{\partial}{\partial x}\left\{\int_y^\infty u^2 dy\right\}dy=\frac{\partial}{\partial x}\int_0^\infty u\left\{\int_y^\infty u^2 dy\right\}dy-\int_0^\infty \frac{\partial u}{\partial x}\int_y^\infty u^2 dy\,dy \qquad (12)$$

Using the equation of continuity (Eq. 3), Eq. (12) reduces to:

$$M_1=\frac{\partial}{\partial x}\int_0^\infty u\left\{\int_y^\infty u^2 dy\right\}dy+\int_0^\infty\left(\int_y^\infty u^2 dy\right)d\left\{\left(1+\frac{y}{R}\right)v\right\} \qquad (13)$$

Integration by parts yields

$$M_1=\frac{\partial}{\partial x}\int_0^\infty u\left\{\int_y^\infty u^2 dy\right\}dy+\left(1+\frac{y}{R}\right)v\int_y^\infty u^2 dy\Big|_0^\infty+\int_0^\infty\left(1+\frac{y}{R}\right)vu^2 dy \qquad (14)$$

Noting that

$$\lim_{y\to\infty}\left(1+\frac{y}{R}\right)v\int_y^\infty u^2 dy=0$$

Equation (14) reduces to:

$$M_1=\frac{\partial}{\partial x}\int_0^\infty u\left\{\int_y^\infty u^2 dy\right\}dy+\int_0^\infty\left(1+\frac{y}{R}\right)vu^2 dy \qquad (15)$$

The integration of the fourth term in Eq. (8) requires certain preliminary steps: Integrating Eq. (2) from y to $y=\infty$, one has

$$\frac{P_t-P_\infty}{\rho}=-\int_y^\infty\frac{u^2}{R\left(1+\frac{y}{R}\right)}dy=\frac{dM_4}{dy} \qquad (16)$$

Repeating the above procedure, one obtains

$$M_4 = \int_y^\infty \frac{P_\infty - P_t}{\rho}\, dy = \int_y^\infty \left[\int_y^\infty \frac{u^2}{R\left(1+\frac{y}{R}\right)}\, dy \right] dy \tag{17}$$

which may be integrated by parts to yield,

$$M_4 = y\int_y^\infty \frac{u^2}{R\left(1+\frac{y}{R}\right)}\, dy \Bigg|_y^\infty + \int_y^\infty y\, \frac{u^2}{R\left(1+\frac{y}{R}\right)}\, dy \tag{17a}$$

Noting that

$$\lim_{y\to\infty}\; y\int_y^\infty \frac{u^2}{R\left(1+\frac{y}{R}\right)}\, dy = 0$$

Equation (17a) may be reduced to:

$$M_4 = -\frac{y}{R}\int_y^\infty \frac{u^2}{1+\frac{y}{R}}\, dy + \int_y^\infty \frac{y}{R}\, \frac{u^2}{1+\frac{y}{R}}\, dy \tag{17b}$$

Now considering the fourth term in Eq. (11) once more, we have

$$I_4 = \int_0^\infty u \left\{ \int_y^\infty \left(-\frac{1}{\rho}\frac{\partial P_t}{\partial x} \right) dy \right\} dy = \int_0^\infty u \left\{ \frac{d}{dx}\int_y^\infty \frac{P_\infty - P_t}{\rho}\, dy \right\} dy$$
$$= \int_0^\infty u\, \frac{dM_4}{dx}\, dy = \frac{d}{dx}\int_0^\infty u M_4\, dy - \int_0^\infty \frac{\partial u}{\partial x} M_4\, dy \tag{18}$$

Re-writing the equation of continuity (Eq. 3), one has

$$-\frac{\partial u}{\partial x} = \frac{\partial}{\partial y}\left\{ \left(1+\frac{y}{R}\right) v \right\} \tag{3}$$

Combining Eqs. (3) and (18) and integrating by parts, we have

$$I_4 = \frac{d}{dx}\int_0^\infty u M_4\, dy + \left(1+\frac{y}{R}\right) v M_4 \Big|_0^\infty - \int_0^\infty \left(1+\frac{y}{R}\right) v \frac{dM_4}{dy}\, dy \qquad (19)$$

Noting that

$$\lim_{y\to\infty} \left(1+\frac{y}{R}\right) v M_4(y) = 0$$

and combining with Eqs. (16) and (17b), yields

$$I_4 = \frac{d}{dx}\int_0^\infty u\left\{\int_y^\infty \frac{y}{R}\frac{u^2}{1+\frac{y}{R}}\, dy - \frac{y}{R}\int_y^\infty \frac{u^2}{1+\frac{y}{R}}\, dy\right\} dy + \int_0^\infty \left(1+\frac{y}{R}\right) v \int_y^\infty \frac{u^2}{R\left(1+\frac{y}{R}\right)}\, dy\, dy \qquad (19a)$$

Evaluating the remaining terms of Eq. (11) in a straightforward manner, as illustrated above, and combining, one finally has

$$\frac{d}{dx}\int_0^\infty u\left(1+\frac{y}{R}\right)\left\{\int_y^\infty \frac{u^2}{1+\frac{y}{R}}\, dy\right\} dy =$$

$$\int_0^\infty \left(1+\frac{y}{R}\right) v\left\{\int_y^\infty \frac{u^2}{R\left(1+\frac{y}{R}\right)}\, dy\right\} dy - \frac{1}{R}\int_0^\infty u\left\{\int_y^\infty uv\, dy\right\} dy - \qquad (20)$$

$$\frac{1}{\rho}\int_0^\infty \left(1+\frac{y}{R}\right) u\tau\, dy + \frac{1}{\rho R}\int_0^\infty u\left\{\int_y^\infty \tau\, dy\right\} dy$$

This equation has been derived here in its most general form for a curved rather than a straight-wall boundary for the purpose of using it in subsequent studies in connection with the comparison of the characteristics of flow along curved and straight Coanda-walls. It is

apparent that for a straight-wall, i.e., for $R \rightarrow \infty$ (for which $\frac{\partial P}{\partial y} = 0$ because of Eq. 2), Eq. (20) reduces to:

$$\frac{d}{dx}\int_0^\infty u\left\{\int_y^\infty u^2 dy\right\}dy = -\frac{1}{\rho}\int_0^\infty u\tau\, dy = -\frac{1}{\rho}\left[\int_0^{y_m} u\tau\, dy + \int_{y_m}^\infty u\tau\, dy\right] \quad (21)$$

Assuming the flow to be laminar, Glauert [8] obtained

$$\frac{d}{dx}\int_0^\infty u\left\{\int_y^\infty u^2 dy\right\}dy = 0 \quad (22)$$

or

$$\int_0^\infty u\left\{\int_y^\infty u^2 dy\right\}dy = \text{constant} \quad (23)$$

The comparison of Eqs. (21) and (22) clearly show the contribution of the turbulent stresses and point out the fact that the integral given by Eq. (23) is not a constant. The significance of this comparison will become apparent later.

Glauert [8], using Eq. (23), assuming the flow to be turbulent, dividing the mean velocity profile into an inner and outer region, invoking similarity hypothesis (the velocity profile plotted non-dimensionally as U/U_m versus $y/y_{m/2}$ is assumed to be the same for all values of x along the jet), and finally by matching the boundary layer flow (for which the eddy viscosity varies with y) to the outer flow (for which the eddy viscosity is assumed constant), found that the outer profile is given by the equation

$$\frac{U}{U_m} = \text{sech}^2 \left\{ 0.88 \left(\frac{y - y_m}{y_{m/2} - y_m} \right) \right\} \qquad (24)$$

Glauert did not give an equation for the inner profile since it was computed numerically in terms of U/U_m versus y/y_m.

The comparison of Eq. (24) with the results obtained herein and the consequences of the dissipation of momentum by viscous forces as depicted by Eq. (21) will be undertaken in section four.

3. Experimental Equipment and Procedures.

The experimental apparatus together with some of the instruments used is shown in Figs. 1 and 2. The only significant change made in the apparatus during the course of the investigation was the replacement of the flexible plastic tubing between the rotometers and the test model with metal piping to permit higher pressures and flow rates.

Air, at approximately 200 psig, was supplied to the basic assembly through a one inch stop valve and then fed into a pressure regulator (maximum input of 400 psig and maximum output of 125 psig). From the regulator the air was directed to one of two Fisher-Porter rotometers. The smaller rotometer had a maximum flow rate of 19.8 standard cubic feet per minute and the larger one had a maximum flow rate of 76.5 standard cubic feet per minute.

All pressures were monitored by a Pace differential-pressure transducer with a rating of plus or minus 50 psi. This transducer was connected to a Hewlett-Packard Model 7712 two channel strip recorder with a Sanborn 350-1100 C carrier preamplifier. To ensure maintenance of a reference zero on the recorder readout, individual pressure readings were taken through a common manifold which could be vented to atmosphere between two successive readings.

Velocity profiles were obtained through the use of a Pitot tube coupled with a micrometer barrel. The Pitot tube was of 0.063 O.D. inches and 0.021 inches I.D. and had four static pressure holes around its shank perimeter. Thus, the output of the Pitot tube measured the local dynamic pressure or the velocity head. The micrometer barrel carriage moved along slots in the side panels in order that velocities

could be measured at various distances from the exit of the power jet and at various distances perpendicular to the surface of the flat plate. The velocities measured at distances closer than 0.057 inches to the wall were not considered accurate because of the proximity effect of the Pitot tube on the flow near the wall boundary.

Construction. The basic test assembly was fabricated from a sheet of one inch plexiglass placed between two one-half inch sheets of plexiglass. Many particulars of the construction are similar to those used in the devices used by Kesler [5] and Johnson [6]. The geometry of all the experimental apparatus utilized was similar to that described by Sarpkaya and Kirschner [4].

The control port was one-eighth of an inch and the setback was 0.025 inches for all the work described herein. The surface of the flat plate was inclined 12 degrees with respect to the axis of the power jet and contained 15 pressure taps one-sixteenth inch in diameter. The first pressure tap was located ¼ inch downstream of the nozzle exit and the remaining pressure taps were located at ½ inch intervals thereafter. With respect to the centerline of the flat plate, the pressure taps were located as follows: centerline, 1/16 inch to the left of centerline, 1/16 inch to the right of centerline, centerline, etc. All sections were firmly assembled and held in place with reference dowels after flow surfaces were carefully hand-polished with rouge.

Procedure. Each run consisted of selecting a proper flow rate and control port condition (open or closed). During the tests the following parameters were recorded: (1) atmospheric pressure and temperature; (2) rotometer outlet pressure; (3) power jet wall pressure; (4) wall

pressure along the flat plate; (5) velocity profiles at various stations along the plate; and (6) the maximum velocity at the center of the power jet immediately downstream of the nozzle.

The first three of the seven stations where velocity profiles were taken were located at 1/8 inch, 5/8 inch, and at 1-5/8 inches from the nozzle exit. The remaining four stations were located at 1-1/2 inch intervals thereafter. These seven stations will be referred to as stations one through seven in the body of this work and in the tabulated data.

Care was taken during the assembly of the device to insure that all dimensions were exactly as desired. The setback of 0.025 inches was set with a depth micrometer. Gage blocks were used to accurately maintain the prescribed dimensions of the control port and power nozzle.

The flow rates were established with the use of two different calibrated (2% accuracy) rotometers depending on the flow rate as mentioned earlier. The flow rates investigated corresponded to Reynolds numbers (based on the power jet width) of 20,000, 37,000, 69,000, 100,000, and 141,000. For each of these flow rates, with the exception of that corresponding to Rew = 100,000, the velocity and pressure distributions were measured for both the open and closed control port conditions. In the case of the flow rate corresponding to Rew = 100,000, only the open control port condition was considered for the reasons which will become evident later during the course of the discussion of results.

The calibration of the system was accomplished by connecting the pressure transducer to a micromanometer and adjusting the gain of the amplifier until a convenient deflection on the readout chart was achieved. The linearity of the recording system was regularly checked and no

deviation from the straight line calibration curve was detected.

After selecting the flow rate and control port condition and balancing and calibrating the amplifier-recorder assembly, a typical run was made as follows:

(1) The atmospheric temperature and pressure were recorded;

(2) The flow rate was set with the rotometer;

(3) The manifold atmospheric vent was opened and the recorder reading positioned to zero;

(4) The manifold vent was closed and the rotometer outlet pressure valve was opened;

(5) After the pressure was recorded, the valve was closed and the vent valve again opened to see if there was any zero shift;

(6) If there was any zero shift it was corrected (In the present study no zero shift was ever observed);

(7) This procedure was repeated for the power jet wall pressure and the fifteen pressure taps along the wall;

(8) Again using the same zeroing procedure, velocity profiles were taken at stations one through seven as previously defined;

(9) And finally a single velocity measurement at the center of the power jet immediately downstream of the power-jet exit was taken.

Data Reduction. The following procedure was used in the reduction of the test data:

(1) The flow rate in standard cubic feet per minute was calculated from

Q=Rotometer reading x 100% full flow x CF(T) x CF(P)

where

CF(P) = pressure correction factor

and

CF(T) = temperature correction factor.

These correction factors were obtained from the Fisher-Porter instruction manual at standard flow conditions, i.e., at 14.7 psig and 70 deg. F.;

(2) The average velocity in the power jet was calculated from

$$U_o = Q/A_c$$

where A_c is the cross sectional area of the power jet;

(3) The static wall pressures were put in dimensionless form as

$$CFP = \frac{P_w}{\rho \frac{U_o^2}{2}}$$

where P_w is the wall pressure;

(4) Velocities were calculated from

$$U = \sqrt{\frac{2P_d}{\rho}}$$

where P_d is the differential pressure sensed by the Pitot tube; and

(5) Reynolds numbers were evaluated as

$$Rew = \frac{U_o w}{\nu}$$

Experimental Uncertainty. Uncertainty in the velocity parameters was estimated using standard techniques. The following equation

$$\frac{\Delta(U/U_o)}{U/U_o} = \left[\frac{1}{4}\left(\frac{\Delta P_t}{P_t}\right)^2 + \left(\frac{\Delta Q}{Q}\right)^2 + \frac{1}{4}\left(\frac{\Delta \rho}{\rho}\right)^2\right]^{1/2}$$

and the following approximate individual uncertainties (calculated for the worst possible conditions),

$$\frac{\Delta P_t}{P_t} \approx 0.030$$

$$\frac{\Delta Q}{Q} \approx 0.020$$

$$\frac{\Delta \rho}{\rho} \approx 0.016$$

yielded a maximum uncertainty interval of

$$\frac{U}{U_o} \approx 0.026$$

An identical procedure gave a maximum uncertainty interval for the wall pressure coefficient of

$$\frac{\Delta CFP}{CFP} \approx 0.05$$

4. Discussion of Results.

The various velocity distributions obtained through the procedures previously described will be discussed both with respect to their inner and outer regions and with respect to the control port conditions. Then the discussion of the pressure distribution along the wall will be taken up.

Each velocity profile is considered to be composed of two parts: an inner profile which extends from the boundary to the point where the velocity reaches its maximum value and an outer profile which extends from the point of maximum velocity to infinity (for all intents and purposes, to the region where ambient conditions prevail).

Figures 3 through 31 represent the dimensionless velocity parameter U/U_m as a function of the normalized distance y/y_m from the wall. In these profiles, Figs. 3 through 16 depict both the inner and outer regions of the velocity distribution. Figures 17 through 31 show the inner velocity at various stations along the wall for different Reynolds numbers.

The purpose of these plots was, in part, to give a clear idea of the evolution of the velocity along the wall and along the normal to the wall and at the same time to present some of the data obtained in graphical form. The complete data is presented in numerical form in Appendix I. It is apparent that these profiles cannot, as they stand, be compared with those predicted theoretically. The outer region of all the velocity profiles for all Reynolds numbers tested for the stations from station 3 through 7 are plotted via computer in Fig. 32. The velocity profiles for stations 1 and 2 are not incorporated into this figure and the reason for this will be discussed separately.

A close examination of Fig. 32 reveals the following facts: (a) within the range of experimental uncertainties encountered, the velocity profiles for the outer region are similar in terms of the parameters $(y-y_m) / (y_{m/2}-y_m)$ and U/U_m; (b) the outer velocity profile predicted by Glauert [8] on the basis of the conservation of linear momentum (Eq. 22), which is plotted in Fig. 33, is in good agreement with the data shown in Fig. 32 in spite of the fact that momentum is not conserved as proved through the theoretical analysis as previously discussed (Eq. 21). Before we present the reasons for this rather unexpected agreement between the data and Glauert's solution, it should be pointed out that the theoretical curve representing Eq. (24) was not plotted in Fig. 32 for it would have been practically impossible to distinguish it from the experimental curves. For this reason Eq. (24) was plotted in Fig. 33. The reader can easily observe the perfect agreement between the Figs. 32 and 33.

It is now necessary that the reasons for the unexpected agreement between Glauert's solution and the experimental data be explained. Clearly, the right hand side of Eq. (21) is comprised of two terms. The first part (the third term) as given by

$$-\frac{1}{\rho}\int_0^{y_m} u\,\tau\,dy \qquad (25)$$

represents the rate of change of specific momentum in the inner region and the second part (the fourth term) as given by

$$-\frac{1}{\rho}\int_{y_m}^{\infty} u\,\tau\,dy \qquad (26)$$

represents the rate of change of specific momentum in the outer region. Obviously the momentum loss given by Eq. (26) is quite small due to the rapid decrease of both the shear stress and the velocity in the outer region. In order that this loss of momentum have an appreciable effect on the overall momentum of the outer region, the jet must extend sufficiently long distances along the wall.

In other words if the length of the side wall had been several times longer than that used in the current investigation, then the loss of momentum and hence the disappearance of the similarity of the outer profiles would have become evident. Thus the boundary layer along a rather short wall behaves as if the Reynolds number based on distance was nearly constant. Even though one might question why the experiments were not carried out along much longer walls and why the validity of the theoretical findings were not brought fourth, one must remember that the primary objective of this, as well as other investigations pertaining to the Coanda effect, are for the understanding of the operation of wall-attachment type fluid amplifiers where the side wall is very short and certainly not much longer than 10w to 20w, (in the present investigation this would correspond to a distance from the nozzle of 2.5 to 5 inches). The distance from the nozzle to the last station was 7.625 inches in the present investigation. Obviously, one can undertake additional studies to determine the range of applicability of the results obtained on the basis of the conservation of momentum as a function of the distance along the wall for a specified degree of uncertainty.

As mentioned previously, the inner profiles were plotted in Figs. 17 through 31. Had there been a similarity between these profiles, or in other words, had the momentum in a region along the wall been conserved,

it would have been possible, at least according to Glauert, to plot them in terms of U/U_m versus y/y_m and obtain a single experimental profile. The plots presented in Figs. 17 through 31 clearly show that there is no such similarity. The reason for the lack of similarity may now be discussed with reference to Eq. (21) or with reference to Eqs. (25) and (26). As cited previously Eq. (25) represents the rate of change of momentum or loss of momentum (since both τ and u are positive, the result of the integral in Eq. (25) is negative). The shear stress is quite large within the inner region and even though the velocity changes from zero to U_m, the momentum loss represented by Eq. (25) is sufficiently large even for short distances along the wall to destroy the hypothesis of the conservation of momentum and hence the hypothesis of similarity for the profiles. In order to illustrate the point, the power law similarity hypothesis, commonly represented by

$$U/U_m = (y/y_m)^{1/n} \qquad (27)$$

was plotted in Fig. 34 for three values of n, namely, n = 7, n = 12, and n = 15. Also shown in Fig. 34 are the mean curves passing through the data points shown in Figs. 17 through 32. It is apparent that the experimental data does not follow a single power law profile and the majority of the data falls somewhere between the curves corresponding to n = 7 and n = 15. This result is in agreement with the work done by Schwarz and Cosart [14], Myers, Schauer, and Eustis [24] on a plane wall, and by Sridhar and Tu [20] on a wall with various setbacks and control port openings. The last investigators have carried their experiments for only one Reynolds number in the order of 20,000.

In concluding the discussion of the velocity profiles it can be stated, for the range of Reynolds numbers tested, that there is a similarity in the

velocity profiles of the outer region because of the negligible effect of the loss of momentum within that region and that there is no similarity of the velocity profiles within the inner region due to the appreciable effect of the loss of momentum. As stated in the introduction to the theoretical analysis the prediction of the characteristics of turbulent jets along straight or curved walls, particularly in the inner region, is quite limited partly because of the lack of information regarding the turbulent shear stress distribution. Thus it is quite difficult to evaluate Eq. (21) to determine the variation of the non-similar velocity profiles along the normal to the wall. The possibility of exploring various eddy viscosity approximations together with Eq. (21) is left for further studies.

The velocity profiles obtained at stations 1 and 2 were excluded from the foregoing discussion and conclusions. A comparison of these profiles as illustrated by Figs. 3, 4, 10, and 11 with the inner and outer velocity profiles illustrated by Figs. 32 and 34 have shown that there is no similarity either in the inner or the outer regions. This is not unexpected, partly because of the complex interaction of the control port and setback on the initial evolution or transition of the jet. The significant fact, however, is that the outer profile obeys similarity at least by the time the jet reaches the third station, i.e., at $x = 6.5w$. Had the jet been laminar, this region of transition would have been much larger due to the lack of eddy mixing. It should also be pointed out that, the transition discussed above is of three-dimensional character because of the effect of the side walls. This type of transition was investigated by Bettoli [25]. It would indeed be a very complex problem to study the transition of the velocity profiles between the two confining walls anywhere along the jet. Thus the reader is reminded that the similarities in the

outer profile and the dissimilarities in the inner profile all refer to the centerline velocities. The comforting fact, however, is that the results reported by Johnson [6] and the measurements made by the writer show that the velocities at a given distance from the wall and at a given station remain uniform within 3/4 inch wide center-region of the one inch thick jet.

The pressure coefficients are plotted in Figs. 35 through 43 as a function of x/w for various Reynolds numbers and for open and closed control port conditions. It is evident that the pressure along the wall starts from a high negative value and reaches a peak at a distance approximately 5w from the nozzle. This is the region which was previously termed as the transition region. The rapid variation of the pressure once again points out the difficulty of predicting the behavior of the jet within that region.

It is also apparent from these curves that the pressure remains fairly constant along the wall extending from 5w to 30w. For relatively small Reynolds numbers (20,000, 37,000) the wall pressure, with the exception of that in the transition region, is nearly zero. This is indeed in conformity with the hypothesis made by Glauert and its validity is illustrated by the data presented herein. As a matter of fact, it should, in passing, be noted that the constancy of the pressure, in addition to the constancy of linear momentum in the outer region, is another reason for the validity of Glauert's solution for relatively small Reynolds numbers. For larger Reynolds numbers (69,000, 100,000, and 141,000) the pressure along the wall deviates from zero in amounts increasing with Reynolds number as observed in Figs. 39 through 43. Thus in order to develop a relatively more reliable analysis for the velocity distribution along the wall one must take into consideration the deviation of pressure from that of the surroundings. It may safely be

surmised that the pressure within a given section reaches very quickly the ambient pressure. However, the effect of the existence of a pressure other than ambient, in the inner region, stands out as another reason, particularly for flow with larger Reynolds numbers, for the dissimilarity of the velocity profiles. Celarly the velocity distribution, loss of momentum, and the side wall effects are inseparably interconnected. In view of this, it is rather surprising that a researcher such as Glauert can, with assumptions justifiable at least within certain regions and Reynolds numbers, predict the behavior of such an enormously complex turbulent flow.

In conclusion it can be stated, for the range of Reynolds numbers tested, that:

(1) There is a transition region where the jet changes from a free jet to a wall jet. The complex interaction of the control port, setback, and three-dimensional characteristics resulting from the proximity of the boundary walls preclude the possibility of a theoretical analysis of the transition region;

(2) Beyond the transition region, there is similarity among the velocity profiles of the outer region for such distances along the wall that the loss of momentum is insignificant (see Eq. 26);

(3) There is no similarity with respect to the inner profiles because the momentum loss of Eq. (25) is sufficiently large even for short distances along the wall.

(4) The total pressure, rather than the static pressure, is constant across the boundary layer (see Eq. 6) when turbulent flow is considered. Many investigators assumed

the static pressure to be constant in investigating turbulent jet flow. Particularly at high Reynolds numbers, this assumption introduces significant errors.

(5) The static pressure along the wall does, however, remain fairly constant for lengths of less than about 30w with the exception of that in the transition region. For small Reynolds numbers (20,000, 37,000) the static pressure is nearly zero which is in conformity with Glauert's hypothesis. For larger Reynolds numbers (69,000, 100,000, and 141,000) the pressure along the side-wall, while still fairly constant, deviates from zero in amounts increasing with increasing Reynolds numbers. The effect of the existence of a pressure other than ambient in the inner flow region is another reason for the dissimilarity of the inner velocity profiles.

5. Recommendations for Further Work.

The investigation described herein should be extended to the study of the following problems:

(1) The effect of the variation of setback on the length of the transition region;

(2) Evaluation of the root-mean-square values of various turbulence-intensity terms across the jet;

(3) Theoretical analysis of the inner region through the use of various eddy-viscosity models;

(4) Comparison of the characteristics of jet flows along straight and curved walls for the purpose of evaluating the effect of the curved Coanda-wall on the performance of wall-attachment devices; and

(5) The effect of higher Mach and Reynolds numbers on the conclusions drawn in this work.

REFERENCES

1. Young, T., "Outlines of Experiments and Inquiries Respecting Sound and Light," (16 January 1800), Quoted by J. L. Pritchard: "The Dawn of Aerodynamics," Journal of the Royal Aeronautical Society, March 1957.

2. Reynolds, O., "Suspension of a Ball by a Jet of Fluid," Proc. Manch. Lit. Phil. Soc., 1870.

3. Reba, I., "Applications of the Coanda Effect," Scientific American, June 1966.

4. Sarpkaya, T. and Kirshner, J., "The Comparative Performance Characteristics of Vented and Unvented, Cusped, and Straight and Curved-Wall Bistable Amplifiers," Proceedings of the Third Cranfield Fluidics Conference, Turin, Paper F3, May 1968.

5. Kesler, K., Turbulent Jet Attachment to Convex Walls, MS Thesis, Naval Postgraduate School, Monterey, June 1968.

6. Johnson, L. D., Experimental Investigation of Turbulent Jet Attachment to a Convex Wall, MS Thesis, Naval Postgraduate School, Monterey, Sept. 1968.

7. Gőrtler, H., "Berechnung von Aufgaben der freien Turbulenz auf Grund eines neuen Näherungsanstazes," Zeitschrift fűr angewandte Mathematik und Mechanik, Vol. 22, 1942.

8. Glauert, M. D., "The Wall Jet," Journal of Fluid Mechanics, Vol. 1, 1956.

9. Newman, B. G., "The Deflection of Plane Jets by Adjacent Boundaries-Coanda Effect," Boundary Layer and Flow Control - Its Principles and Applications, ed. G. V. Lachmann, Vol. 1, Pergamon Press, 1961.

10. Főrthmann, E., "Uber Turbulente Strahlausbreitung," Ing. - Arch., 1934, N.A.C.A. TM 789, 1936.

11. Schlichting, H., "Boundary-Layer Theory," McGraw-Hill, 1968.

12. Sigalla, A., "Measurements of Skin Friction in a Plane Turbulent Wall Jet," Journal of the Royal Aeronautical Society, 1958.

13. Bourque, C. and Newman, B. G., "Reattachment of a Two-Dimensional, Incompressible Jet to an Adjacent Flat Plate," Journal of the Royal Aeronautical Society, August 1960.

14. Schwarz, W. H. and Cosart, W. P., "Two Dimensional Turbulent Wall Jet," Journal of Fluid Mechanics, Vol. 10, Part 4, 1961.

15. Sawyer, R. A. "The Flow due to a Two-Dimensional Jet Issuing Parallel to a Flat Plate," Journal of Fluid Mechanics, December 1960.

16. Sawyer, R. A., "Two-Dimensional Reattaching Jet Flows Including the Effects of Curvature on Entrainment," Journal of Fluid Mechanics, December 1963.

17. Kadosch, M., "Attachment of a Jet to a Curved Wall," Proceedings of the Second Fluid Amplification Symposium, Vol. 4, May 1964.

18. McGlaughlin, D. W. and Taft, C. K., "Fluidic Electrofluid Converter," Transactions of the ASME, June 1967.

19. McGlaughlin, D. W. and Greber, I., "Experiments on the Separation of a Fluid Jet from a Curved Surface," Advances in Fluidics, ASME, 1967.

20. Sridhar, K. and Tu, P. K. C., "Effects of an Initial Gap on the Flow in a Turbulent Wall Jet," Journal of the Royal Aeronautical Society, Vol. 70, June 1966.

21. Paranjpe, S. C. and Sridhar, K., "Effects of an Initial Gap on the Turbulent Jet Flow over a Curved Wall," Journal of the Royal Aeronautical Society, January 1968.

22. Korbacher, G. K., "The Coanda Effect at Deflection Surfaces Detached from the Jet Nozzle," Canadian Aeronautics and Space Journal, Volume 8, Number 1, January 1962.

23. USATRECOM Technical Report 64-70, "The Coanda Effect at Deflection Surfaces Widely Separated from the Jet Nozzle," by the Institute for Aerospace Studies at the University of Toronto, December 1964.

24. Myers, G. E., Schauer, J. J., and Eustis, R. N., Plane Turbulent Wall Jet, Part I: Jet Development and Friction Factor, Stanford University, Dept. Mech. Eng., TR No. 1, 1961.

25. Bettoli, R., Experimental Study of Spreading of Semi-Confined Jets, MS Thesis, Pennsylvania State University, March 1968.

BIBLIOGRAPHY

1. Akatnow, N. I., Die Ausbreitung eines ebenen laminaren Flüssigkeits-strahles längs einer festen Wand, (in Russian), Trudy Leningr. Polytechn. Inst. (Energiemaschinenbau, Techn. Hydromechanik) Maschgis, Nr. 5, 1953.

2. Bradshaw, P. and Gee, M. T., Turbulent Wall Jets With and Without an External Stream, R & M 3252, 1962.

3. Eskinazi, S. and Kruka, V., "Mixing of a Turbulent Wall-Jet into a Free-Stream," Journal Engineering Mechanics, Division Proc. ASCE, 1962, Vergl. auch Trans. ASCE Vol. 128, 1963.

4. Fekete, G. I., Coanda Flow of a Two-Dimensional Wall Jet on the Outside of a Circular Cylinder, McGill University, Report 63-11, 1963.

5. Fernholz, H. H., Zur Umlenkung von Freistrahlen an Konvex gekrümmten Wänden (Coanda-Effekt), DLR FB 66-21, 1966. (Habilitationsschrift der TU Berlin 1965)

6. Gartshore, I. S., Jets and Wall Jets in Uniform Streaming Flow, McGill University, Montreal, Report 64-4, 1964.

7. Gartshore, I. and Hawaleshka, O., The Design of a Two-Dimensional Blowing Slot and its Application to a Turbulent Wall Jet in Still Air, McGill Univeristy, Montreal, Report 65-5, 1964.

8. Gersten, K., Flow Along Highly Curved Surfaces, Vortrag auf EUROMECH 1, Berlin 1965, Vergl. auch (2) vgl. auch Diskussion zu H. H. Fernholz: Umlenkung von Freistrahlen an Gekrümmten Wänden Jahrbuch 1964 der WGLR.

9. Giles, J. A., Hays, A. P., and Sawyer, R. A., "Turbulent Wall Jets on Logarithmic Spiral Surfaces," The Aeronautical Quarterly, Vol. 17, 1966.

10. Goldstein, S., "Modern Developments in Fluid Dynamics," At the Clarendon Press, Oxford, Vol. 1, 1938.

11. Guitton, D. E., Two-Dimensional Turbulent Wall Jets Over Curved Surfaces, McGill University, Montreal, Report 64-7, 1964.

12. Harris, G. L., The Turbulent Wall Jet on Plane and Curved Surfaces Beneath an External Stream, VKI TN 27, 1965.

13. Köster, H. and Löhr, R., Untersuchungen der Umlenkung eines ebenen Strahles durch einen Kreiszylinder (Coanda-Effekt), DFL - Bericht Nr. 0272, 1964.

14. Kruka, V. and Eskinazi, S., "The Wall Jet in a Moving Stream," Journal of Fluid Mechanics, Vol. 20, 1964.

15. Loitsianski, L. G., Laminare Grenzschichten, Akademie-Verlag, Berlin, 1967.

16. Mathieu, J. and Tailland, A., Étude d'un Jet Plan Dirigé Tangentiellement á une Paroi, Comptes Rendus des Séances de l'Académie des Sciences, Vol. 252, 1961, Vol. 256, 1963, Vol. 257, 1963.

17. Mathieu, J. and Tailland, A., Jet Pariétal, Comptes Rendus des Séances de l'Académie des Sciences, Vol. 261, 1965.

18. Myers, G. E., Schauer, J. J., and Eustis, R. N., Plane Turbulent Wall Jet, Part II: Heat Transfer, Stanford University, Dept. Mech. Eng., TR No. 2, 1961.

19. Myers, G. E., Schauer, J. J., and Eustis, R. N., "Plane Turbulent Wall Jet Flow Development and Friction Factor," Transactions of the ASME, Vol 85, Series D, Journal of Basic Engineering, 1963.

20. Nakaguchi, H., Jet Along a Curved Wall, T. Moriya Memorial Seminar for Aerodynamics Research Memorandum No. 4, Tokyo, 1961.

21. Patel, R. P., Self-Preserving Two-Dimensional Turbulent Jets and Wall Jets in a Moving Stream, M. Eng. Thesis, McGill University, 1962.

22. Rajaratnam, K. and Subramanya, K., An Annotated Bibliography of Wall Jets, Report of Department of Civil Engineering, University of Alberta, Edmonton, Canada, July 1967.

23. Rajaratnam, N. and Subramanya, K., "Plane Turbulent Free Jet and Wall Jet," Journal Royal Aeronautical Society, Vol. 71, 1967.

24. Sawyer, R. A., Two-Dimensional Turbulent Jets With Adjacent Boundaries, Ph.D. Thesis, Cambridge University, 1962.

25. Schauer, J. J. and Eustis, R. H., The Flow Development and Heat Transfer Characteristics of Plane Turbulent Impinging Jets, Stanford University, Dept. Mech. Eng., TR No. 3, 1963.

26. Schlichting, H., Grenzschichttheorie, Verlag G. Braun, Karlsrule, 5, Aufl., 1965.

27. Schultz-Grunow, F. and Breuer, W., "Laminar Boundary Layers on Cambered Walls," Basic Developments in Fluid Dynamics, Ed. M. Holt, Vol. 1, Academic Press, New York, 1965.

28. Sigalla, A., "Experimental Data on Turbulent Wall Jets," Aircraft Engineering, Vol. 30, 1958.

29. Stratford, B. S., Jawor, Z. M., and Golesworthy, G. T., The Mixing With Ambient Air of a Cold Airstream in a Centrifugal Field, ARC C. P. No. 687, 1963.

30. Tailland, A. and Mathieu, J., Jet Pariétal, Journal de Méchanique, Vol. 6, 1967.

31. Thomas, P., "Untersuchungen über die Grenzschicht an einer Wand Stromabwärts von einem Ausblasespalt," Adhandlungen der BWG, Bd. XV, 1963.

32. Townsend, A. A., The Structure of Turbulent Shear Flow, Cambridge University Press, Cambridge, 1956.

33. Verhoff, A., The Two-Dimensional Turbulent Wall Jet With and Without an External Stream, Princeton University, Report No. 636, 1963.

34. Wille, R. and Fernholz, H., "Report on the First European Mechanics Colloquium, on the Coanda Effect," Journal of Fluid Mechanics, 23, 1965.

35. Wygnanski, I. J. and Champagne, F. H., "The Laminar Wall-Jet over a Curved Surface," Journal of Fluid Mechanics, Vol. 31, 1968.

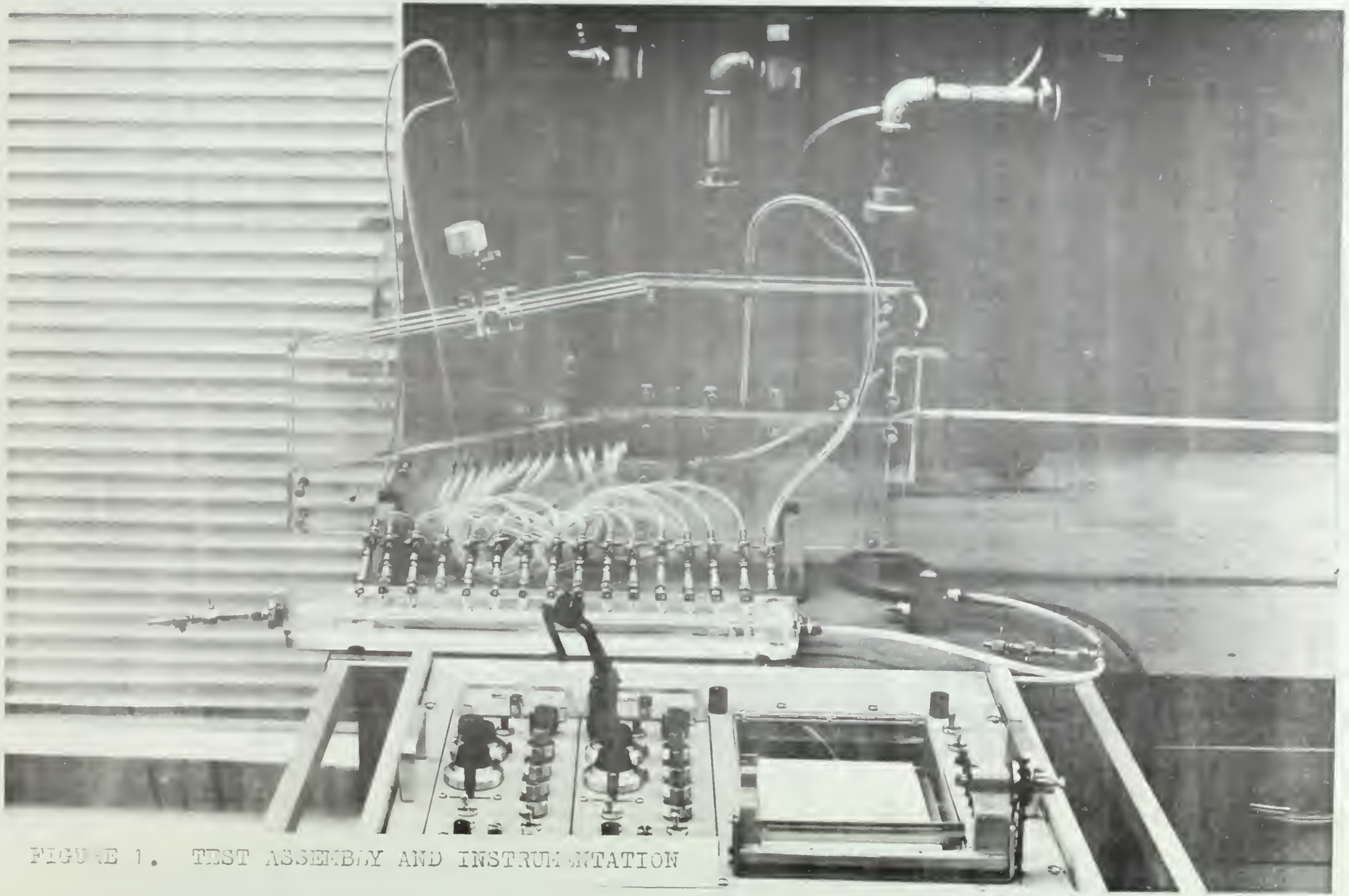

FIGURE 1. TEST ASSEMBLY AND INSTRUMENTATION

NOTE:
NOT TO SCALE
DIMENSIONS IN INCHES

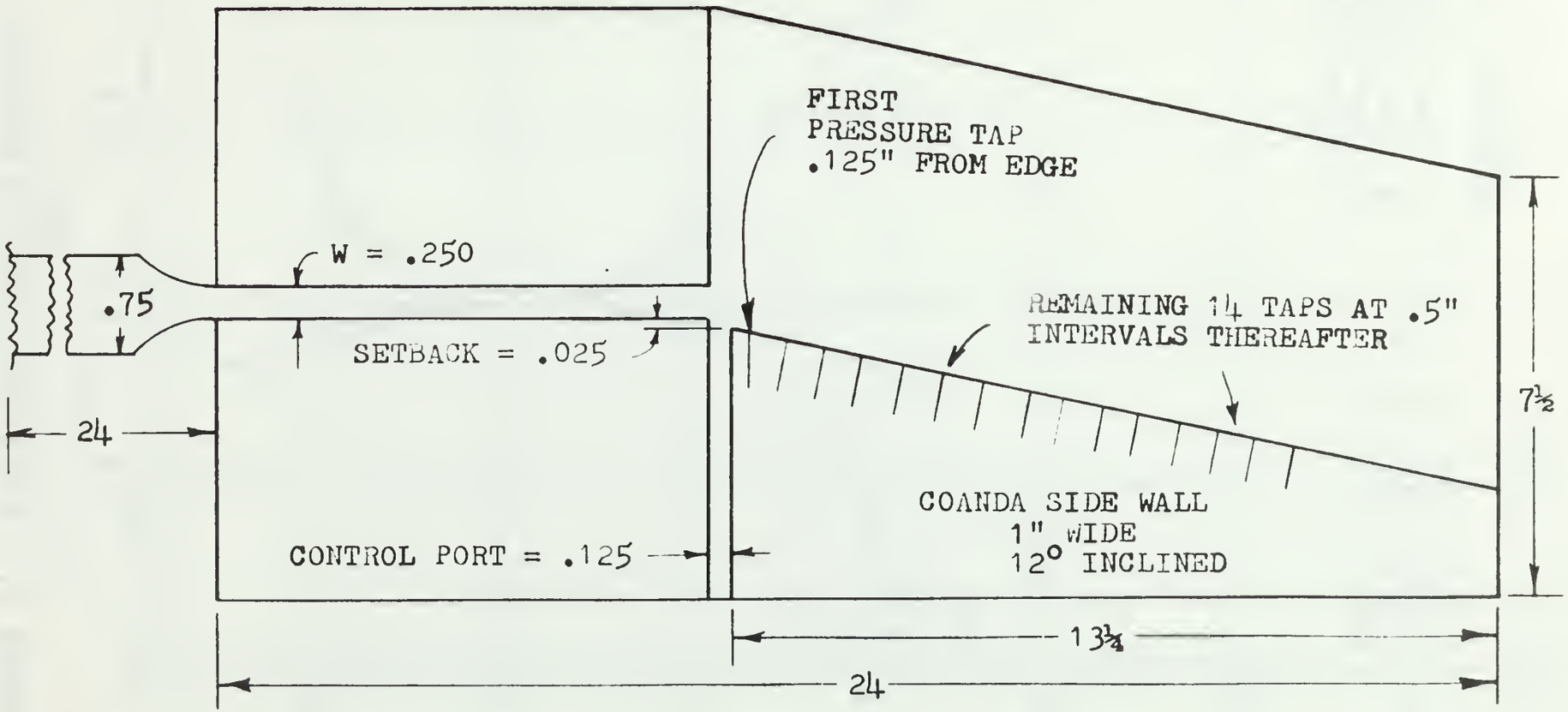

FIGURE 2. SCHEMATIC OF TEST SECTION

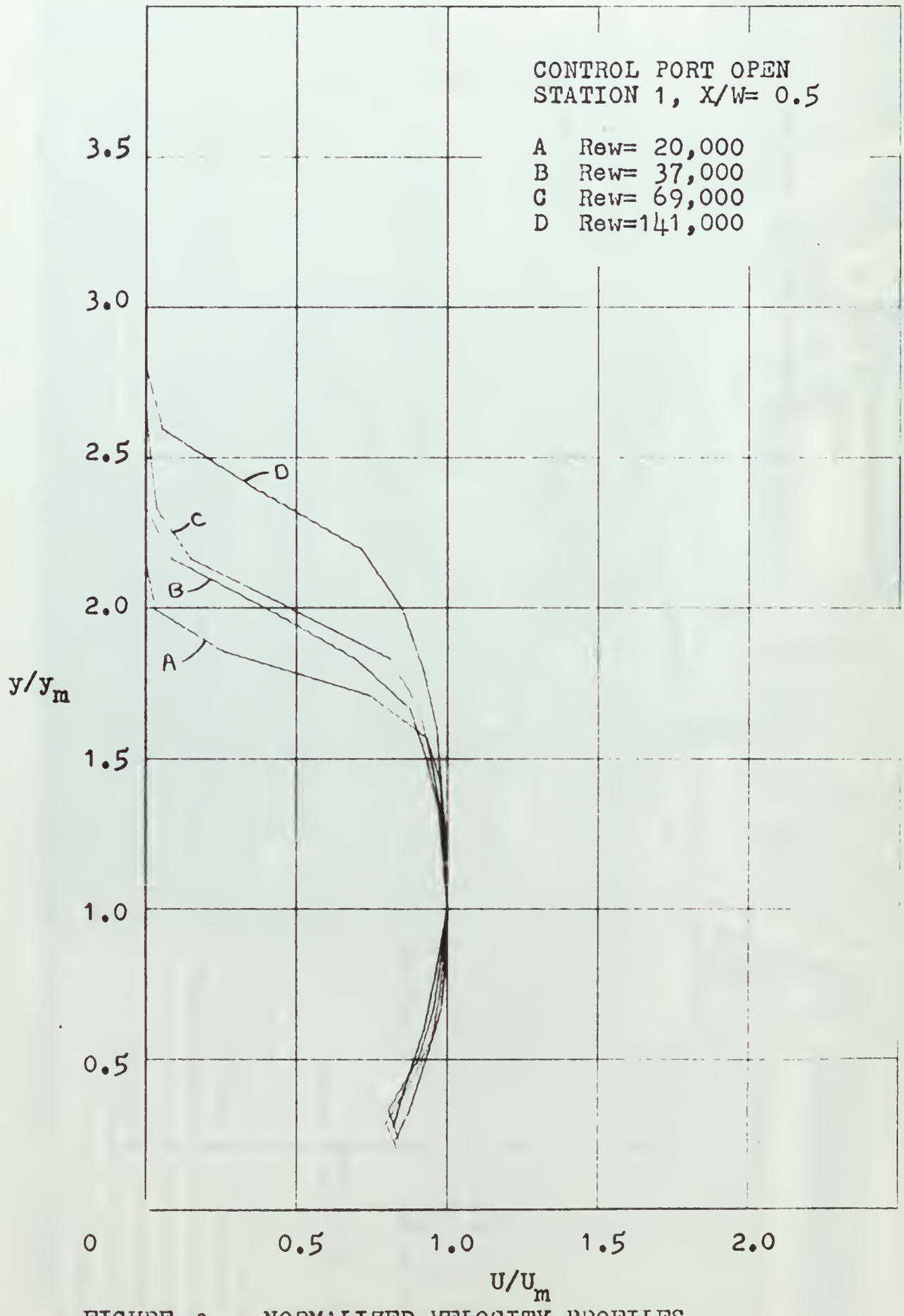

FIGURE 3. NORMALIZED VELOCITY PROFILES

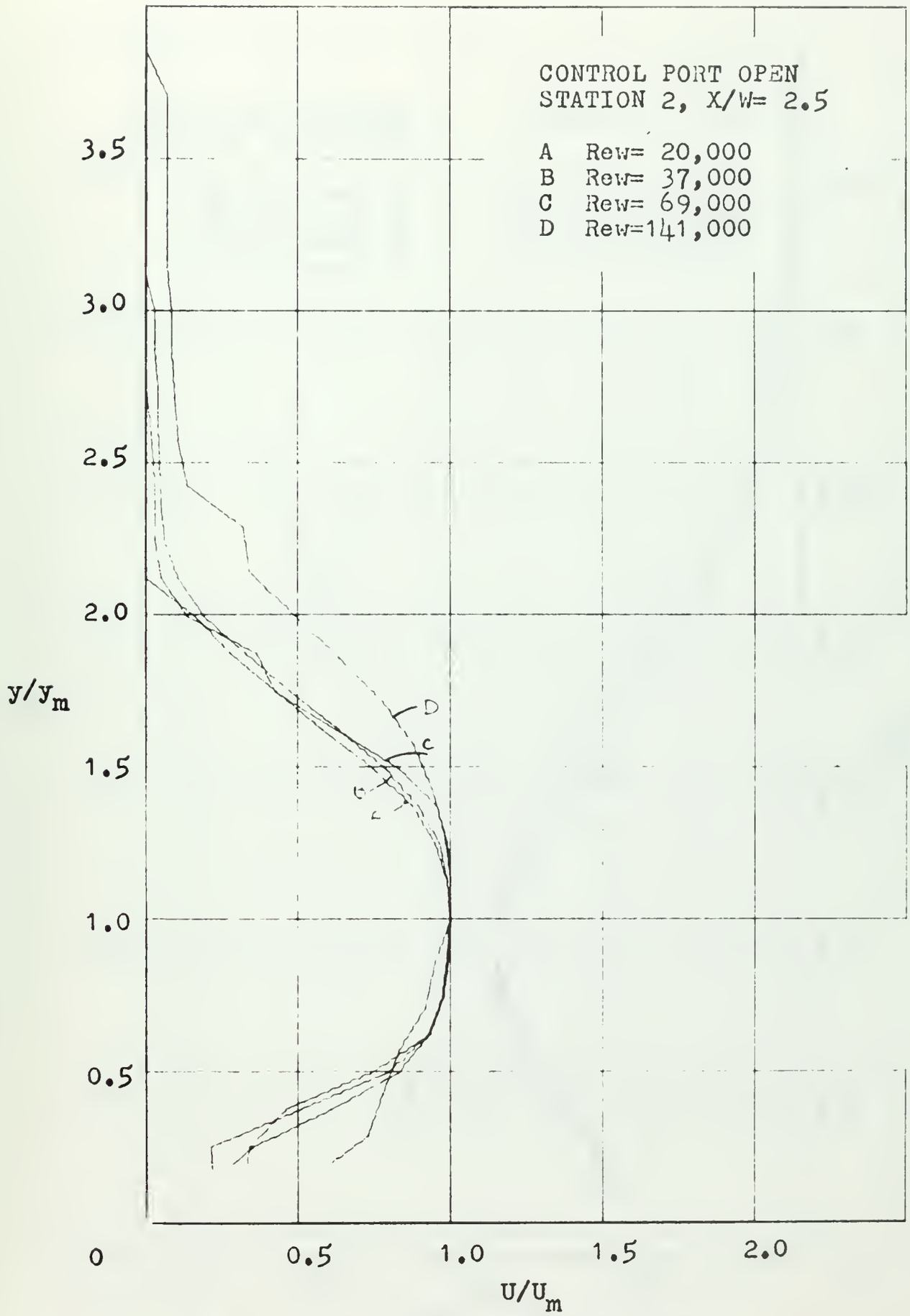

FIGURE 4. NORMALIZED VELOCITY PROFILES

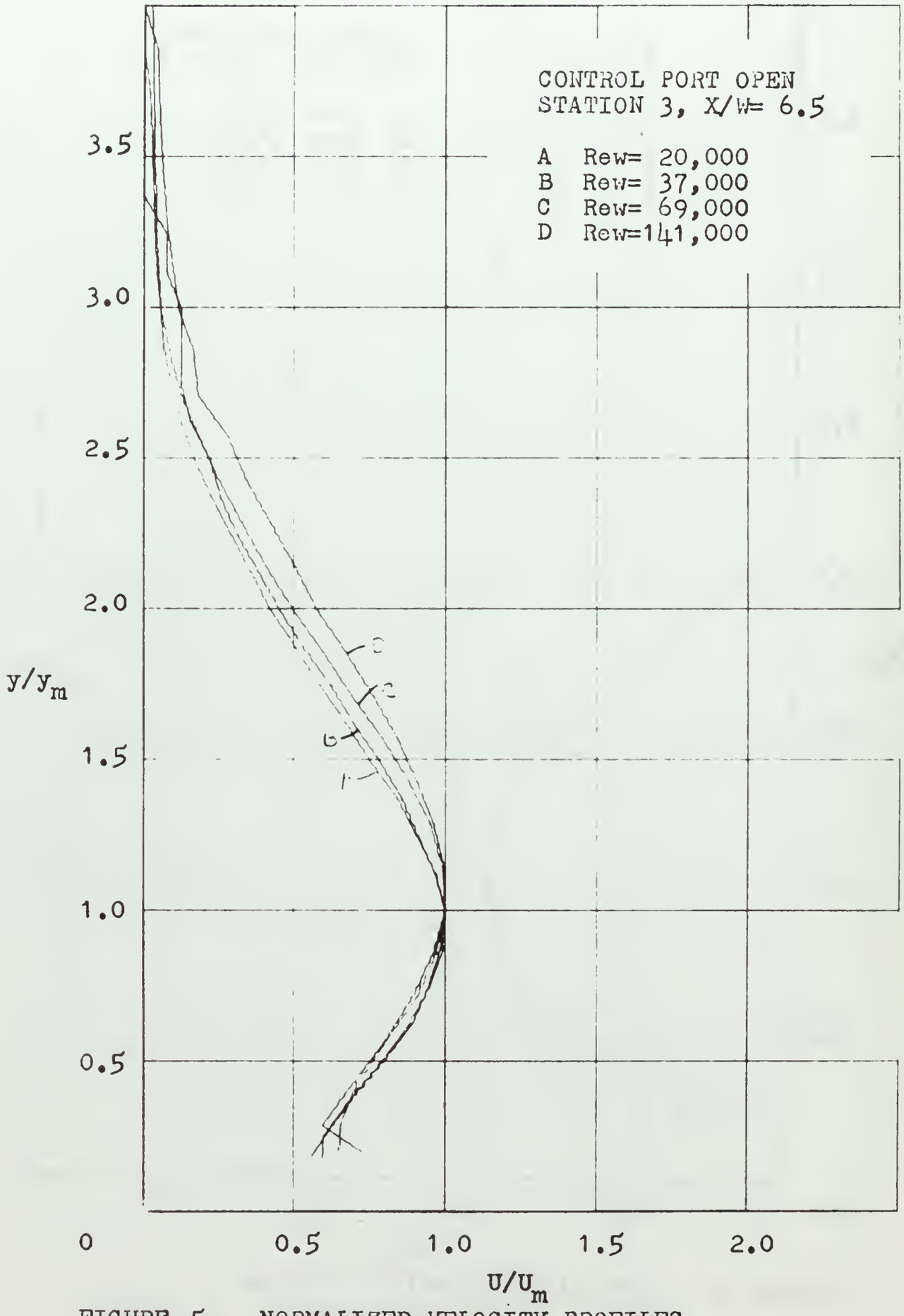

FIGURE 5. NORMALIZED VELOCITY PROFILES

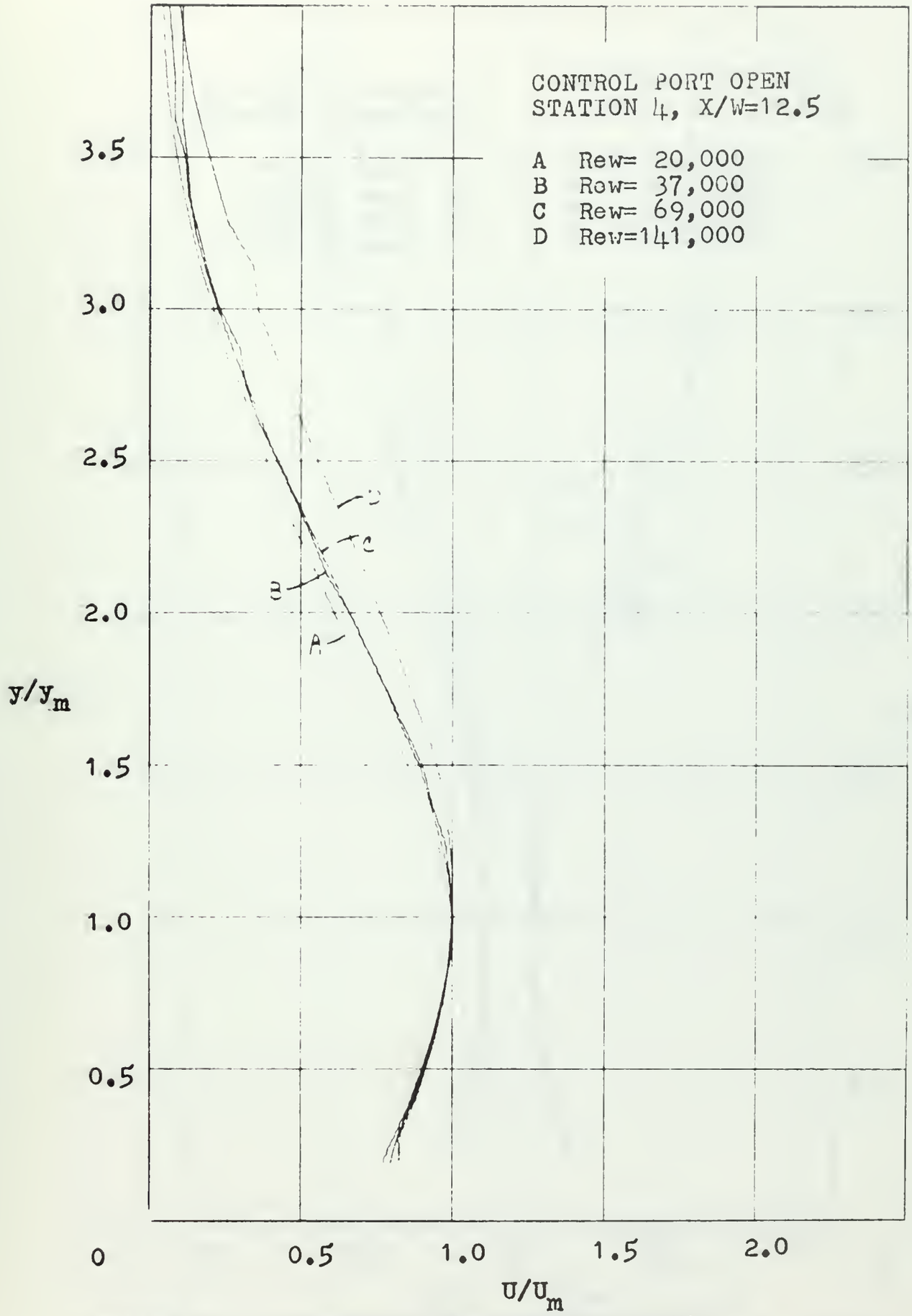

FIGURE 6. NORMALIZED VELOCITY PROFILES

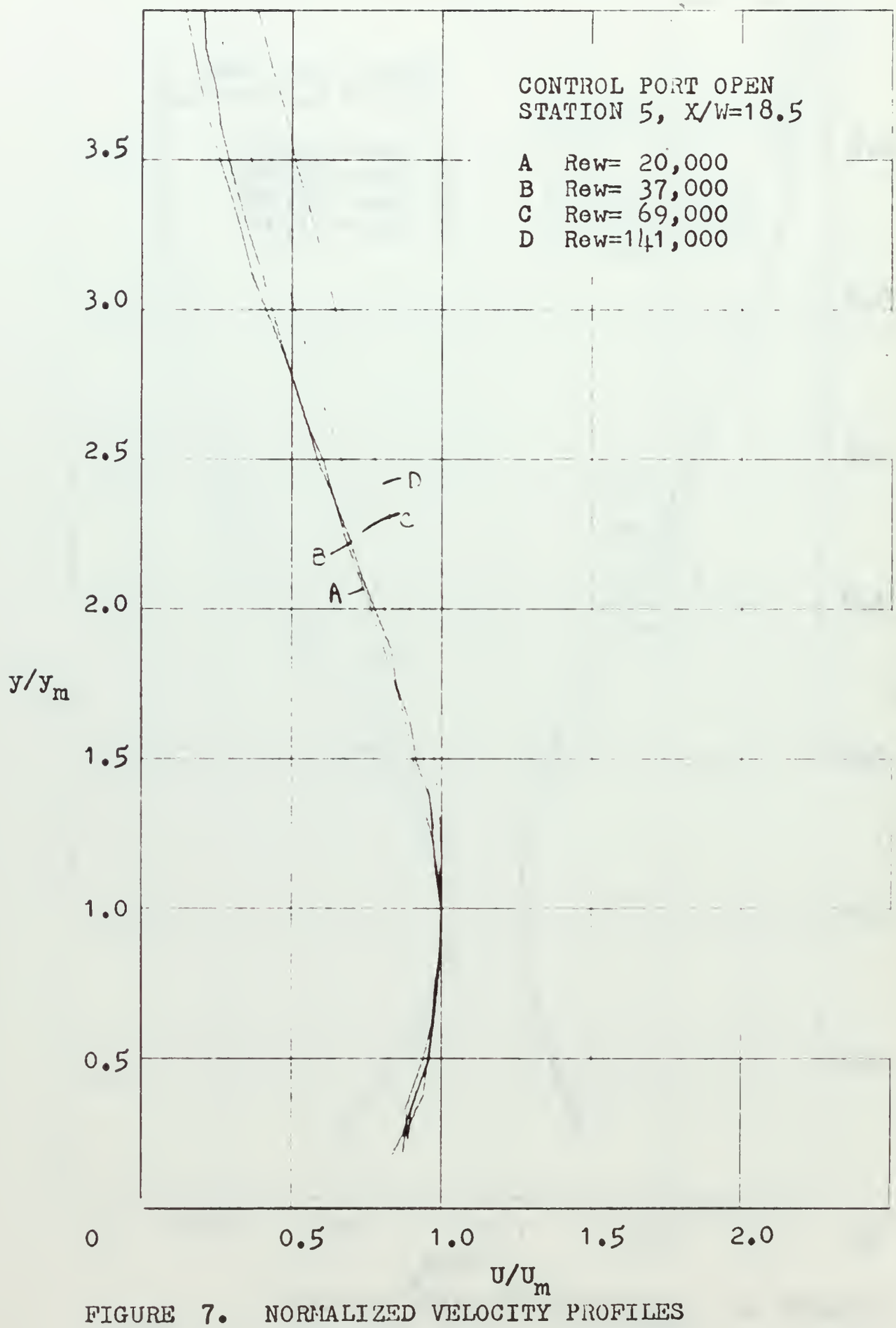

FIGURE 7. NORMALIZED VELOCITY PROFILES

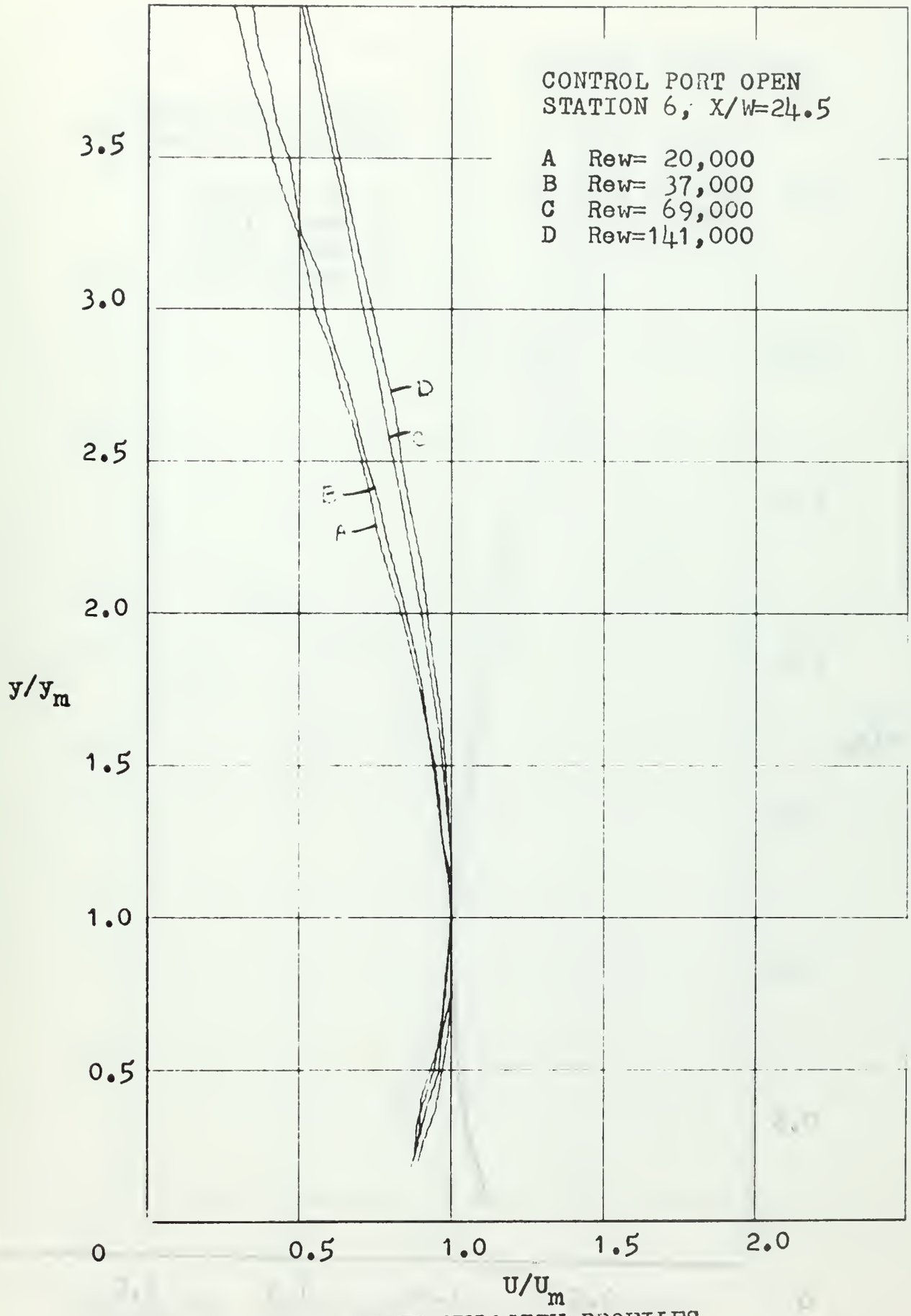

FIGURE 8. NORMALIZED VELOCITY PROFILES

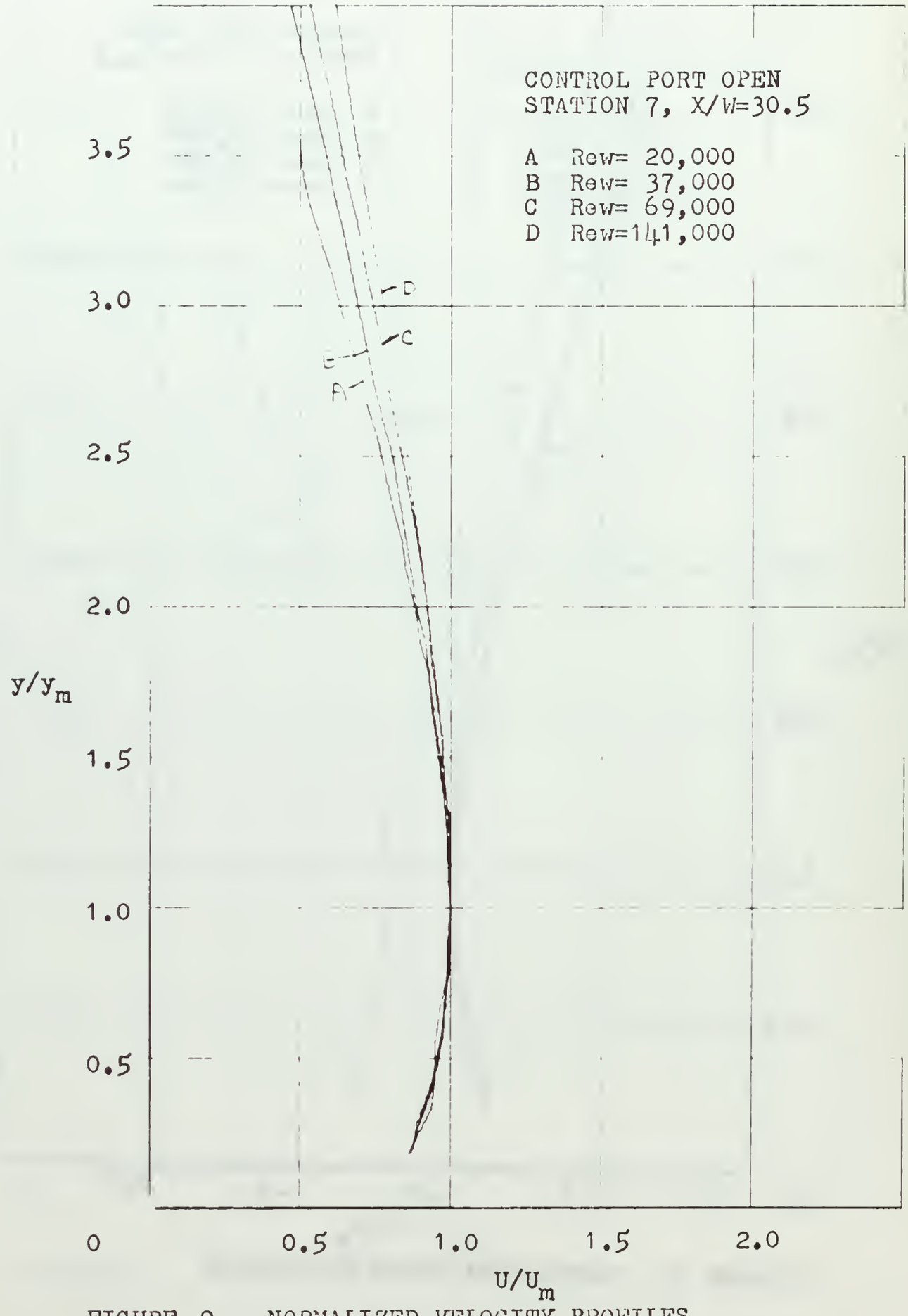

FIGURE 9. NORMALIZED VELOCITY PROFILES

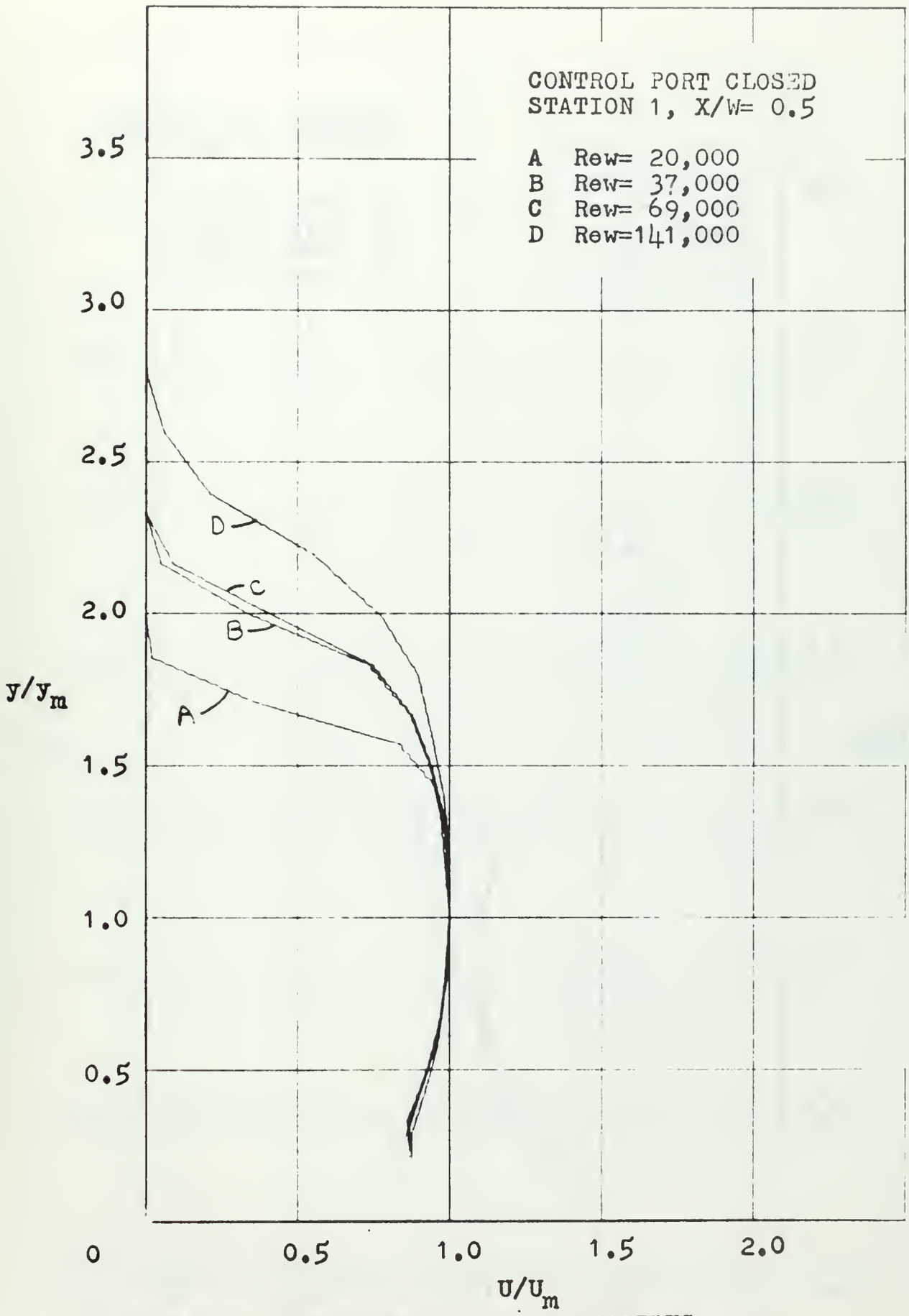

FIGURE 10. NORMALIZED VELOCITY PROFILES

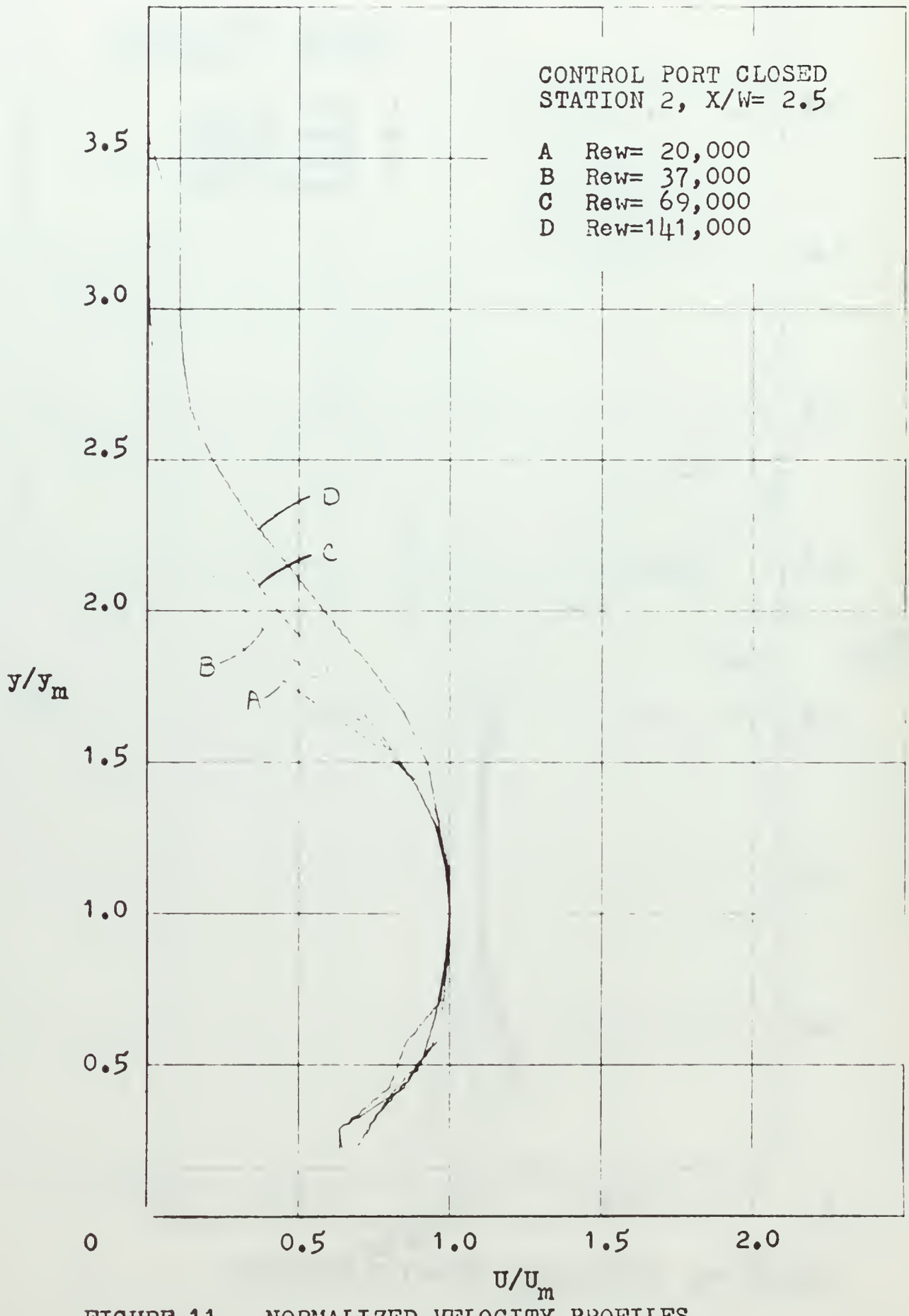

FIGURE 11. NORMALIZED VELOCITY PROFILES

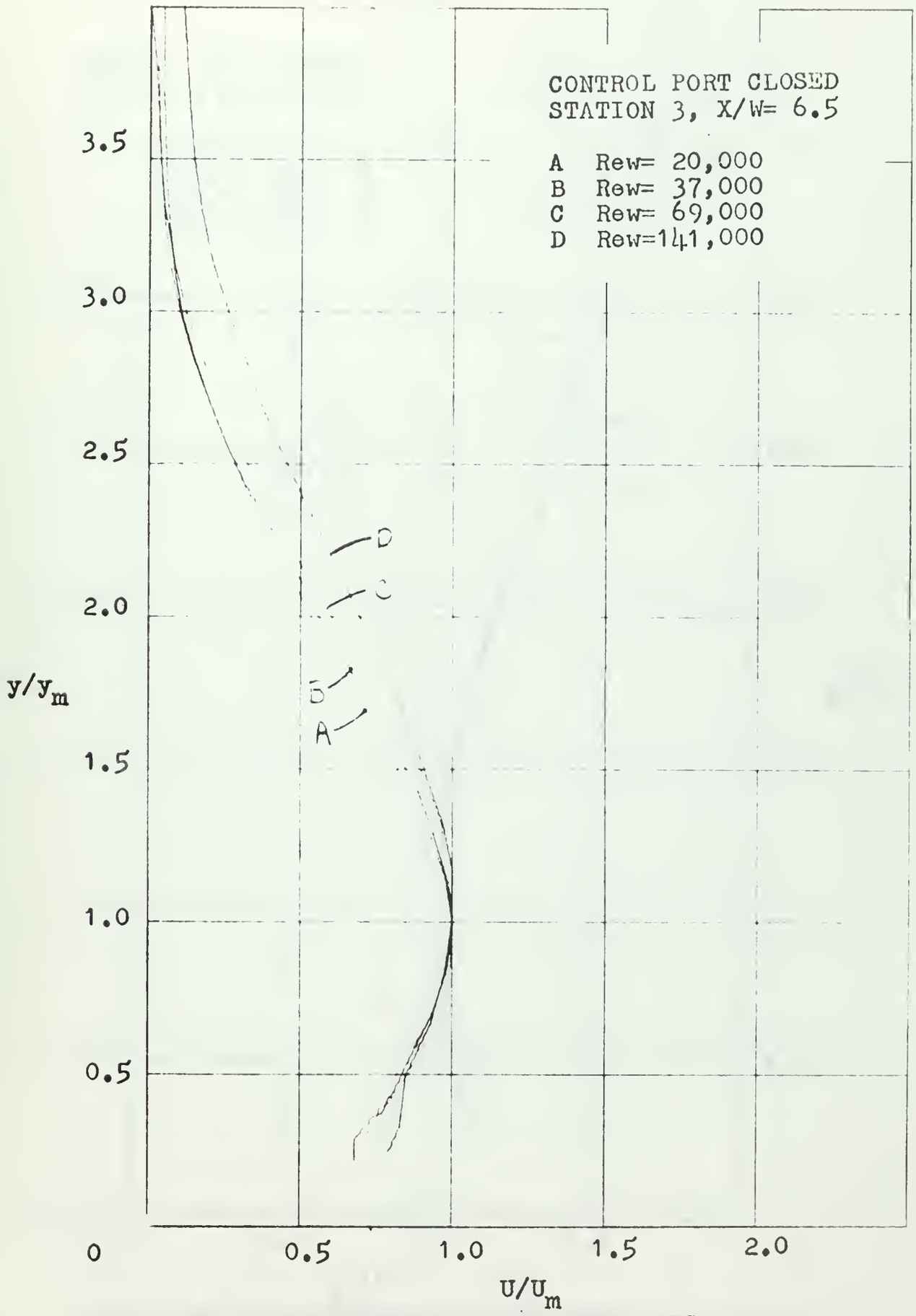

FIGURE 12. NORMALIZED VELOCITY PROFILES

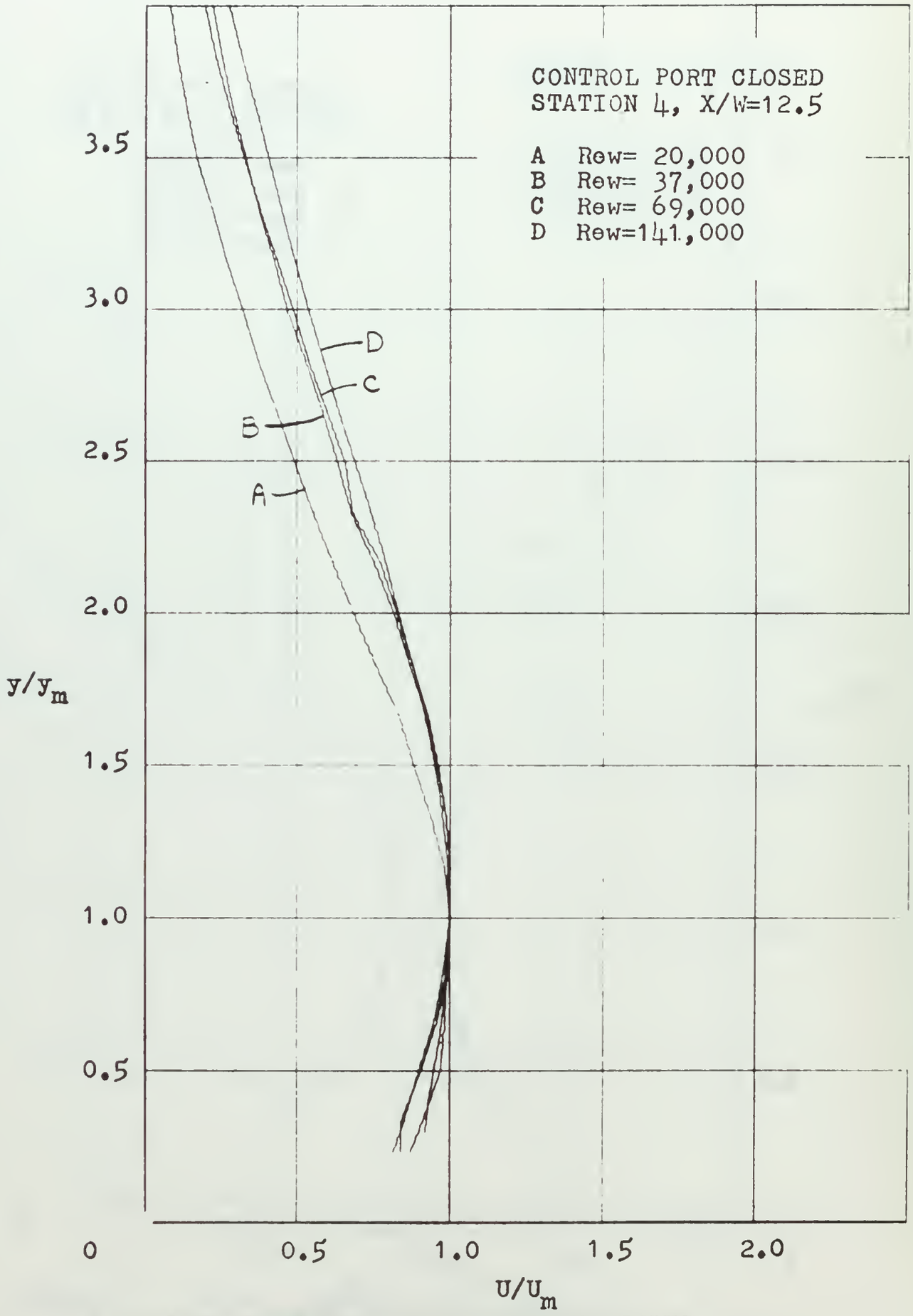

FIGURE 13. NORMALIZED VELOCITY PROFILES

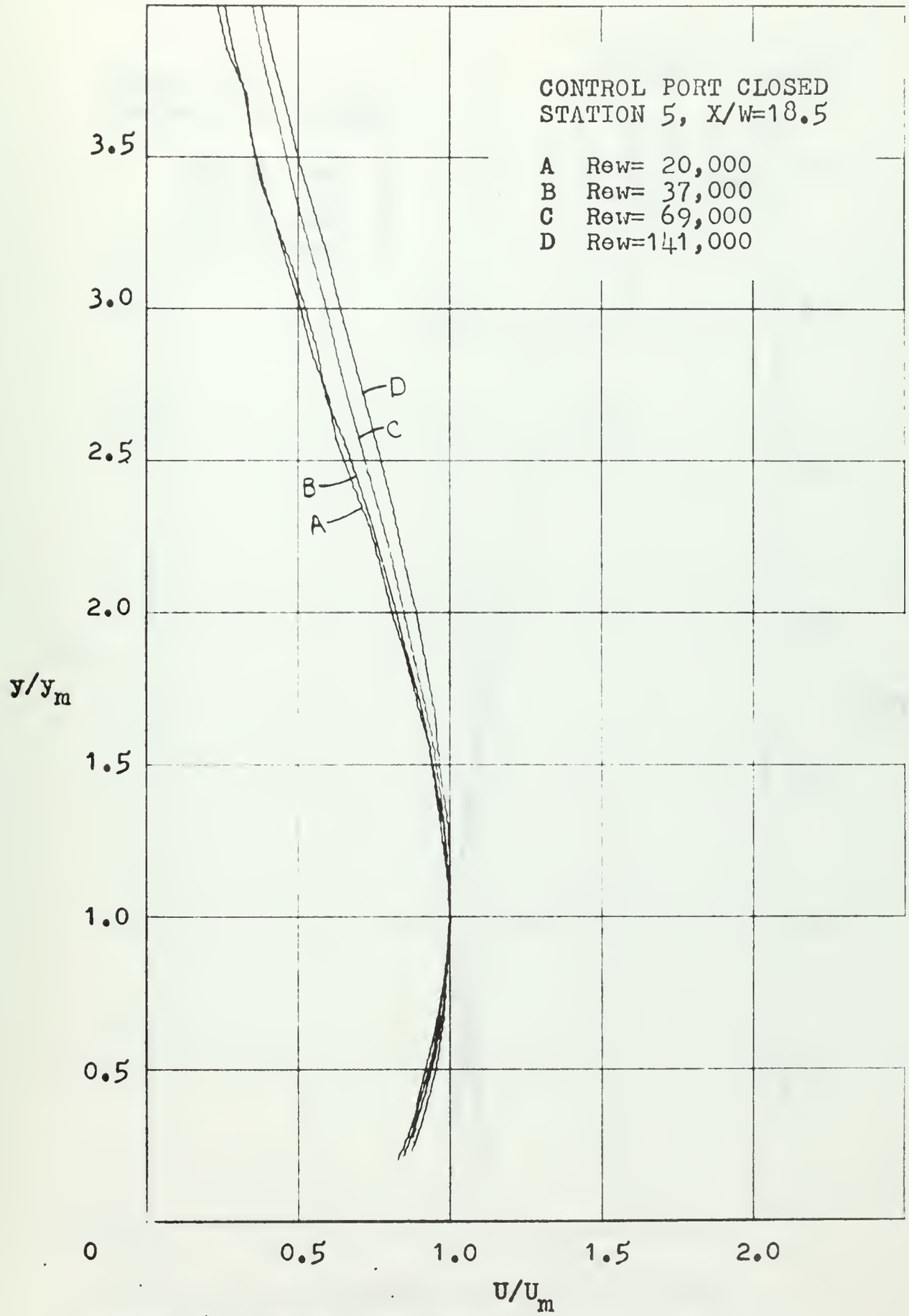

FIGURE 14. NORMALIZED VELOCITY PROFILES

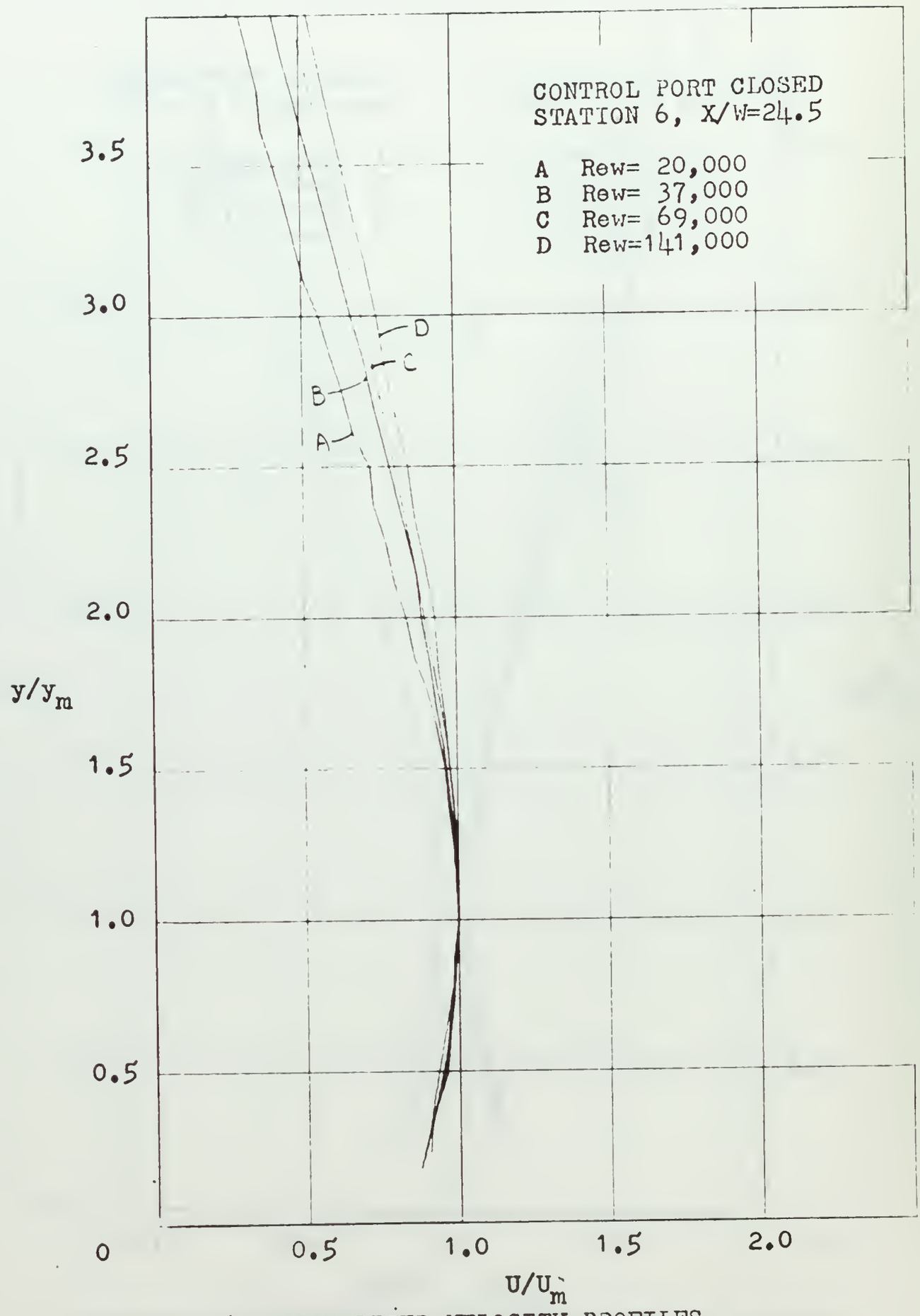

FIGURE 15. NORMALIZED VELOCITY PROFILES

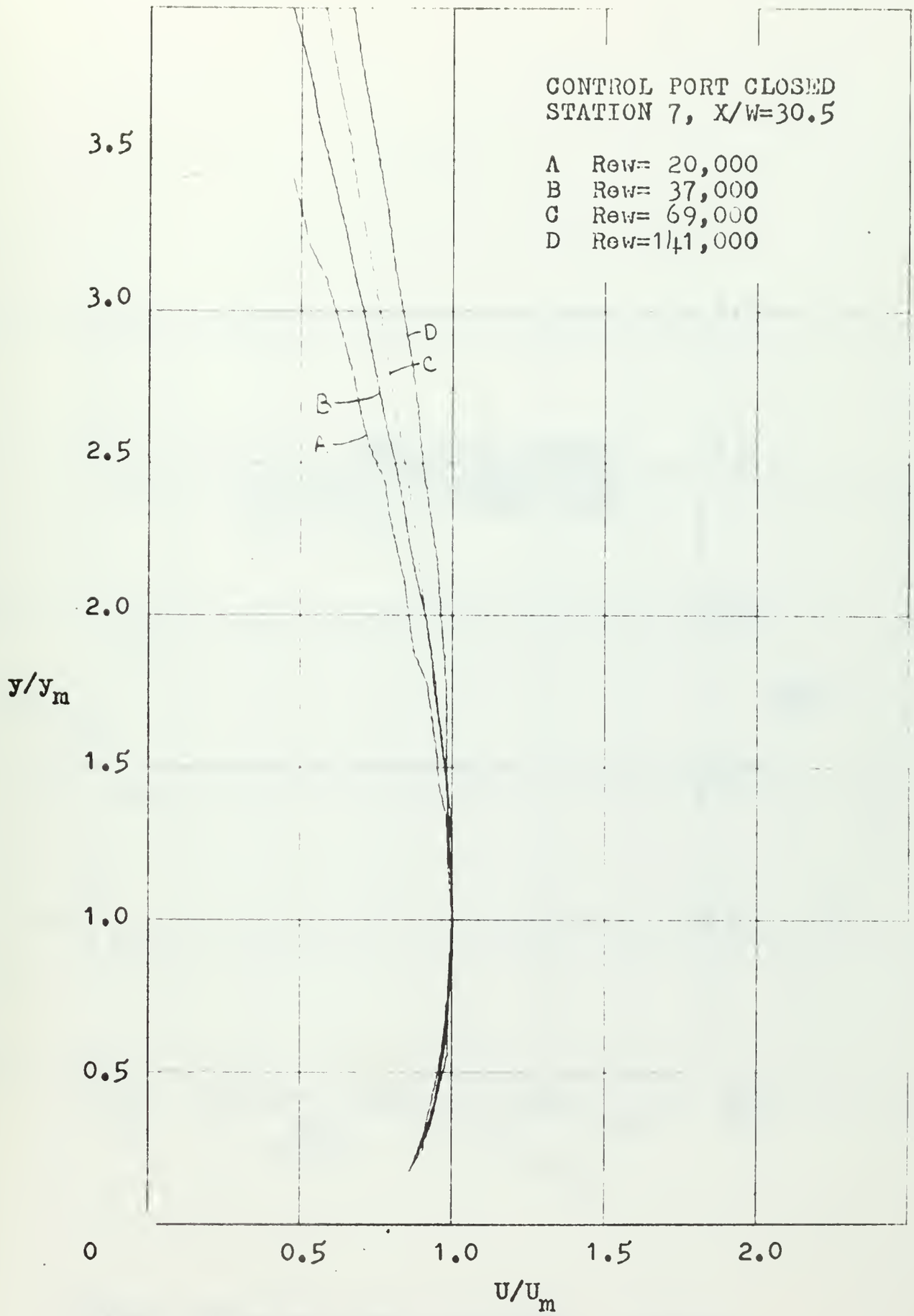

FIGURE 16. NORMALIZED VELOCITY PROFILES

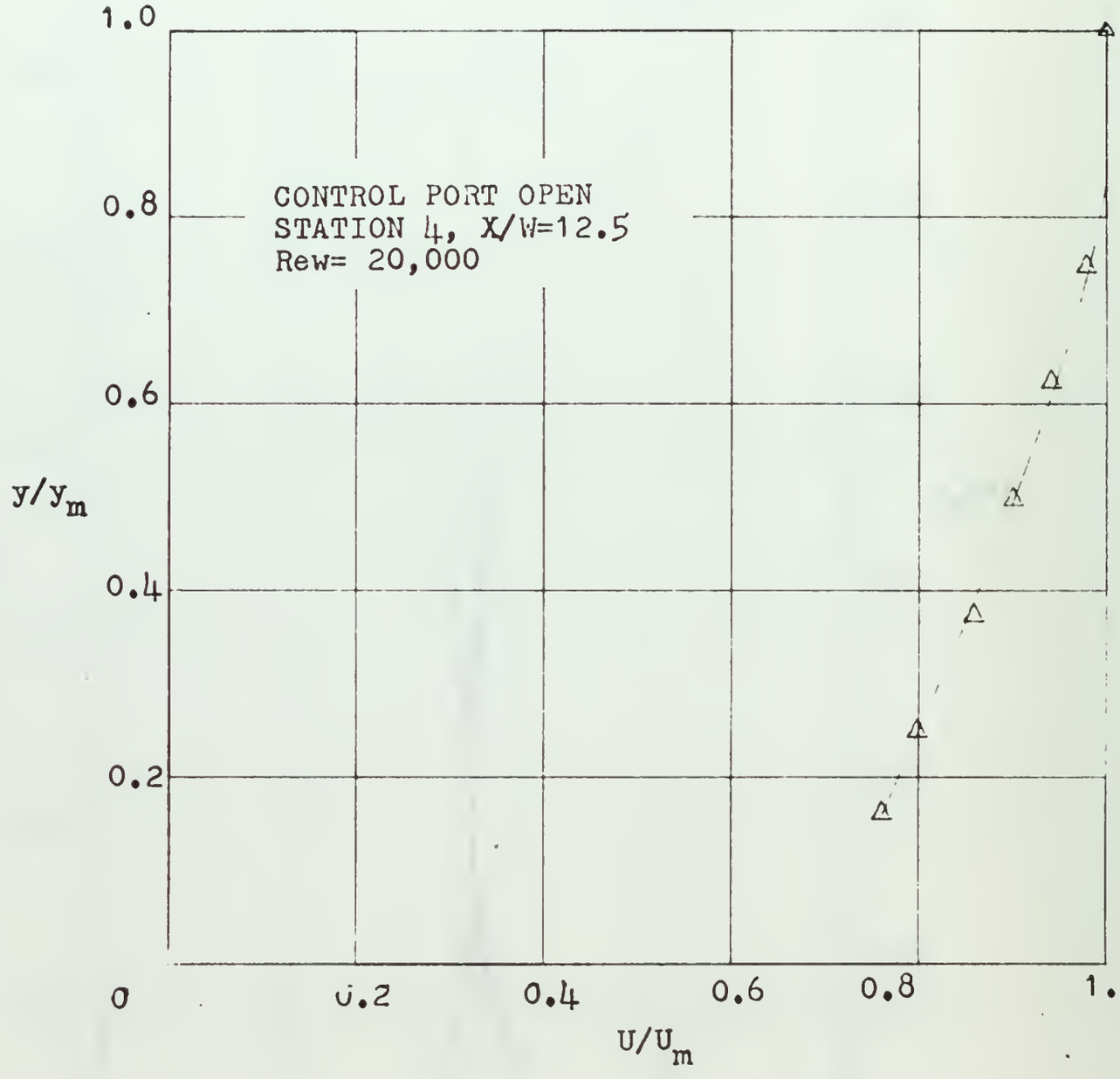

FIGURE 17. NORMALIZED INNER VELOCITY PROFILE

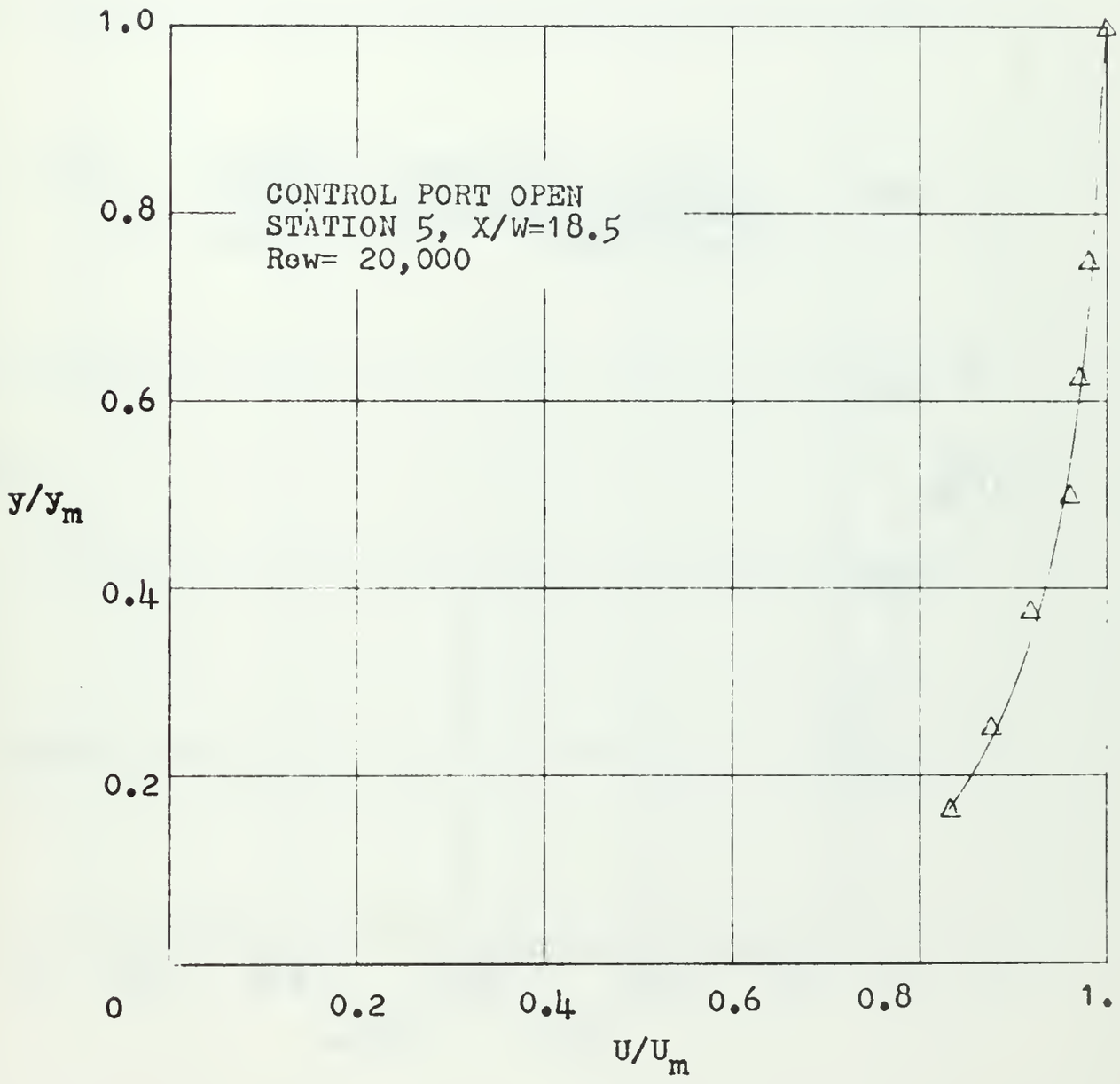

FIGURE 18. NORMALIZED INNER VELOCITY PROFILE

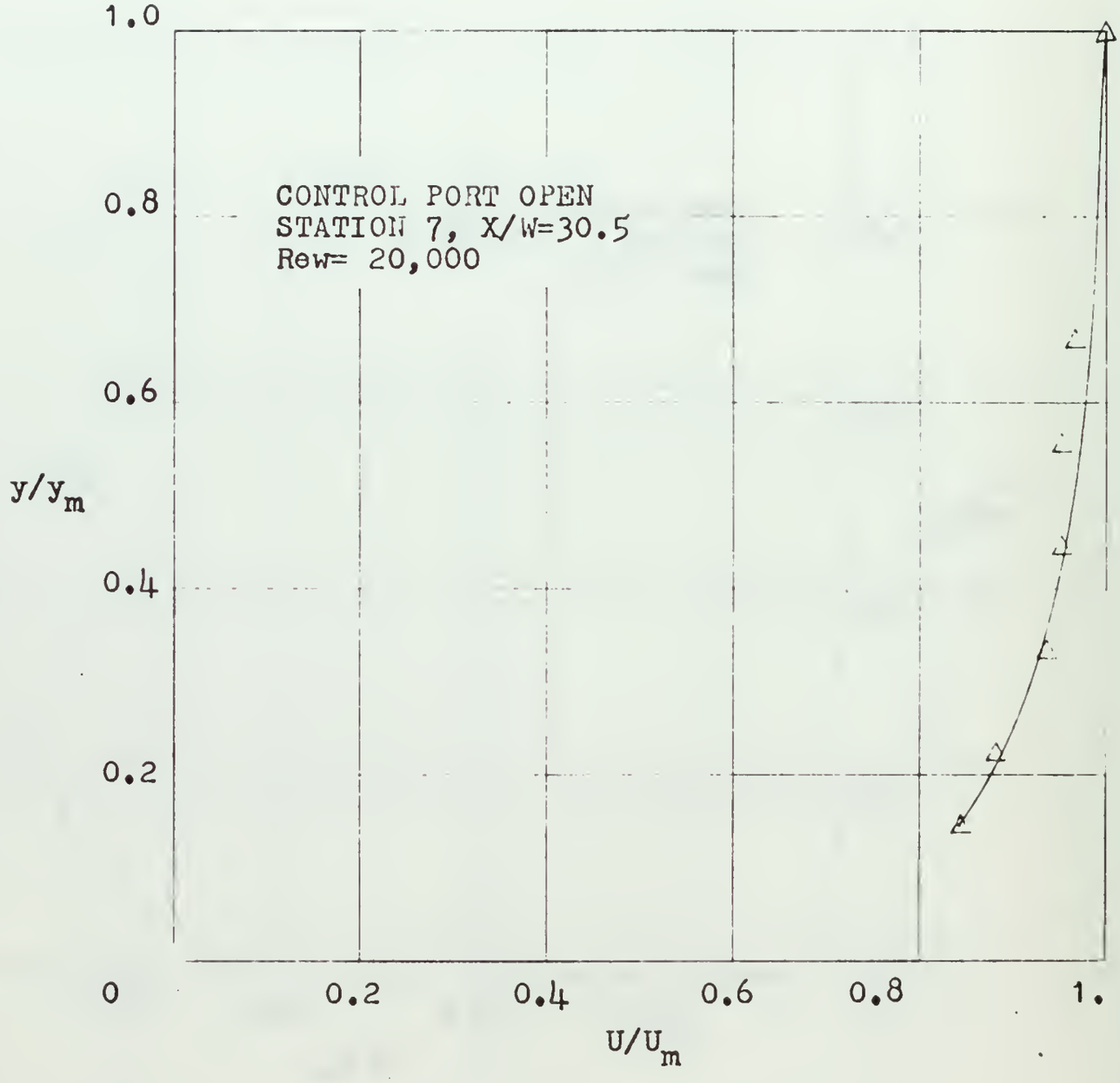

FIGURE 19. NORMALIZED INNER VELOCITY PROFILE

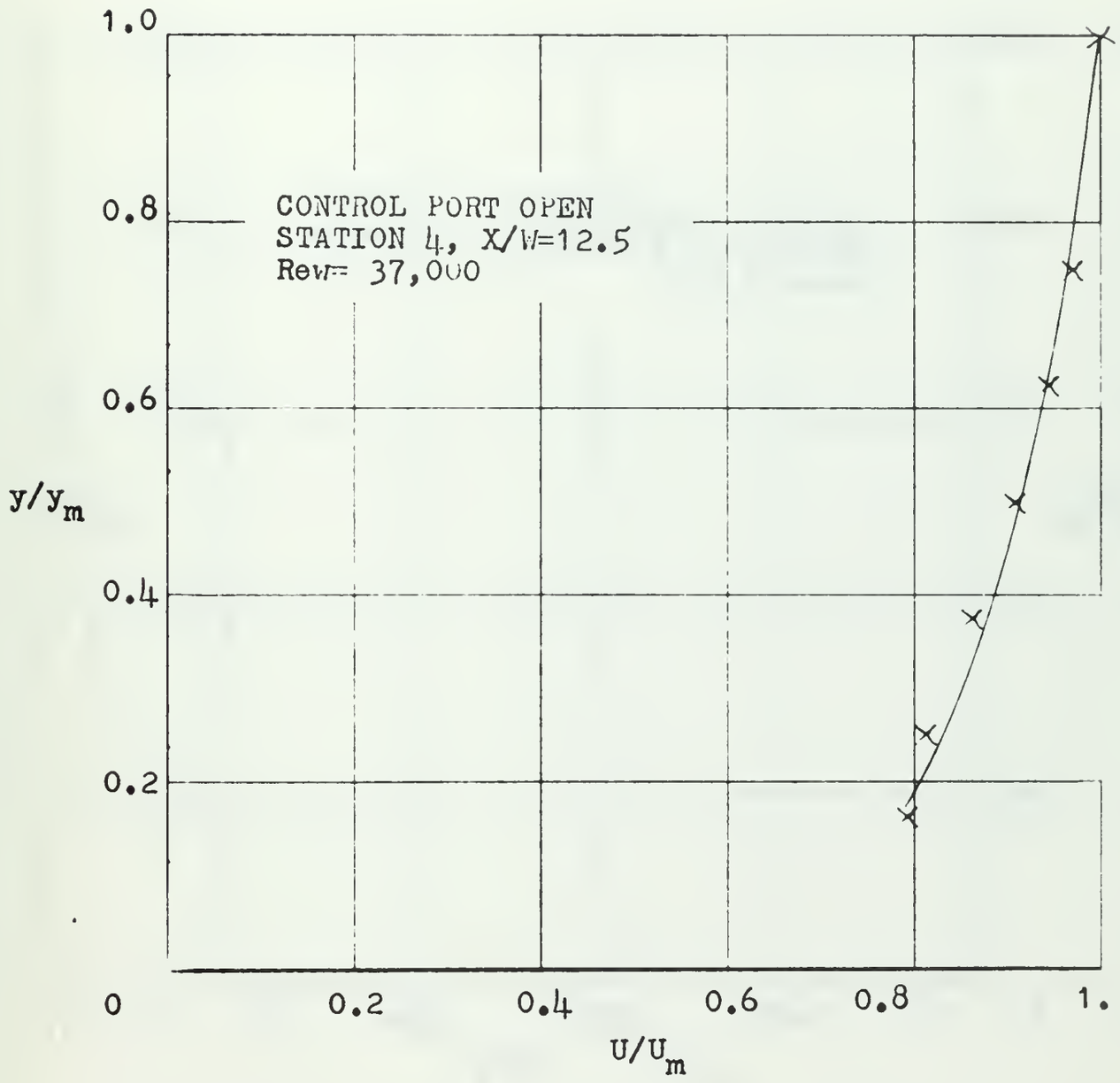

FIGURE 20. NORMALIZED INNER VELOCITY PROFILE

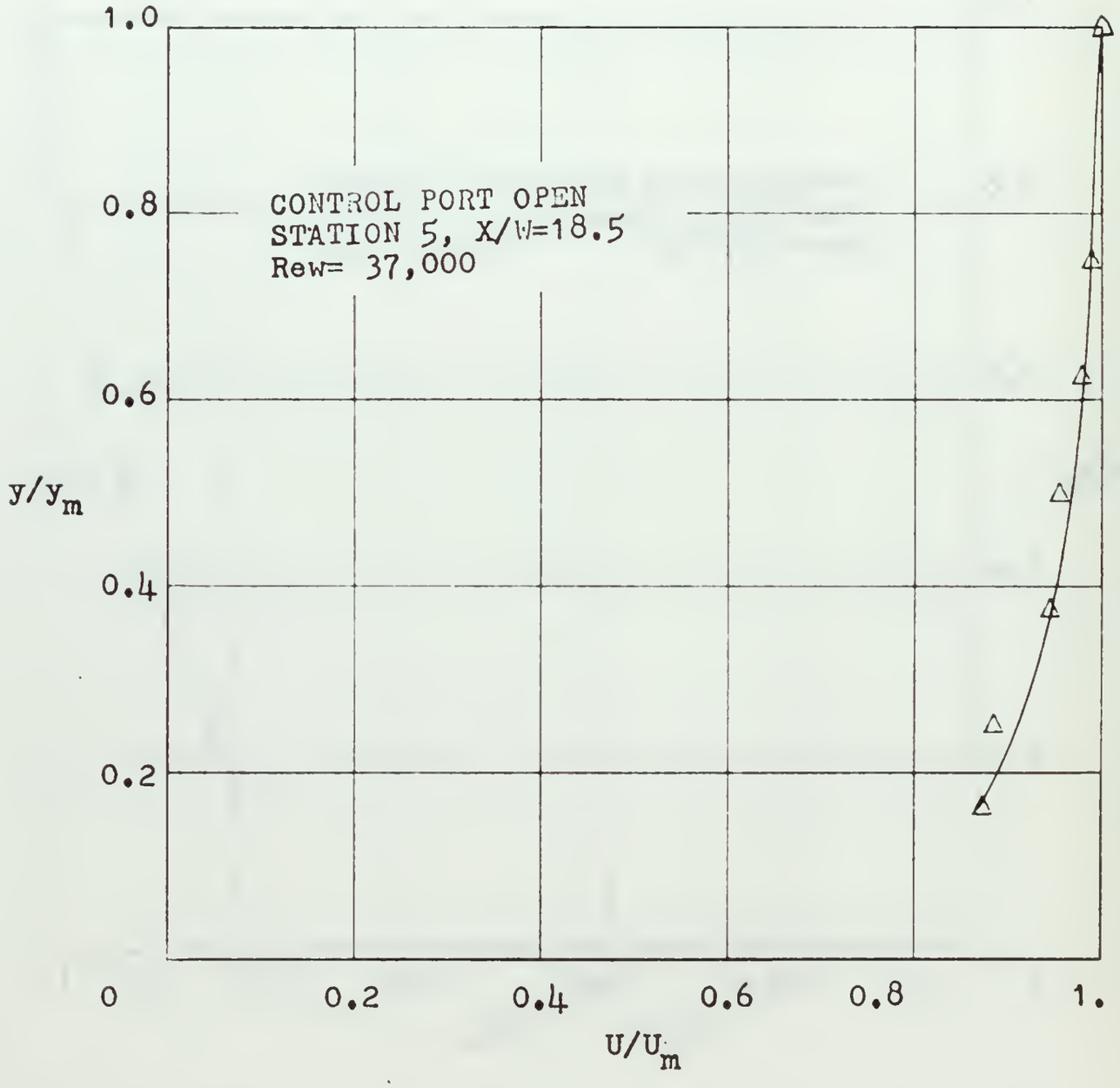

FIGURE 21. NORMALIZED INNER VELOCITY PROFILE

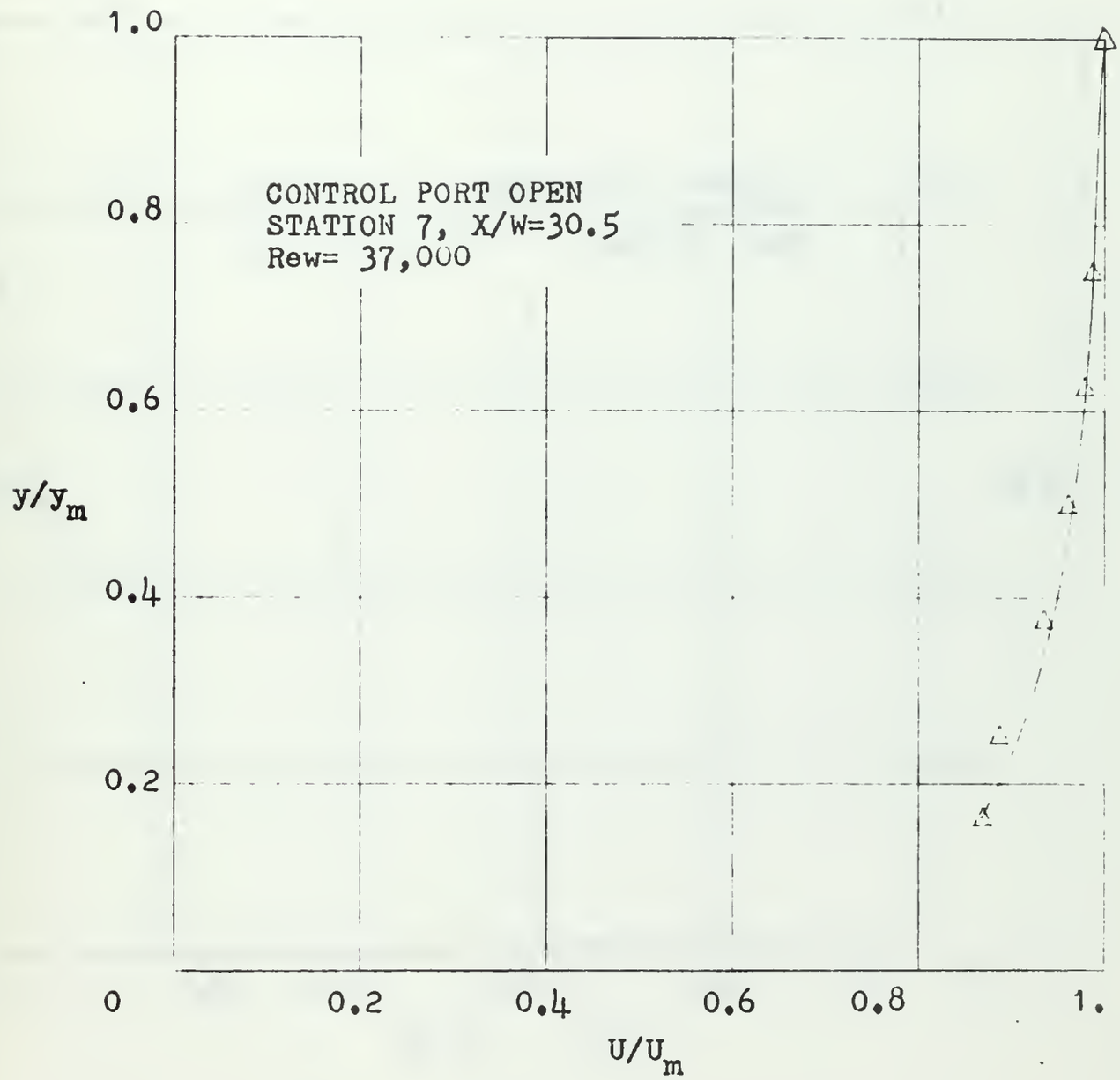

FIGURE 22. NORMALIZED INNER VELOCITY PROFILE

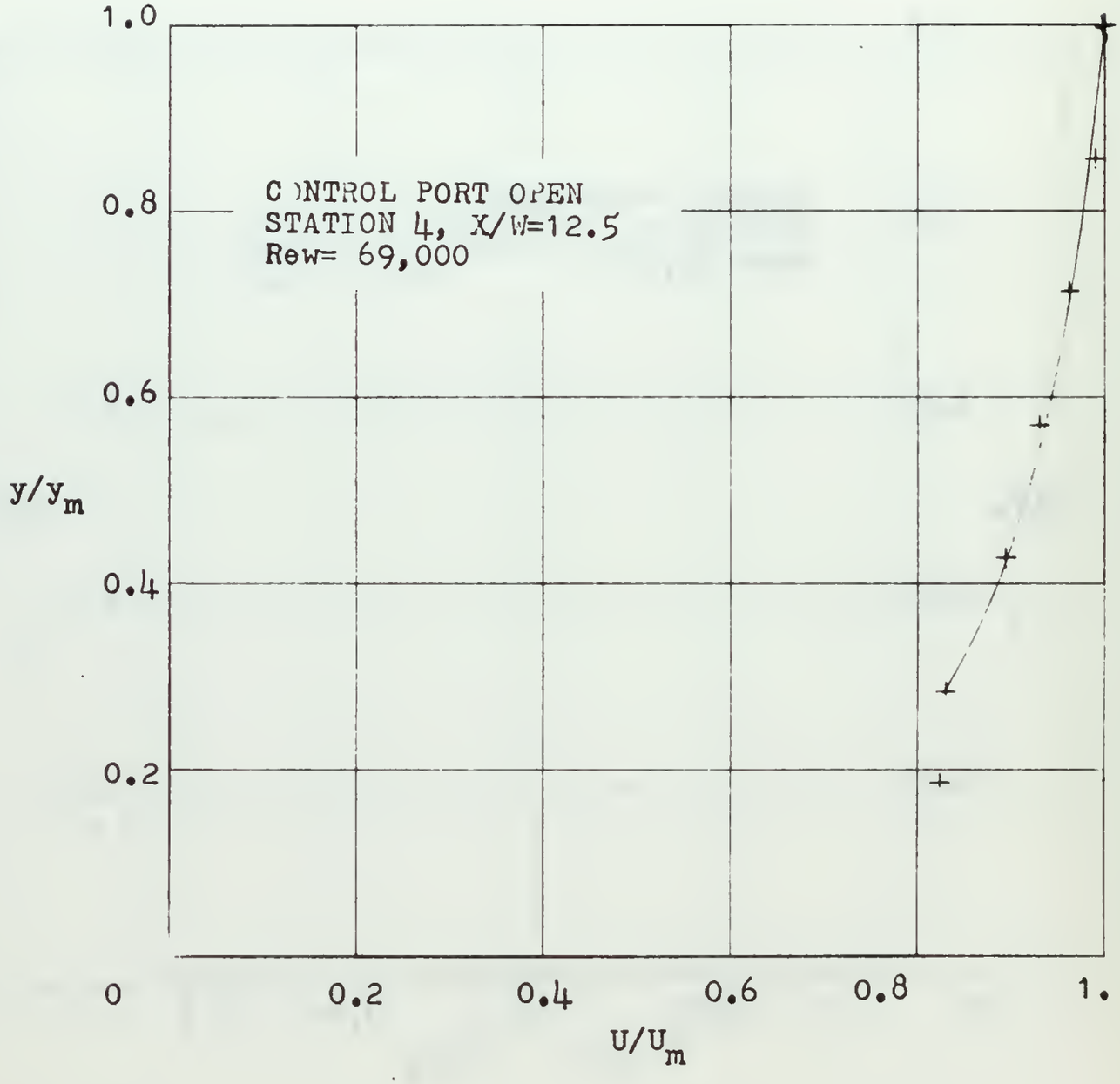

FIGURE 23. NORMALIZED INNER VELOCITY PROFILE

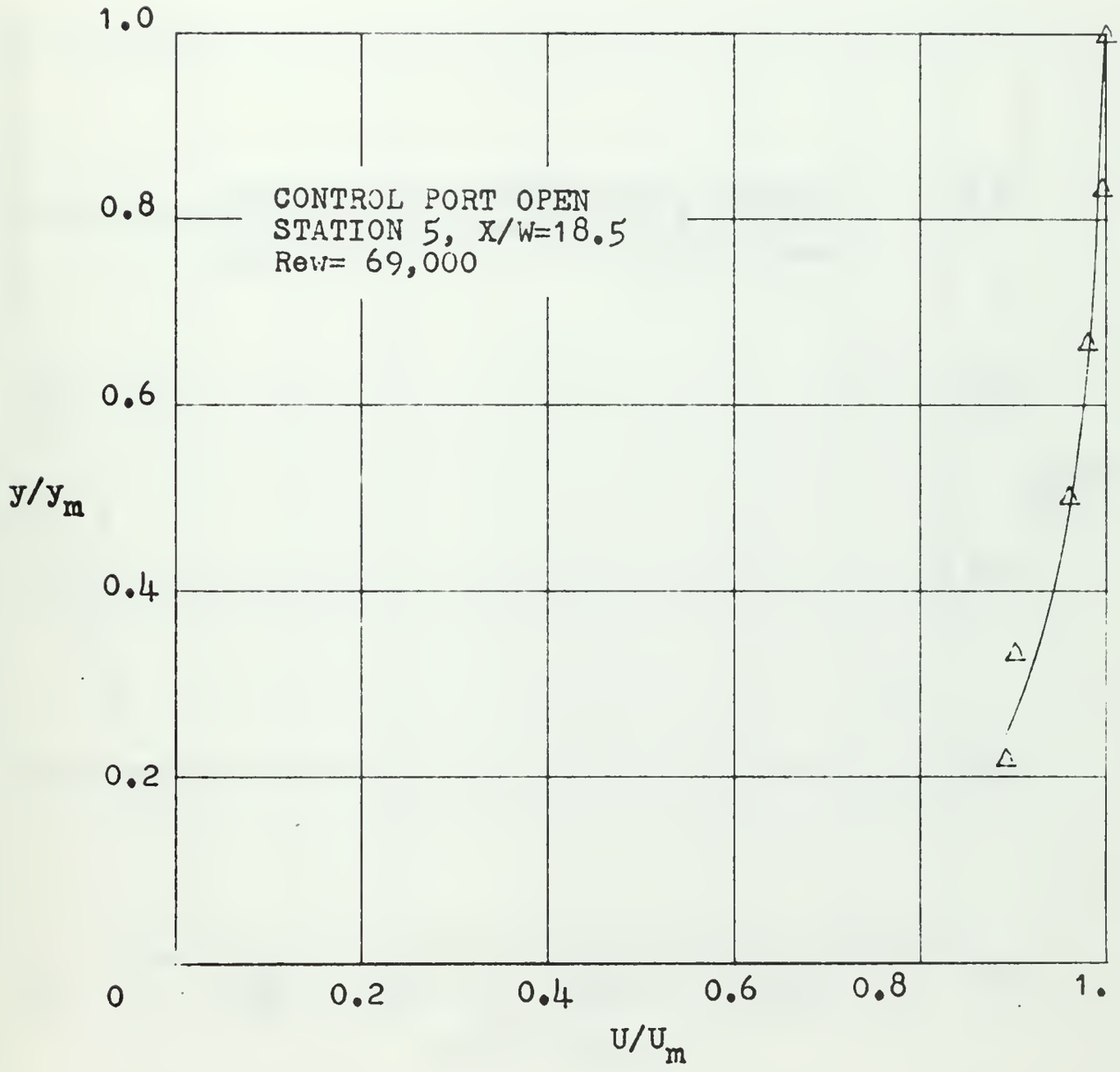

FIGURE 24. NORMALIZED INNER VELOCITY PROFILE

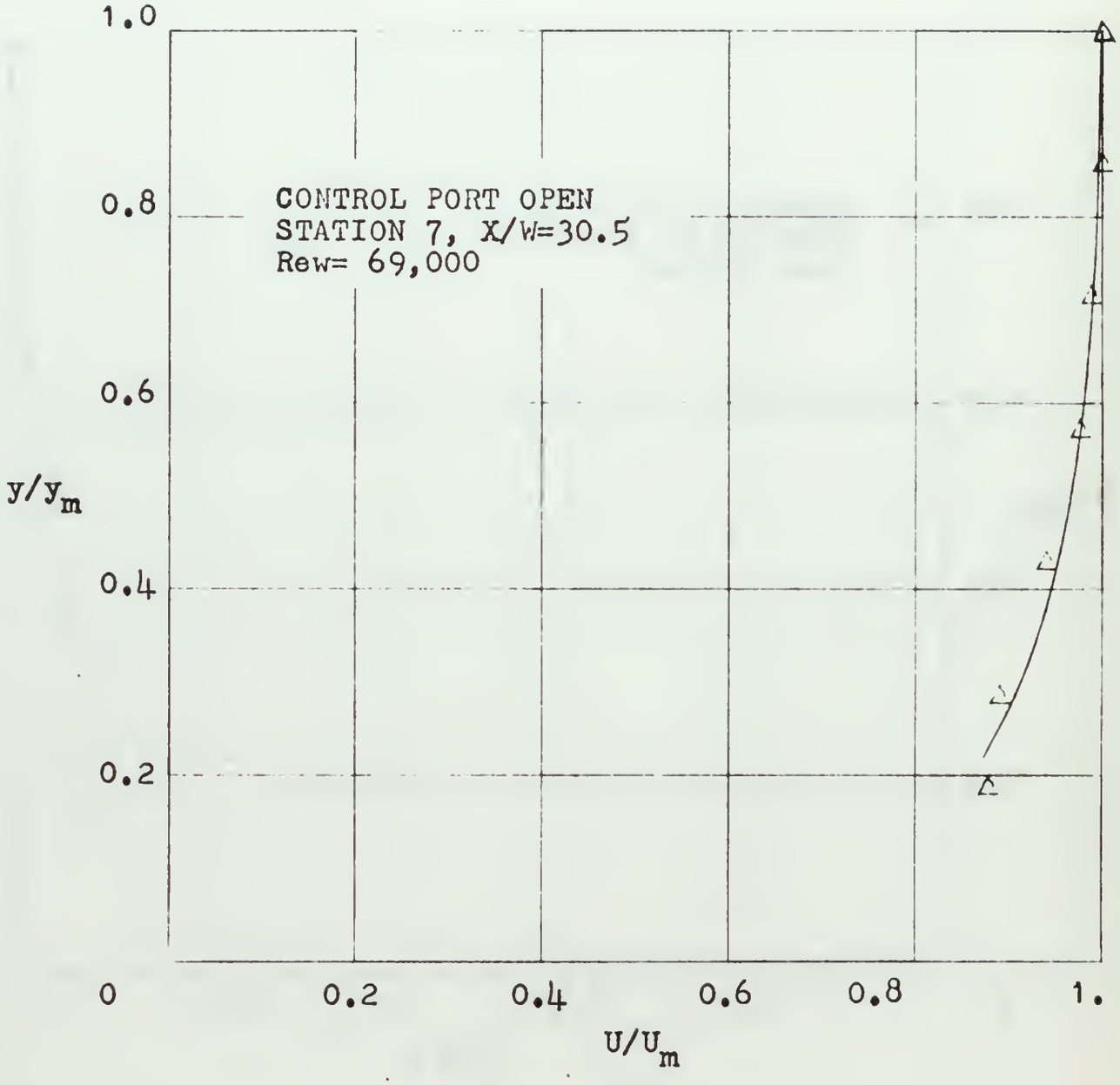

FIGURE 25. NORMALIZED INNER VELOCITY PROFILE

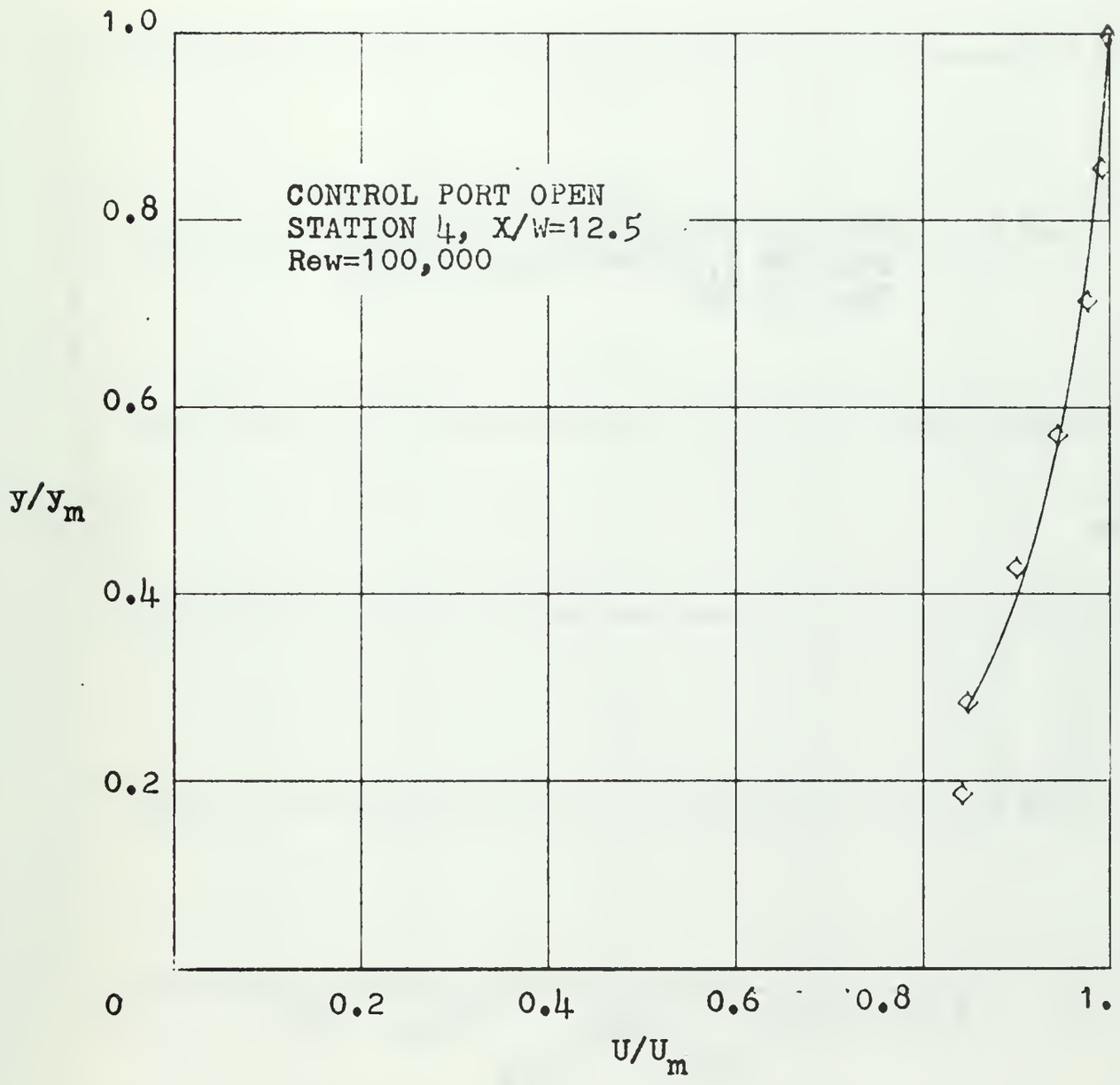

FIGURE 26. NORMALIZED INNER VELOCITY PROFILE

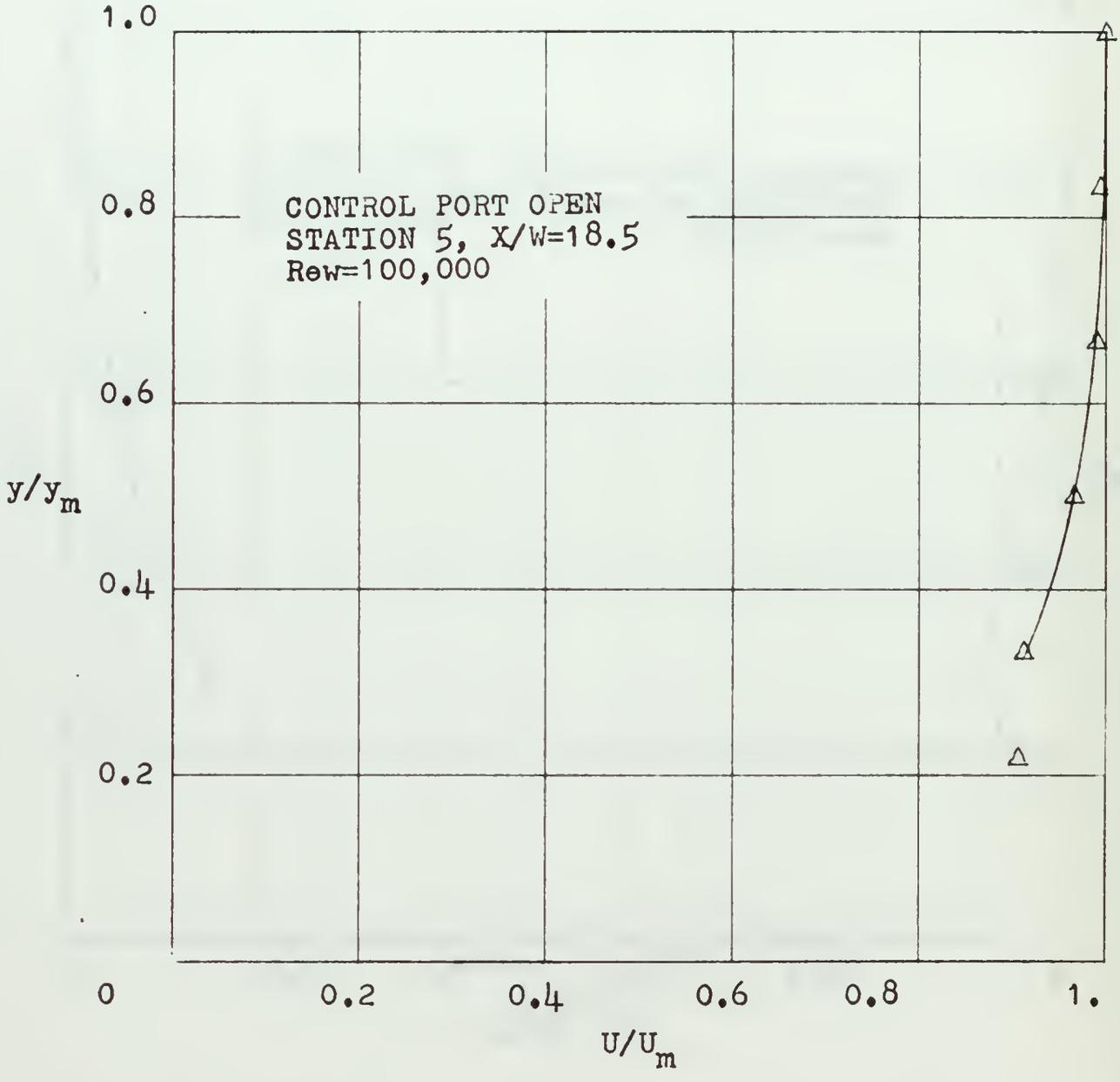

FIGURE 27. NORMALIZED INNER VELOCITY PROFILE

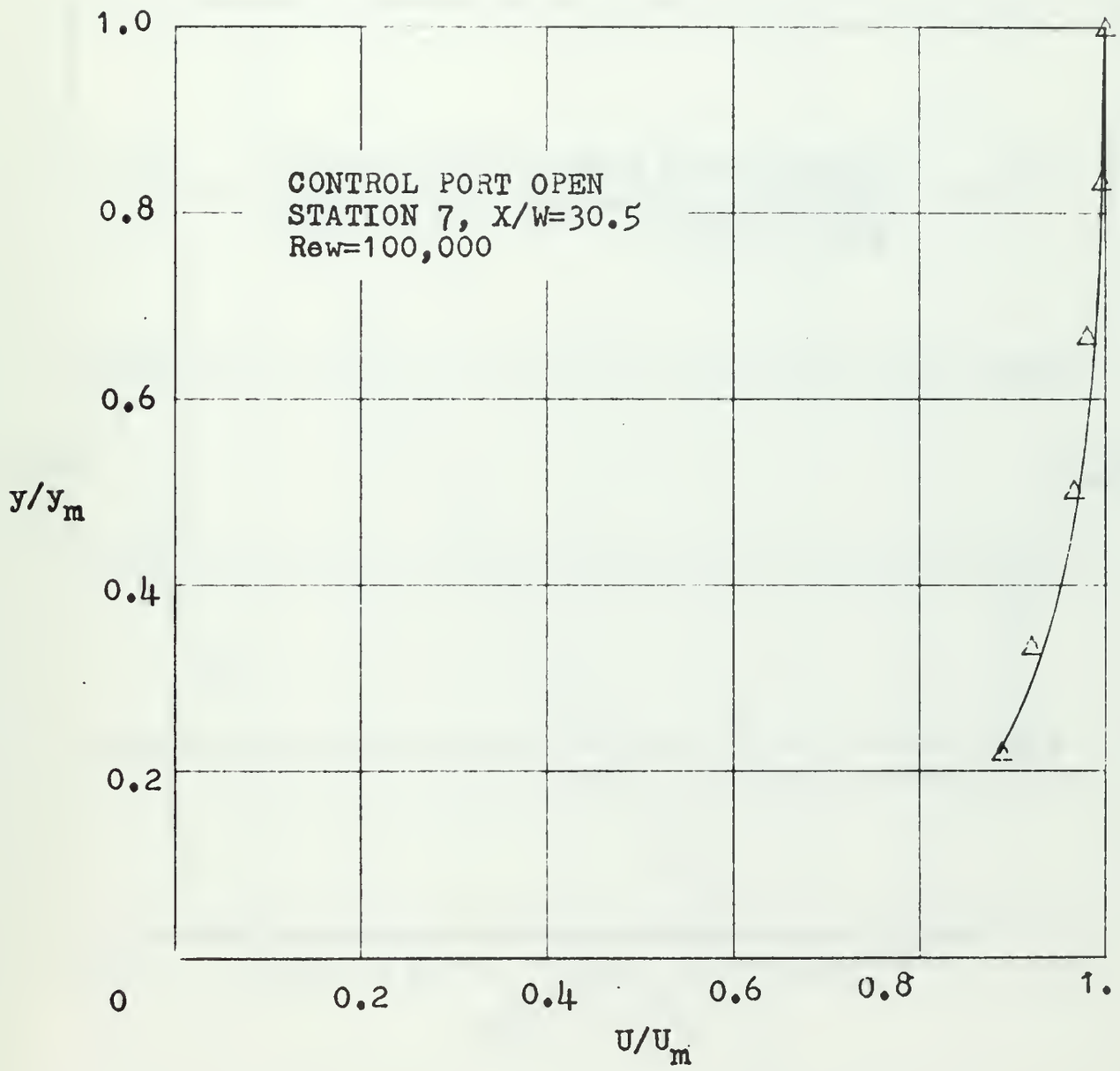

FIGURE 28. NORMALIZED INNER VELOCITY PROFILE

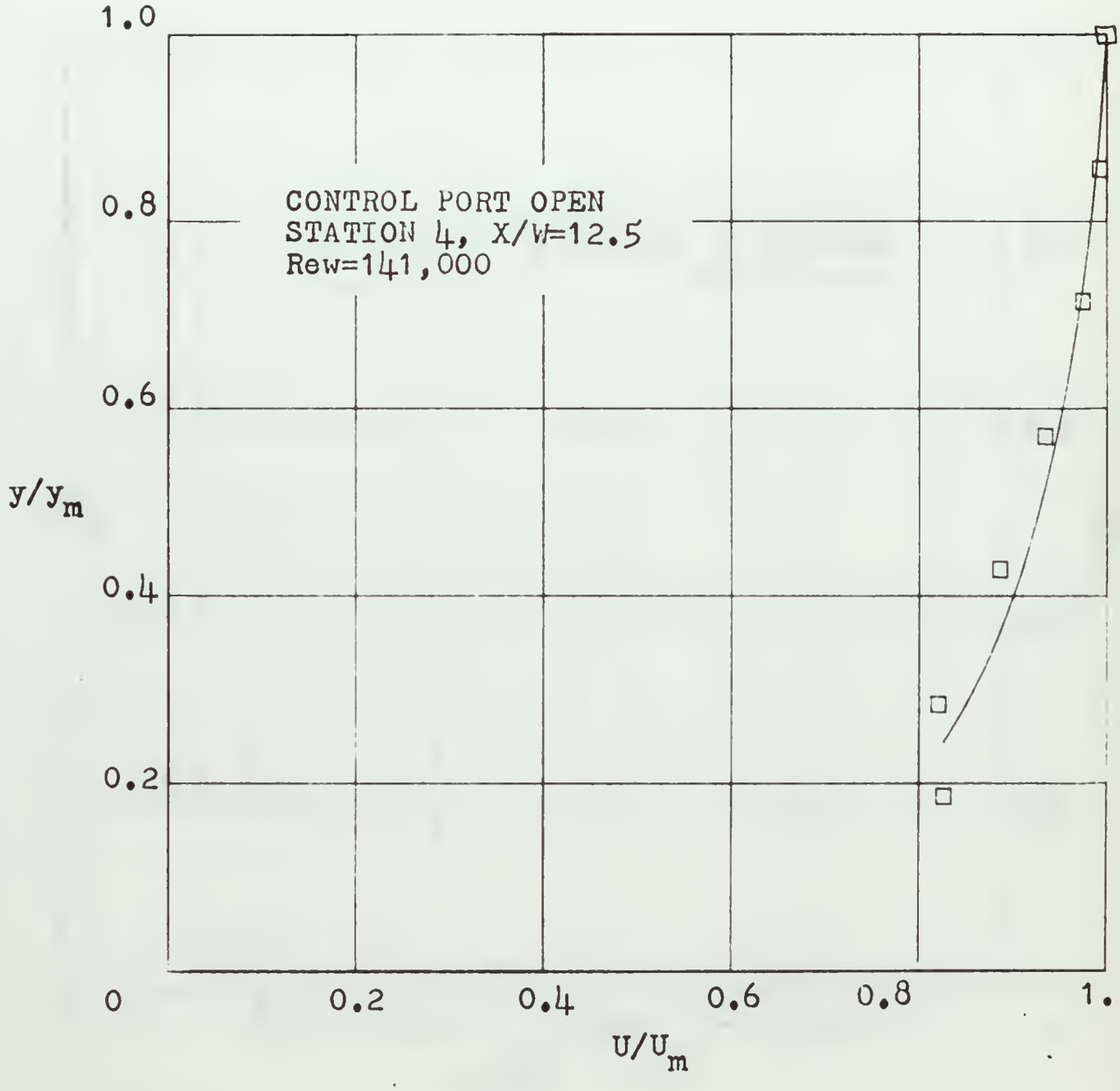

FIGURE 29. NORMALIZED INNER VELOCITY PROFILE

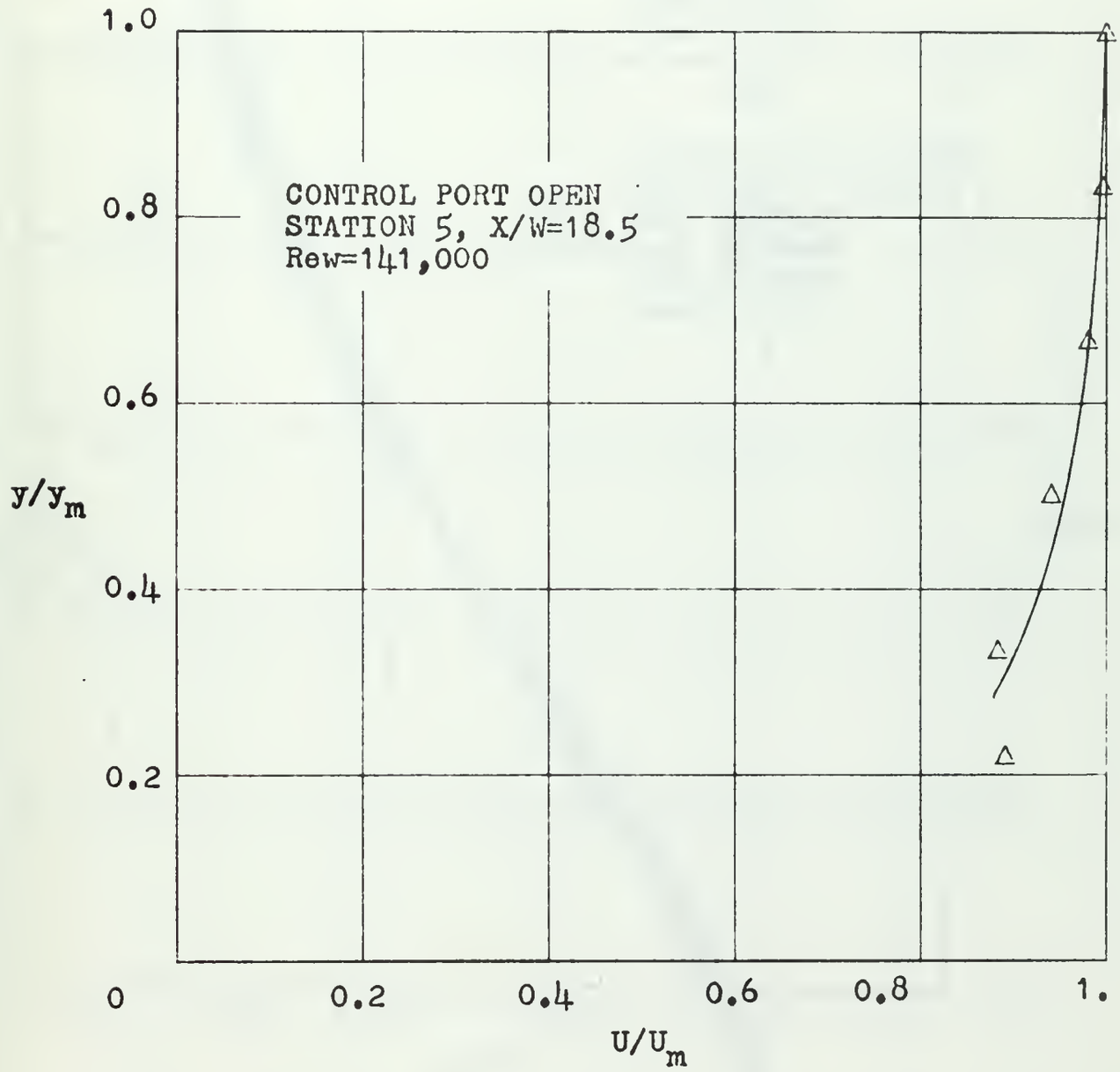

FIGURE 30. NORMALIZED INNER VELOCITY PROFILE

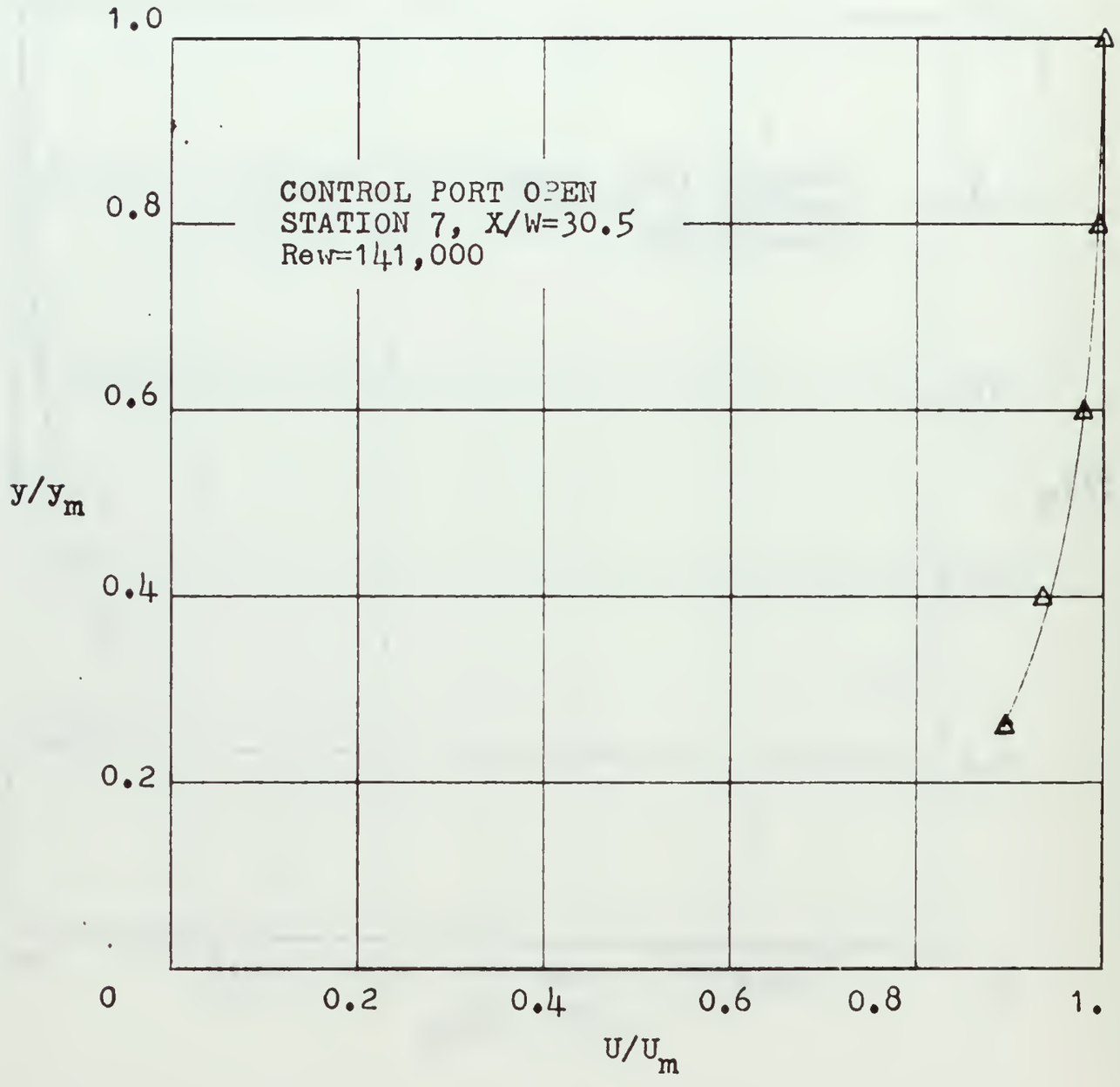

FIGURE 31. NORMALIZED INNER VELOCITY PROFILE

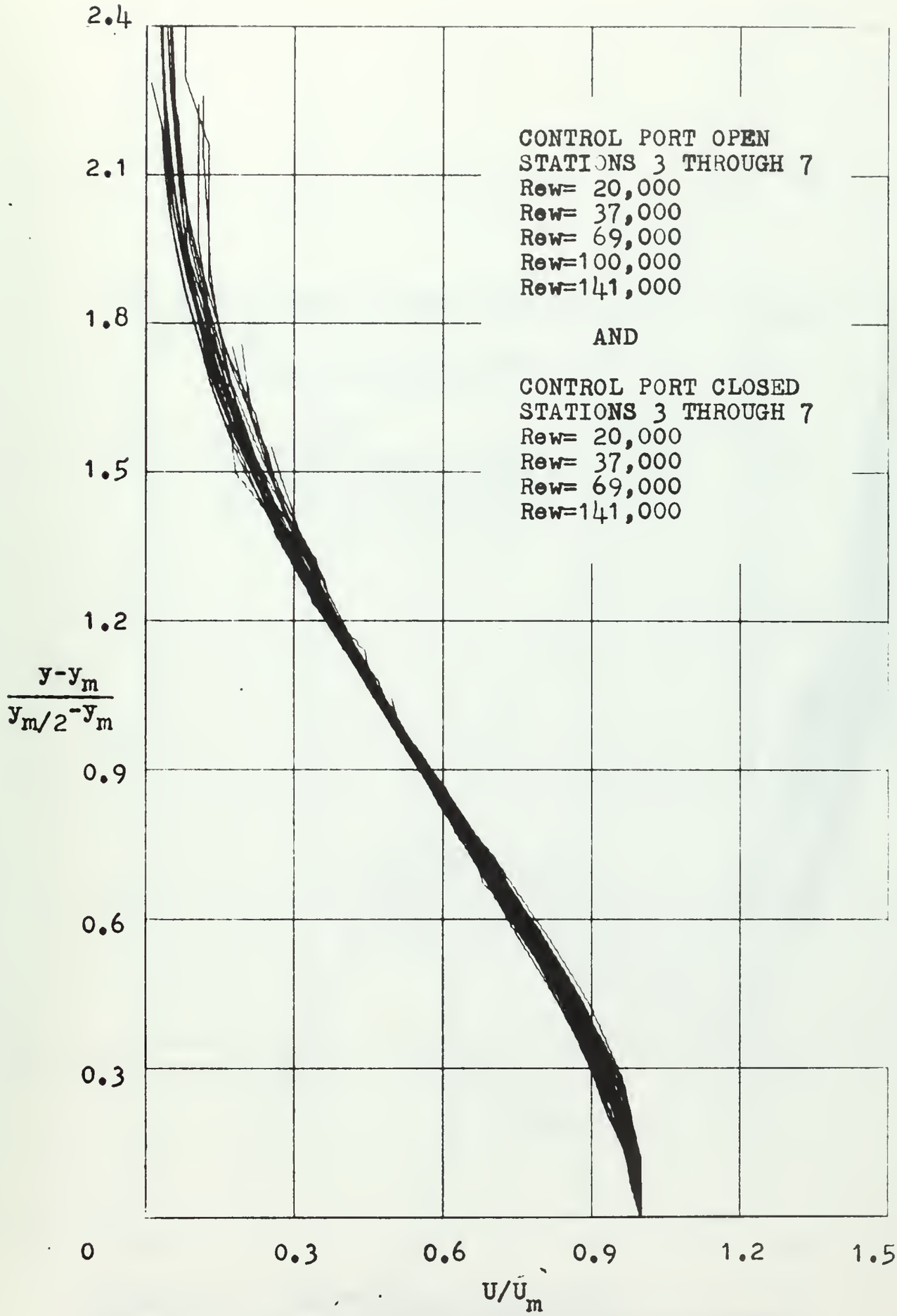

FIGURE 32. NORMALIZED OUTER VELOCITY PROFILES

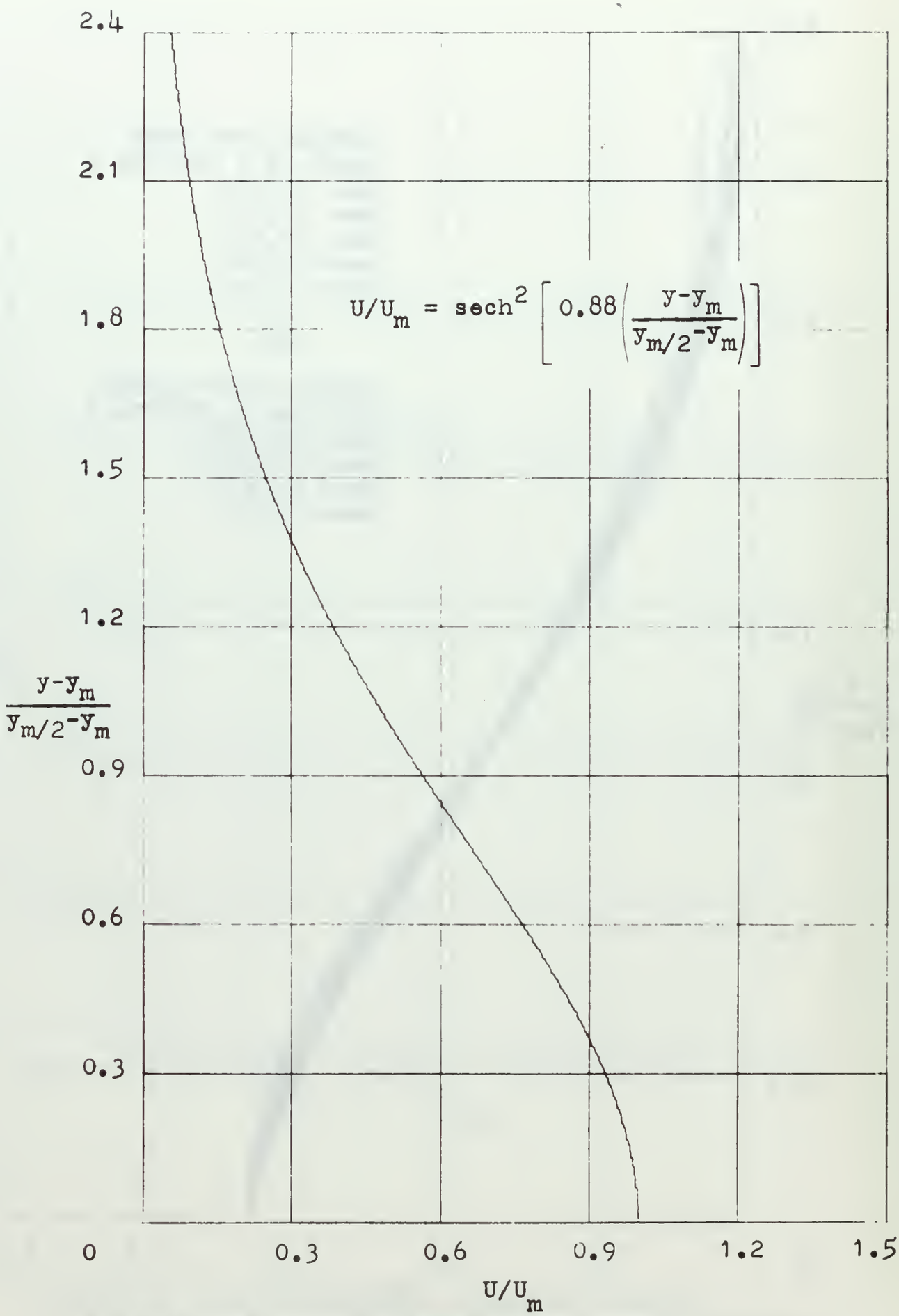

FIGURE 33. PLOT OF EQUATION 24

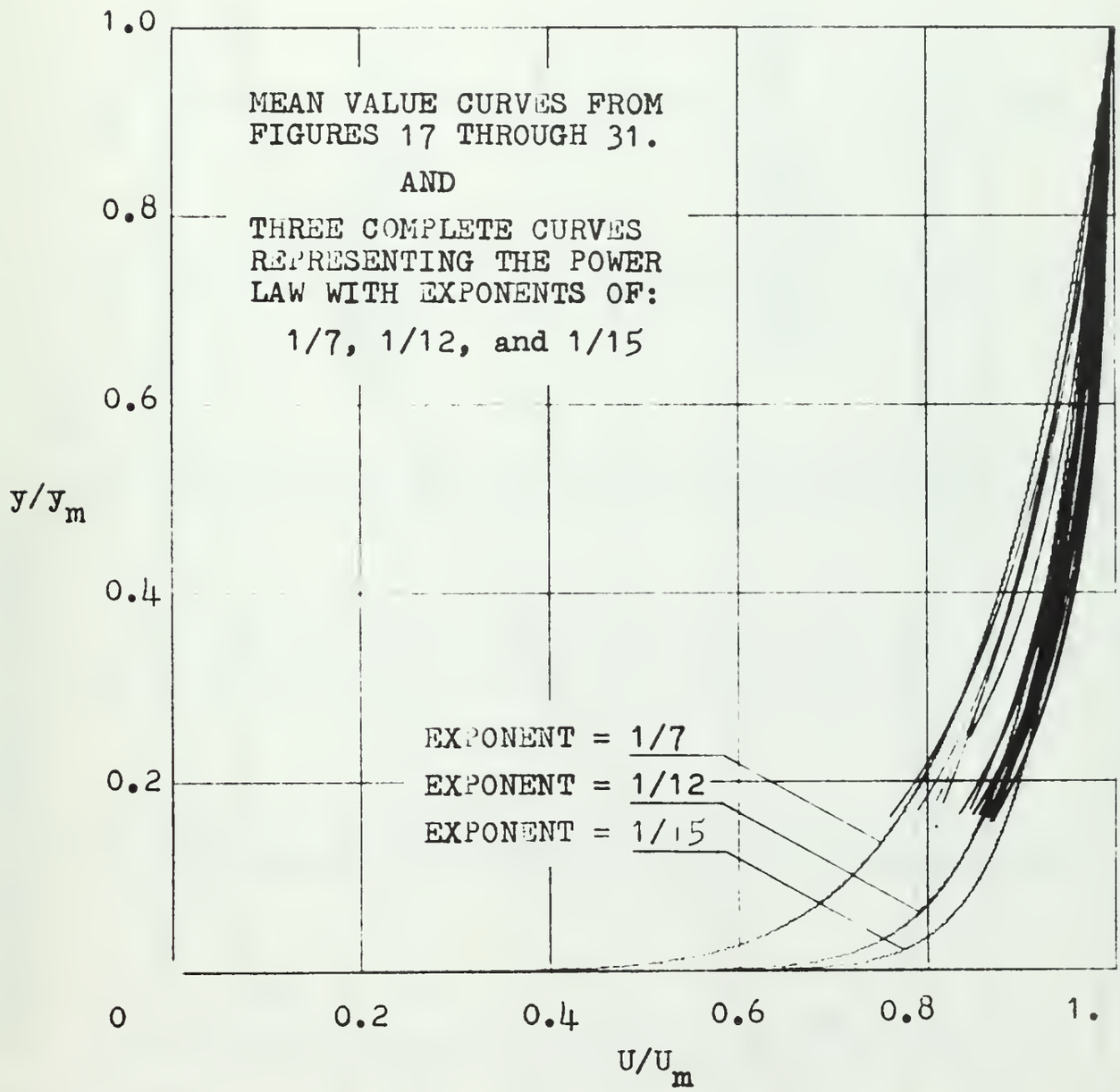

FIGURE 34. INNER VELOCITY PROFILES

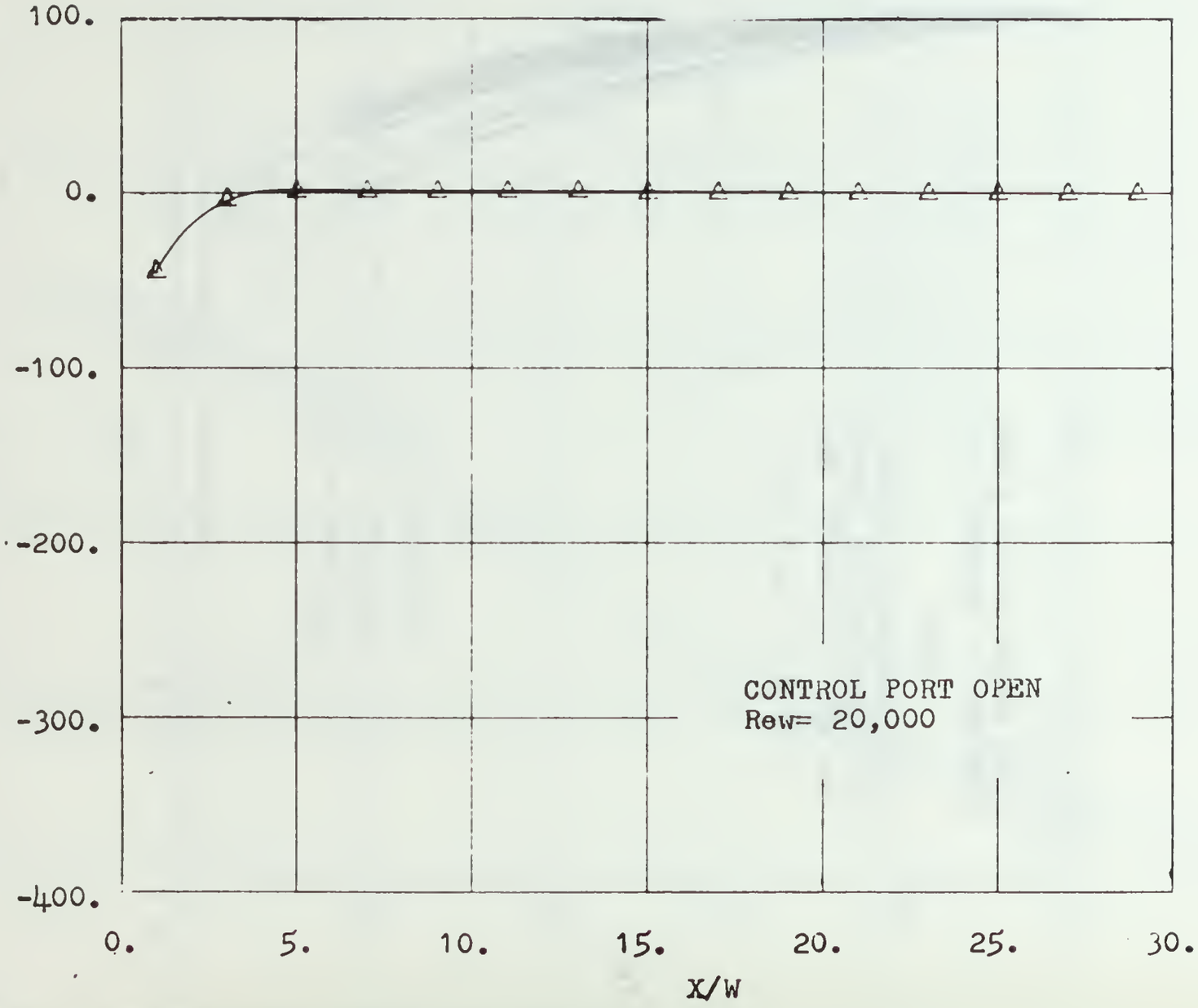

FIGURE 35. NORMALIZED PRESSURE PROFILE

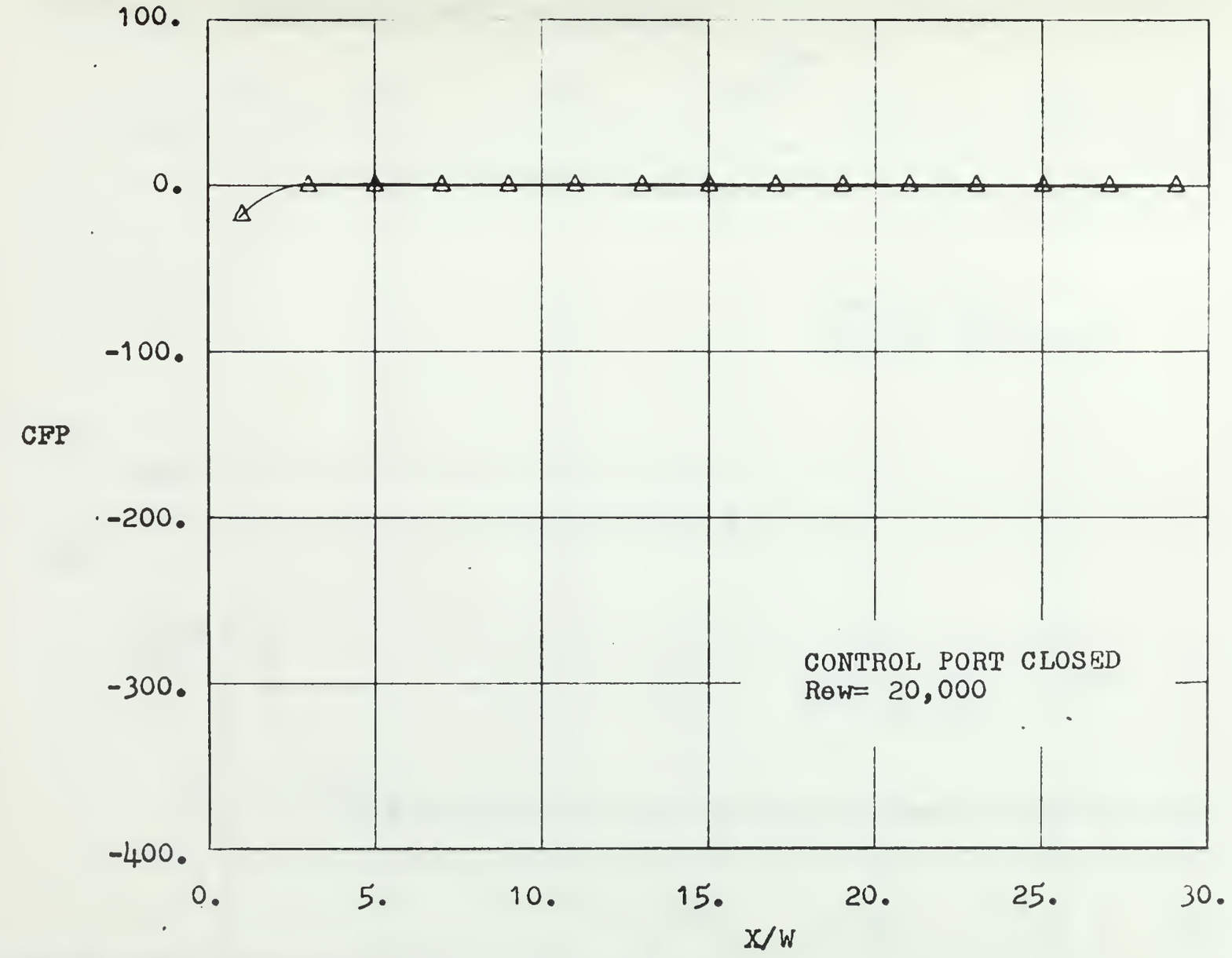

FIGURE 36. NORMALIZED PRESSURE PROFILE

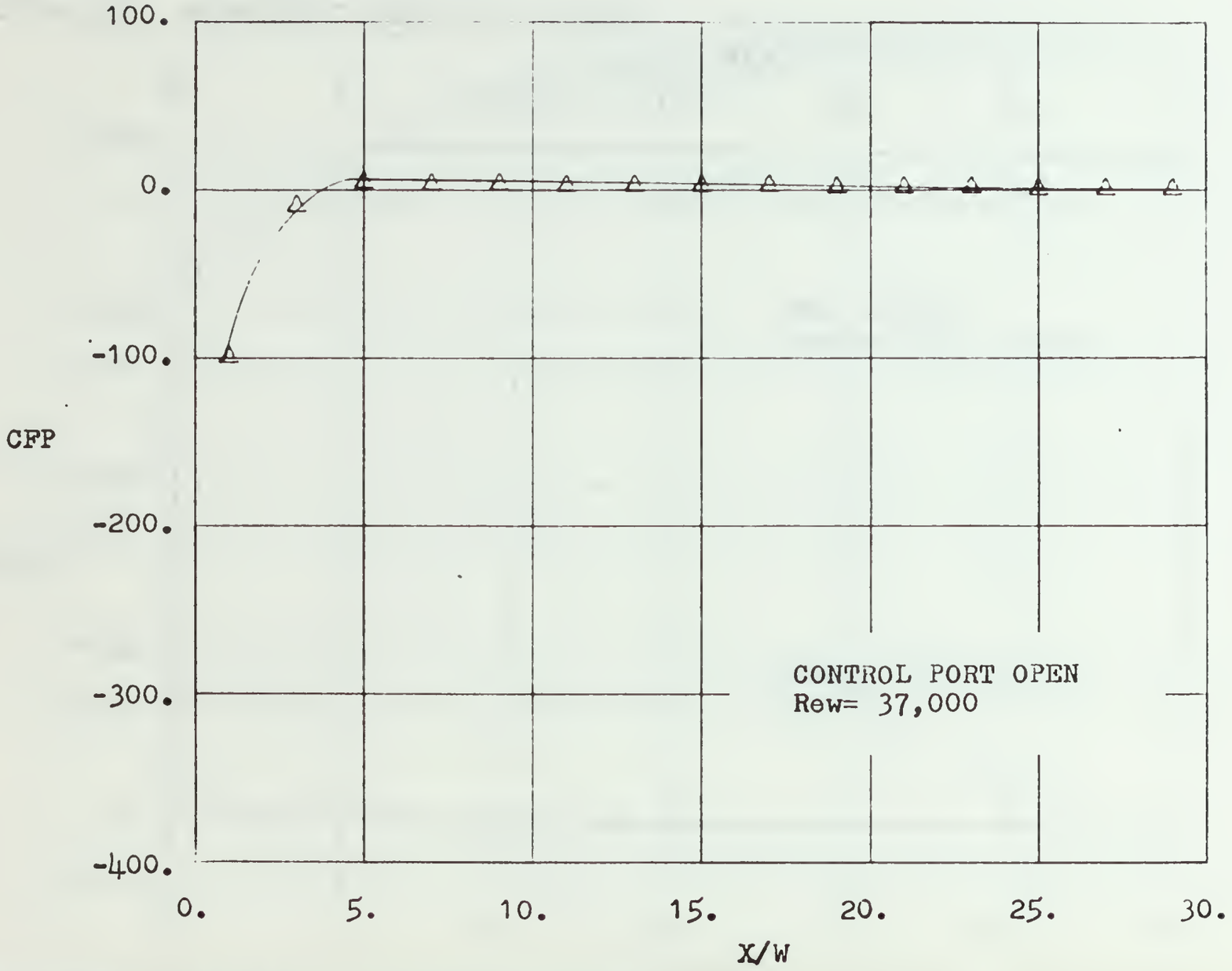

FIGURE 37. NORMALIZED PRESSURE PROFILE

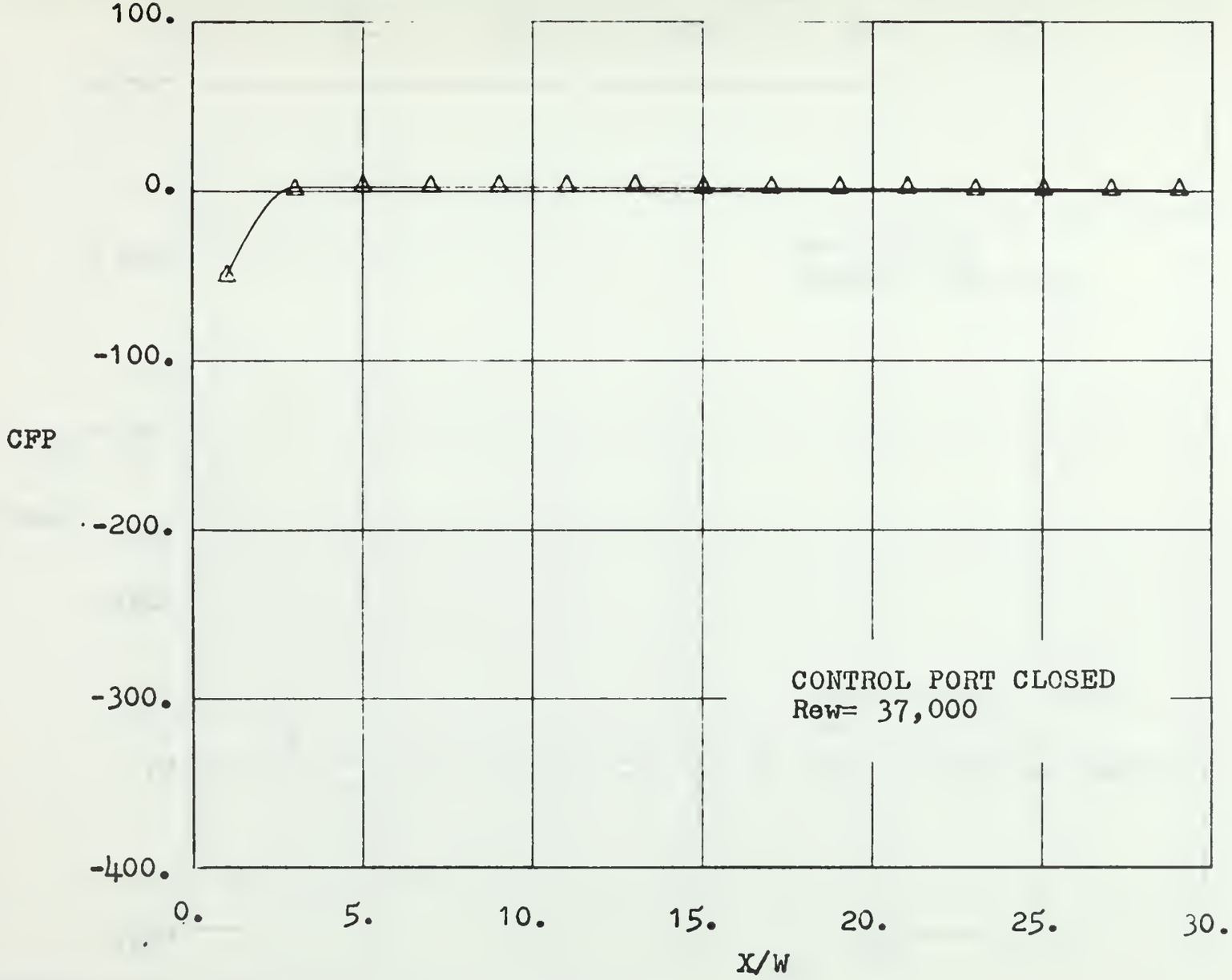

FIGURE 38. NORMALIZED PRESSURE PROFILE

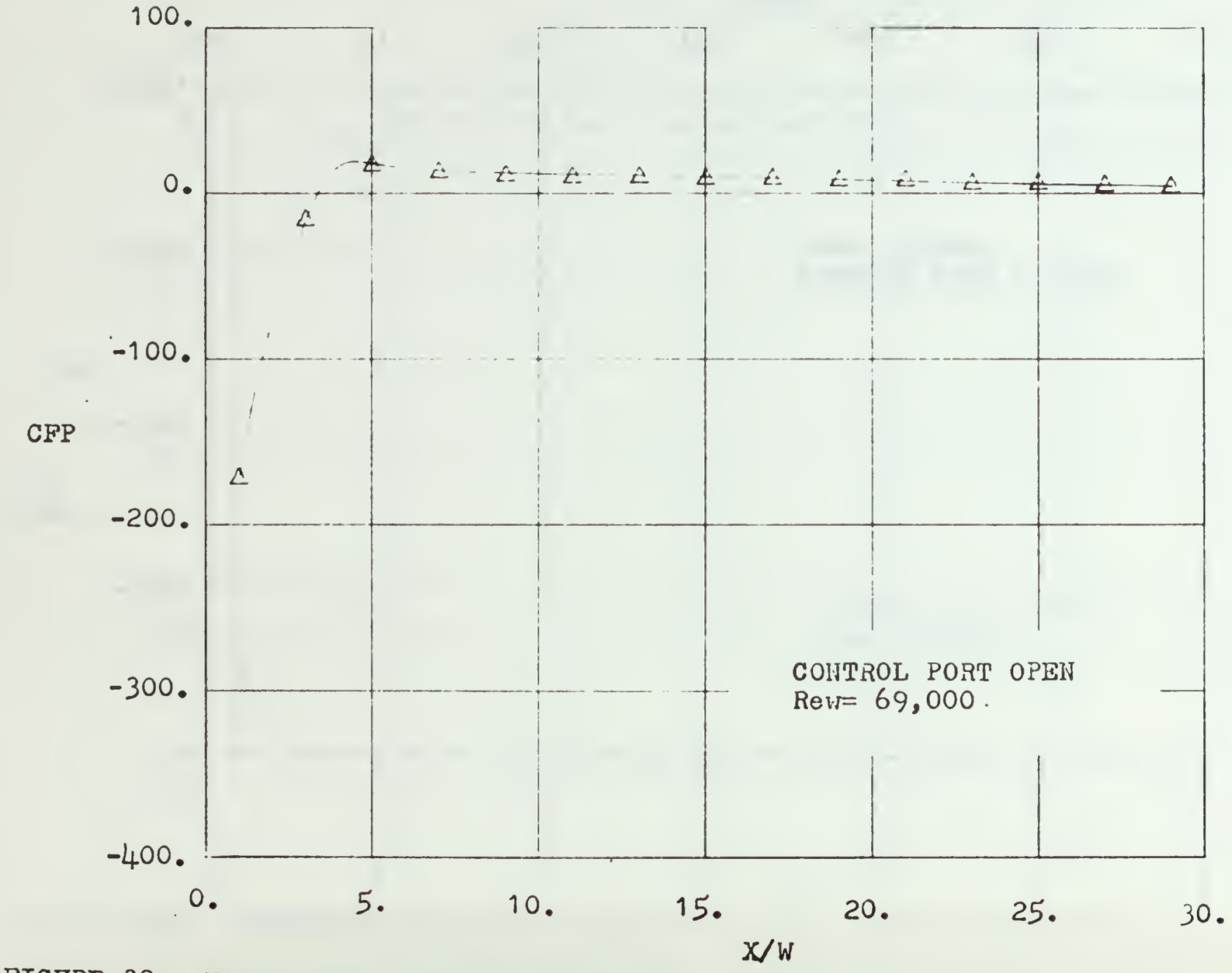

FIGURE 39. NORMALIZED PRESSURE PROFILE

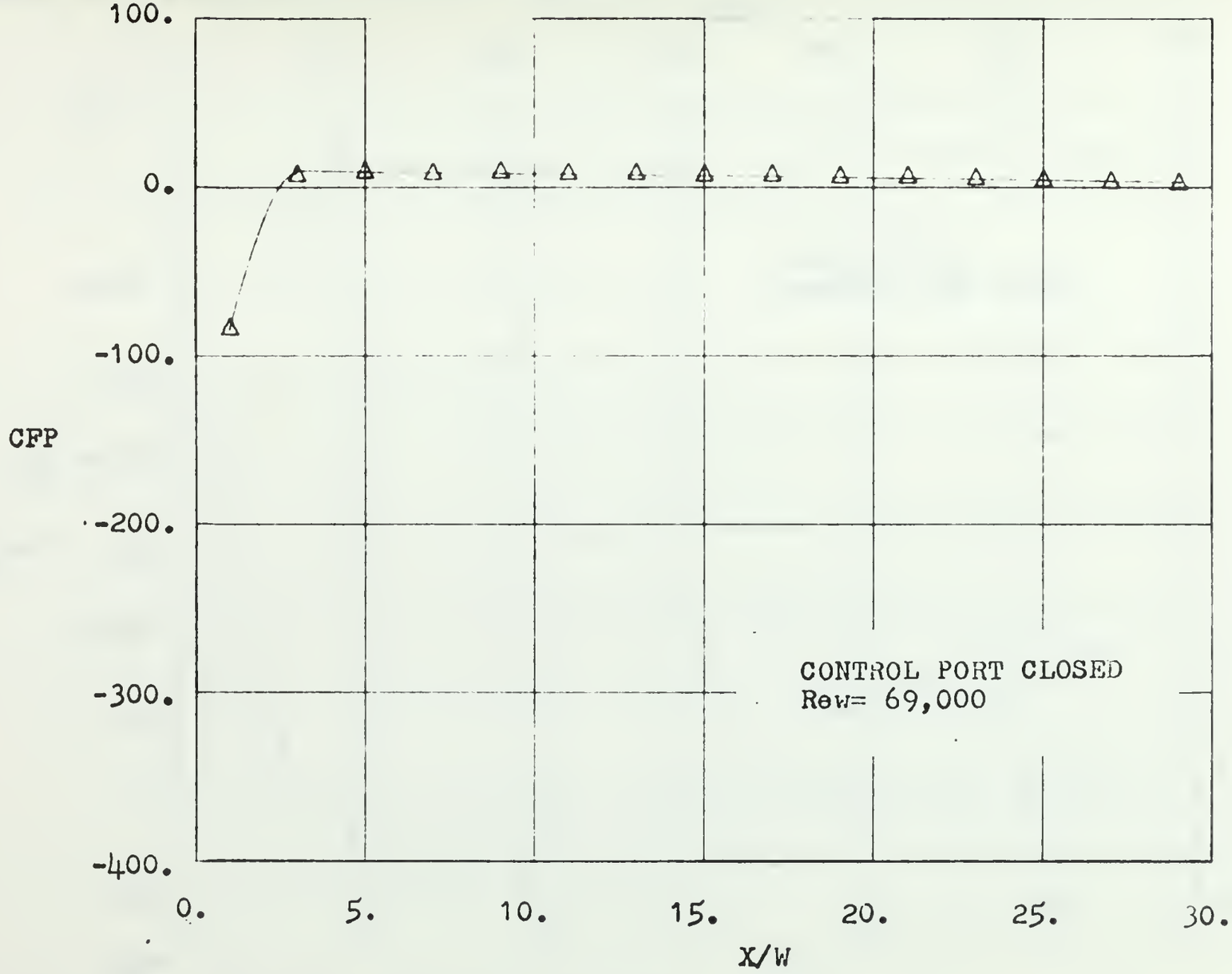

FIGURE 40. NORMALIZED PRESSURE PROFILE

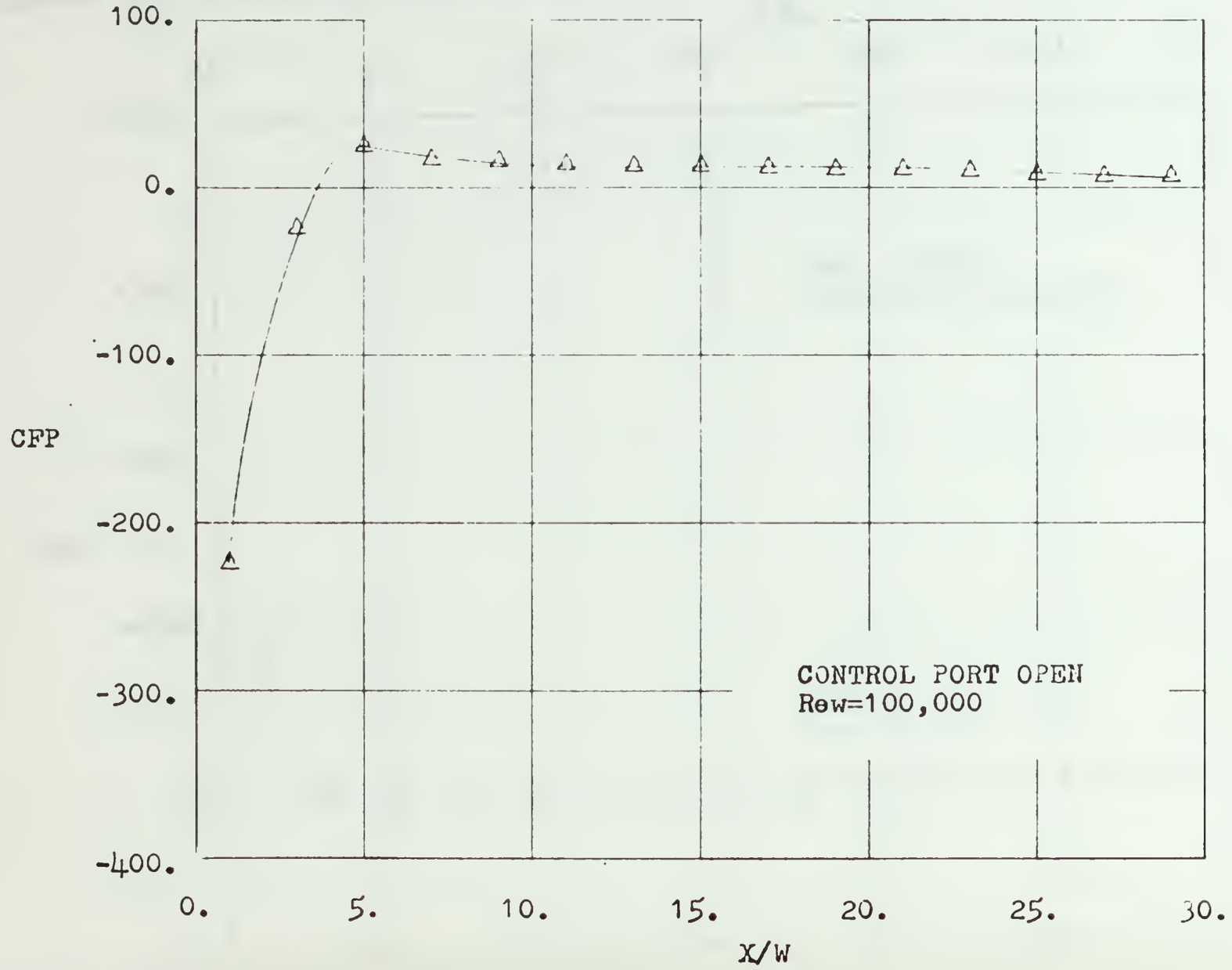

FIGURE 41. NORMALIZED PRESSURE PROFILE

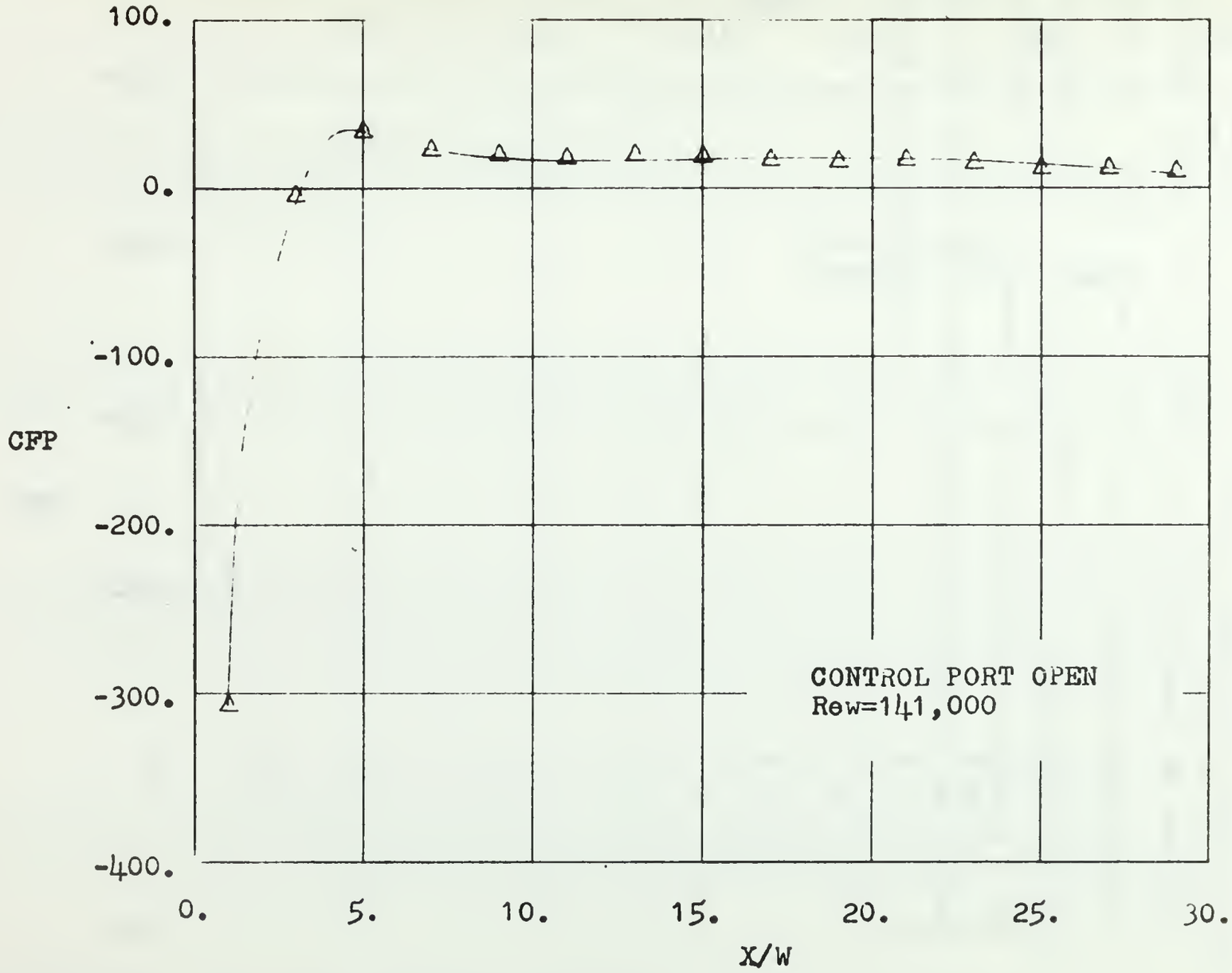

FIGURE 42. NORMALIZED PRESSURE PROFILE

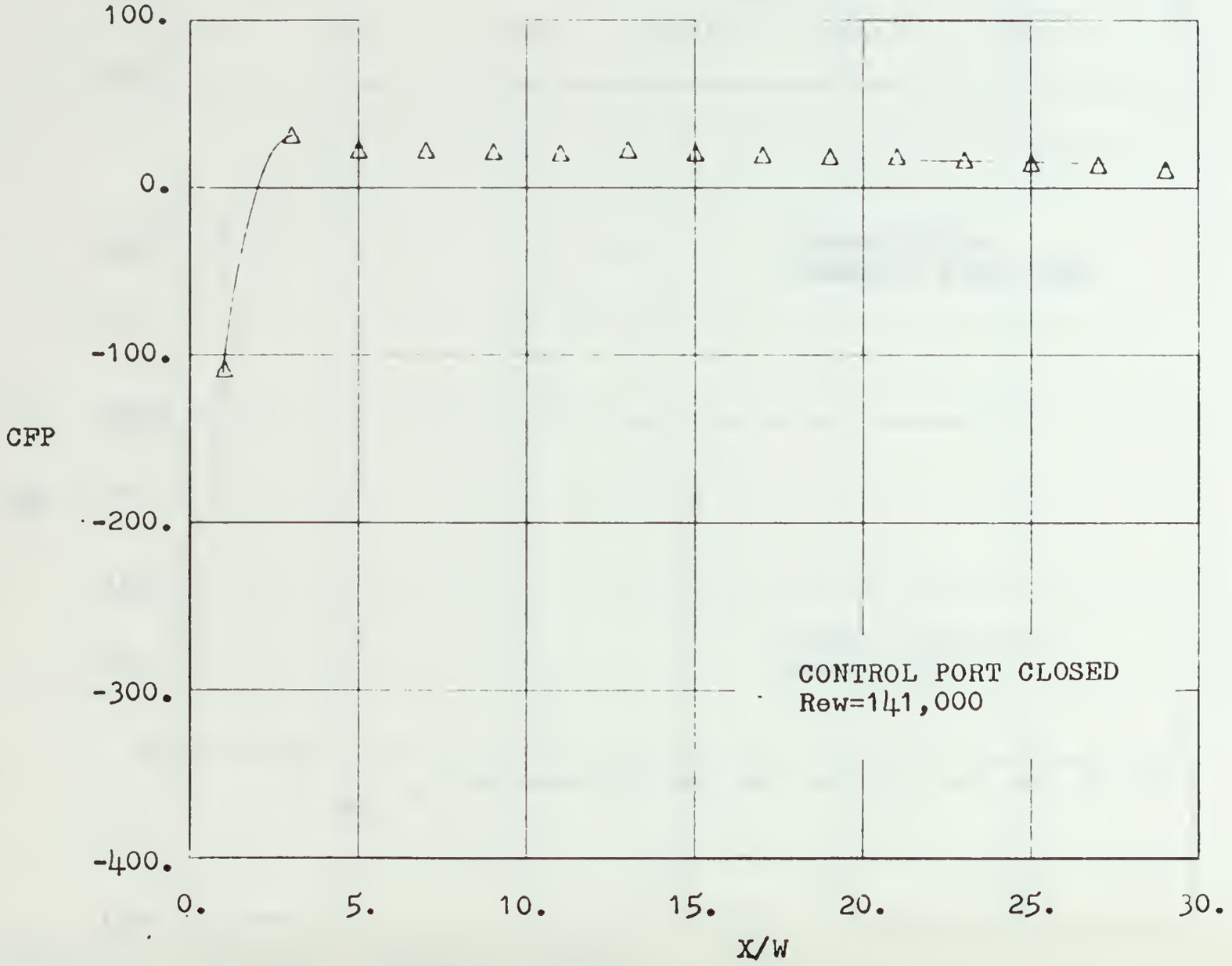

FIGURE 43. NORMALIZED PRESSURE PROFILE

APPENDIX I

Tabulated Data

The following pages contain tabulated data taken during the course of this investigation. The velocity data is indexed with respect to the run number (there is no run number 1) and station number as described previously. The "Y" value is the distance in inches perpendicular to the surface of the flat plate and the "U" value is the local velocity at that point in feet per second. The tabulated data for pressure is indexed with respect to run number, control port condition, and distance from the jet exit in inches.

TABULATED DATA

REYNOLDS NUMBER 20,000 CONTROL PORT OPEN

RUN NO.	STATION NO.	Y	U
2	1	0.03	168.58
2	1	0.05	176.81
2	1	0.07	190.35
2	1	0.10	197.68
2	1	0.12	204.74
2	1	0.15	203.00
2	1	0.17	201.24
2	1	0.20	197.68
2	1	0.22	188.48
2	1	0.25	174.79
2	1	0.27	147.21
2	1	0.30	75.39
2	1	0.32	11.92
2	1	0.13	195.87
2	2	0.03	116.19
2	2	0.05	143.54
2	2	0.07	153.12
2	2	0.10	164.31
2	2	0.12	180.78
2	2	0.15	186.58
2	2	0.17	195.87
2	2	0.20	195.87
2	2	0.22	192.21
2	2	0.25	184.67
2	2	0.27	172.74
2	2	0.30	153.12
2	2	0.32	125.02
2	2	0.35	96.11
2	2	0.37	67.43
2	2	0.40	63.08
2	2	0.42	26.65
2	2	0.45	20.65
2	2	0.47	18.85
2	2	0.50	16.86
2	2	0.52	16.86
2	2	0.55	14.60
2	2	0.57	14.60
2	2	0.60	14.60
2	2	0.62	14.60
2	2	0.65	14.60
2	3	0.03	102.54
2	3	0.05	113.09
2	3	0.07	130.58
2	3	0.10	148.41
2	3	0.12	166.46
2	3	0.15	176.81
2	3	0.17	184.67
2	3	0.20	186.58
2	3	0.22	180.78
2	3	0.25	170.67
2	3	0.27	159.93
2	3	0.30	145.99
2	3	0.32	130.58
2	3	0.35	116.19
2	3	0.37	99.73
2	3	0.40	84.29
2	3	0.42	71.52
2	3	0.45	58.40
2	3	0.47	47.68
2	3	0.50	41.29

TABULATED DATA

REYNOLDS NUMBER 20,000 CONTROL PORT OPEN

RUN NO.	STATION NO.	Y	U
2	3	0.52	29.20
2	3	0.55	23.84
2	3	0.57	23.84
2	3	0.60	23.84
2	3	0.62	14.60
2	3	0.65	14.60
2	4	0.03	119.20
2	4	0.05	125.02
2	4	0.07	134.60
2	4	0.10	141.04
2	4	0.12	147.21
2	4	0.15	153.12
2	4	0.17	155.42
2	4	0.20	156.56
2	4	0.22	155.42
2	4	0.25	153.12
2	4	0.27	145.99
2	4	0.30	141.04
2	4	0.32	131.93
2	4	0.35	122.15
2	4	0.37	113.09
2	4	0.40	103.92
2	4	0.42	92.33
2	4	0.45	84.29
2	4	0.47	75.39
2	4	0.50	66.37
2	4	0.52	58.40
2	4	0.55	50.57
2	4	0.57	42.98
2	4	0.60	35.76
2	4	0.62	29.20
2	4	0.65	23.84
2	4	0.67	20.65
2	4	0.70	18.85
2	4	0.72	16.86
2	4	0.75	16.86
2	4	0.77	16.86
2	4	0.80	16.86
2	4	0.82	16.86
2	5	0.03	113.09
2	5	0.05	119.20
2	5	0.07	125.02
2	5	0.10	130.58
2	5	0.12	131.93
2	5	0.15	133.27
2	5	0.17	135.91
2	5	0.20	135.91
2	5	0.22	133.27
2	5	0.25	131.93
2	5	0.27	130.58
2	5	0.30	125.02
2	5	0.32	122.15
2	5	0.35	116.19
2	5	0.37	113.09
2	5	0.40	106.62
2	5	0.42	99.73
2	5	0.45	93.86
2	5	0.47	87.60
2	5	0.50	82.59
2	5	0.52	75.39

TABULATED DATA

REYNOLDS NUMBER 20,000 CONTROL PORT OPEN

RUN NO.	STATION NO.	Y	U
2	5	0.55	69.51
2	5	0.57	64.19
2	5	0.60	59.60
2	5	0.62	54.63
2	5	0.65	49.15
2	5	0.67	44.60
2	5	0.70	39.54
2	5	0.72	35.76
2	5	0.75	33.72
2	5	0.77	29.20
2	5	0.80	27.96
2	5	0.82	26.65
2	6	0.03	103.23
2	6	0.05	106.62
2	6	0.07	109.90
2	6	0.10	114.65
2	6	0.12	116.19
2	6	0.15	119.20
2	6	0.17	119.20
2	6	0.20	119.20
2	6	0.22	119.20
2	6	0.25	116.19
2	6	0.27	114.65
2	6	0.30	113.09
2	6	0.32	109.90
2	6	0.35	107.94
2	6	0.37	105.28
2	6	0.40	101.85
2	6	0.42	98.30
2	6	0.45	93.86
2	6	0.47	90.78
2	6	0.50	85.96
2	6	0.52	82.59
2	6	0.55	79.07
2	6	0.57	73.48
2	6	0.60	69.51
2	6	0.62	67.43
2	6	0.65	60.78
2	6	0.67	58.40
2	6	0.70	55.91
2	6	0.72	50.57
2	6	0.75	47.68
2	6	0.77	42.98
2	6	0.80	41.29
2	6	0.82	37.70
2	7	0.03	88.40
2	7	0.05	92.33
2	7	0.07	97.94
2	7	0.10	99.73
2	7	0.12	99.73
2	7	0.15	101.15
2	7	0.17	103.92
2	7	0.20	103.92
2	7	0.22	104.60
2	7	0.25	103.92
2	7	0.27	103.92
2	7	0.30	102.54
2	7	0.32	101.15
2	7	0.35	99.73
2	7	0.37	98.30

TABULATED DATA

REYNOLDS NUMBER 20,000 CONTROL PORT OPEN

RUN NO.	STATION NO.	Y	U
2	7	0.40	96.84
2	7	0.42	93.86
2	7	0.45	92.33
2	7	0.47	89.20
2	7	0.50	87.60
2	7	0.52	84.29
2	7	0.55	81.72
2	7	0.57	79.07
2	7	0.60	75.39
2	7	0.62	73.48
2	7	0.65	69.51
2	7	0.67	66.37
2	7	0.70	63.08
2	7	0.72	59.60
2	7	0.75	55.91
2	7	0.77	53.31
2	7	0.80	51.96
2	7	0.82	49.15
2	7	0.85	46.17
2	7	0.87	42.98
2	7	0.90	41.29
2	7	0.92	37.70
2	7	0.95	35.76

TABULATED DATA

REYNOLDS NUMBER 20,000 CONTROL PORT CLOSED

RUN NO.	STATION NO.	Y	U
3	1	0.03	164.31
3	1	0.05	172.74
3	1	0.07	184.67
3	1	0.10	190.35
3	1	0.12	192.21
3	1	0.15	192.21
3	1	0.17	188.48
3	1	0.20	180.78
3	1	0.22	172.74
3	1	0.25	148.41
3	1	0.27	106.62
3	1	0.30	41.29
3	1	0.32	11.92
3	1	0.13	197.68
3	2	0.03	130.58
3	2	0.05	143.54
3	2	0.07	170.67
3	2	0.10	180.78
3	2	0.12	186.58
3	2	0.15	188.48
3	2	0.17	186.58
3	2	0.20	180.78
3	2	0.22	174.79
3	2	0.25	159.93
3	2	0.27	135.91
3	2	0.30	110.55
3	2	0.32	85.13
3	2	0.35	60.78
3	2	0.37	41.29
3	2	0.40	26.65
3	2	0.42	22.30
3	2	0.45	20.65
3	2	0.47	20.65
3	2	0.50	20.65
3	2	0.52	20.65
3	2	0.55	20.65
3	2	0.57	20.65
3	2	0.60	20.65
3	3	0.03	141.04
3	3	0.05	150.78
3	3	0.07	154.28
3	3	0.10	168.58
3	3	0.12	176.81
3	3	0.15	180.78
3	3	0.17	180.78
3	3	0.20	174.79
3	3	0.22	164.31
3	3	0.25	153.12
3	3	0.27	139.78
3	3	0.30	126.43
3	3	0.32	111.82
3	3	0.35	96.84
3	3	0.37	82.59
3	3	0.40	69.51
3	3	0.42	58.40
3	3	0.45	47.68
3	3	0.47	37.70
3	3	0.50	31.54
3	3	0.52	26.65
3	3	0.55	23.84

TABULATED DATA

REYNOLDS NUMBER 20,000 CONTROL PORT CLOSED

RUN NO.	STATION NO.	Y	U
3	3	0.57	22.30
3	3	0.60	20.65
3	3	0.62	20.65
3	4	0.03	138.50
3	4	0.05	145.99
3	4	0.07	155.42
3	4	0.10	157.69
3	4	0.12	158.81
3	4	0.15	159.93
3	4	0.17	159.93
3	4	0.20	157.69
3	4	0.22	153.12
3	4	0.25	147.21
3	4	0.27	138.50
3	4	0.30	130.58
3	4	0.32	120.68
3	4	0.35	108.27
3	4	0.37	101.15
3	4	0.40	93.10
3	4	0.42	84.29
3	4	0.45	74.44
3	4	0.47	67.43
3	4	0.50	59.60
3	4	0.52	53.31
3	4	0.55	46.17
3	4	0.57	40.42
3	4	0.60	35.76
3	4	0.62	31.54
3	4	0.65	27.96
3	4	0.67	26.65
3	4	0.70	25.29
3	4	0.72	23.84
3	5	0.03	113.09
3	5	0.05	119.20
3	5	0.07	125.02
3	5	0.10	130.58
3	5	0.12	133.27
3	5	0.15	135.91
3	5	0.17	137.21
3	5	0.20	135.91
3	5	0.22	133.27
3	5	0.25	130.58
3	5	0.27	127.83
3	5	0.30	122.15
3	5	0.32	117.70
3	5	0.35	111.82
3	5	0.37	106.62
3	5	0.40	101.15
3	5	0.42	93.86
3	5	0.45	85.96
3	5	0.47	82.59
3	5	0.50	75.39
3	5	0.52	70.52
3	5	0.55	64.19
3	5	0.57	58.40
3	5	0.60	51.96
3	5	0.62	47.68
3	5	0.65	44.60
3	5	0.67	39.54
3	5	0.70	35.76

TABULATED DATA

REYNOLDS NUMBER 20,000 CONTROL PORT CLOSED

RUN NO.	STATION NO.	Y	U
3	5	0.72	33.72
3	5	0.75	29.20
3	5	0.77	27.96
3	5	0.80	26.65
3	5	0.82	25.29
3	6	0.03	103.23
3	6	0.05	106.62
3	6	0.07	109.90
3	6	0.10	114.65
3	6	0.12	116.19
3	6	0.15	117.70
3	6	0.17	117.70
3	6	0.20	119.20
3	6	0.22	119.20
3	6	0.25	117.70
3	6	0.27	116.19
3	6	0.30	114.65
3	6	0.32	111.50
3	6	0.35	107.94
3	6	0.37	102.54
3	6	0.40	99.73
3	6	0.42	95.36
3	6	0.45	92.33
3	6	0.47	87.60
3	6	0.50	85.96
3	6	0.52	79.07
3	6	0.55	75.39
3	6	0.57	70.52
3	6	0.60	66.37
3	6	0.62	60.78
3	6	0.65	57.17
3	6	0.67	53.31
3	6	0.70	49.15
3	6	0.72	44.60
3	6	0.75	42.98
3	6	0.77	39.54
3	6	0.80	35.76
3	6	0.82	33.72
3	6	0.90	26.65
3	6	1.00	20.65
3	7	0.03	87.60
3	7	0.05	92.33
3	7	0.07	96.84
3	7	0.10	99.73
3	7	0.12	102.54
3	7	0.15	102.54
3	7	0.17	103.23
3	7	0.20	103.92
3	7	0.22	103.92
3	7	0.25	103.92
3	7	0.27	102.54
3	7	0.30	101.85
3	7	0.32	99.73
3	7	0.35	98.30
3	7	0.37	96.84
3	7	0.40	95.36
3	7	0.42	90.78
3	7	0.45	89.20
3	7	0.47	87.60
3	7	0.50	85.13

TABULATED DATA

REYNOLDS NUMBER 20,000 CONTROL PORT CLOSED

RUN NO.	STATION NO.	Y	U
3	7	0.52	82.59
3	7	0.55	80.85
3	7	0.57	75.39
3	7	0.60	72.51
3	7	0.62	70.52
3	7	0.65	67.43
3	7	0.67	64.19
3	7	0.70	60.78
3	7	0.72	58.40
3	7	0.75	54.63
3	7	0.77	51.96
3	7	0.80	49.15
3	7	0.85	44.60
3	7	0.90	39.54
3	7	0.95	33.72
3	7	1.00	31.54

TABULATED DATA

REYNOLDS NUMBER 37,000 CONTROL PORT OPEN

RUN NO.	STATION NO.	Y	U
4	1	0.03	315.38
4	1	0.05	337.16
4	1	0.07	357.61
4	1	0.10	376.96
4	1	0.12	381.64
4	1	0.15	383.50
4	1	0.17	378.84
4	1	0.20	373.17
4	1	0.22	357.61
4	1	0.25	337.16
4	1	0.27	266.55
4	1	0.30	155.42
4	1	0.32	32.65
4	1	0.13	437.98
4	2	0.03	92.33
4	2	0.05	130.58
4	2	0.07	226.17
4	2	0.10	308.55
4	2	0.12	345.49
4	2	0.15	362.54
4	2	0.17	367.41
4	2	0.20	370.30
4	2	0.22	367.41
4	2	0.25	352.61
4	2	0.27	324.27
4	2	0.30	277.00
4	2	0.32	216.54
4	2	0.35	159.93
4	2	0.37	105.28
4	2	0.40	60.78
4	3	0.03	261.16
4	3	0.05	209.88
4	3	0.07	244.30
4	3	0.10	282.09
4	3	0.12	313.12
4	3	0.15	337.16
4	3	0.17	350.39
4	3	0.20	349.57
4	3	0.22	337.16
4	3	0.25	317.63
4	3	0.27	294.41
4	3	0.30	266.55
4	3	0.32	235.41
4	3	0.35	203.00
4	3	0.37	176.81
4	3	0.40	148.41
4	3	0.42	119.20
4	3	0.45	99.73
4	3	0.47	63.08
4	3	0.50	58.40
4	3	0.52	41.29
4	3	0.55	33.72
4	3	0.57	26.65
4	3	0.60	23.84
4	3	0.62	20.65
4	3	0.65	17.68
4	3	0.67	16.86
4	4	0.03	232.37
4	4	0.05	238.41
4	4	0.07	252.87

TABULATED DATA

REYNOLDS NUMBER 37,000 CONTROL PORT OPEN

RUN NO.	STATION NO.	Y	U
4	4	0.10	266.55
4	4	0.12	277.00
4	4	0.15	284.59
4	4	0.17	291.99
4	4	0.20	292.96
4	4	0.22	291.01
4	4	0.25	282.09
4	4	0.27	271.83
4	4	0.30	261.16
4	4	0.32	244.30
4	4	0.35	229.29
4	4	0.37	211.57
4	4	0.40	194.05
4	4	0.42	176.81
4	4	0.45	159.93
4	4	0.47	143.54
4	4	0.50	125.02
4	4	0.52	106.62
4	4	0.55	92.33
4	4	0.57	87.60
4	4	0.60	67.43
4	4	0.62	55.91
4	4	0.65	47.68
4	4	0.67	37.70
4	4	0.70	33.72
4	4	0.72	23.84
4	4	0.75	23.84
4	4	0.77	20.65
4	4	0.80	18.47
4	5	0.03	223.01
4	5	0.05	226.17
4	5	0.07	241.37
4	5	0.10	244.30
4	5	0.12	250.04
4	5	0.15	252.87
4	5	0.17	255.11
4	5	0.20	255.66
4	5	0.22	252.87
4	5	0.25	247.19
4	5	0.27	238.41
4	5	0.30	232.37
4	5	0.32	226.17
4	5	0.35	216.54
4	5	0.37	206.47
4	5	0.40	195.87
4	5	0.42	184.67
4	5	0.45	172.74
4	5	0.47	164.31
4	5	0.50	150.78
4	5	0.52	141.04
4	5	0.55	130.58
4	5	0.57	119.20
4	5	0.60	106.62
4	5	0.62	93.86
4	5	0.65	85.96
4	5	0.67	77.25
4	5	0.70	67.43
4	5	0.72	58.40
4	5	0.75	50.57
4	5	0.77	44.60

TABULATED DATA

REYNOLDS NUMBER 37,000 CONTROL PORT OPEN

RUN NO.	STATION NO.	Y	U
4	5	0.80	37.70
4	5	0.82	33.72
4	6	0.03	199.47
4	6	0.05	204.74
4	6	0.07	214.90
4	6	0.10	219.80
4	6	0.12	224.60
4	6	0.15	226.17
4	6	0.17	226.17
4	6	0.20	226.17
4	6	0.22	224.60
4	6	0.25	220.45
4	6	0.27	216.54
4	6	0.30	213.24
4	6	0.32	208.18
4	6	0.35	203.00
4	6	0.37	195.87
4	6	0.40	189.23
4	6	0.42	180.78
4	6	0.45	172.74
4	6	0.47	166.46
4	6	0.50	159.93
4	6	0.52	153.12
4	6	0.55	143.54
4	6	0.57	135.91
4	6	0.60	125.02
4	6	0.62	119.20
4	6	0.65	113.09
4	6	0.67	102.54
4	6	0.70	93.86
4	6	0.72	87.60
4	6	0.75	77.25
4	6	0.77	71.52
4	6	0.80	65.29
4	6	0.90	44.60
4	6	1.00	26.65
4	7	0.03	176.81
4	7	0.05	180.78
4	7	0.07	190.35
4	7	0.10	195.87
4	7	0.12	199.47
4	7	0.15	201.24
4	7	0.17	203.00
4	7	0.20	203.70
4	7	0.22	202.65
4	7	0.25	201.24
4	7	0.27	199.47
4	7	0.30	196.60
4	7	0.32	192.95
4	7	0.35	190.35
4	7	0.37	186.58
4	7	0.40	180.78
4	7	0.42	176.81
4	7	0.45	172.74
4	7	0.47	168.58
4	7	0.50	164.31
4	7	0.52	157.69
4	7	0.55	151.72
4	7	0.57	145.99
4	7	0.60	141.04

TABULATED DATA

REYNOLDS NUMBER 37,000 CONTROL PORT OPEN

RUN NO.	STATION NO.	Y	U
4	7	0.62	135.91
4	7	0.65	130.58
4	7	0.67	125.02
4	7	0.70	119.20
4	7	0.72	113.09
4	7	0.75	107.94
4	7	0.77	101.15
4	7	0.80	95.36
4	7	0.90	85.96
4	7	1.00	63.08

TABULATED DATA

REYNOLDS NUMBER 37,000 CONTROL PORT CLOSED

RUN NO.	STATION NO.	Y	U
5	1	0.03	315.38
5	1	0.05	315.38
5	1	0.07	337.16
5	1	0.10	352.61
5	1	0.12	359.59
5	1	0.15	362.54
5	1	0.17	360.58
5	1	0.20	356.62
5	1	0.22	341.35
5	1	0.25	317.63
5	1	0.27	271.83
5	1	0.30	150.78
5	1	0.32	33.72
5	1	0.13	372.21
5	2	0.03	223.01
5	2	0.05	223.01
5	2	0.07	282.09
5	2	0.10	301.56
5	2	0.12	341.35
5	2	0.15	348.76
5	2	0.17	350.79
5	2	0.20	347.94
5	2	0.22	336.32
5	2	0.25	311.76
5	2	0.27	277.00
5	2	0.30	238.41
5	2	0.32	195.87
5	2	0.35	153.12
5	2	0.37	113.09
5	2	0.40	77.25
5	2	0.42	50.57
5	2	0.45	33.72
5	2	0.47	20.65
5	2	0.50	20.65
5	2	0.52	16.86
5	2	0.55	16.86
5	2	0.57	16.86
5	2	0.60	16.86
5	3	0.03	235.41
5	3	0.05	235.41
5	3	0.07	277.00
5	3	0.10	301.56
5	3	0.12	326.45
5	3	0.15	341.35
5	3	0.17	345.49
5	3	0.20	339.26
5	3	0.22	324.27
5	3	0.25	306.24
5	3	0.27	279.56
5	3	0.30	250.04
5	3	0.32	223.01
5	3	0.35	194.05
5	3	0.37	168.58
5	3	0.40	138.50
5	3	0.42	111.82
5	3	0.45	87.60
5	3	0.47	68.48
5	3	0.50	50.57
5	3	0.52	37.70
5	3	0.55	29.20

TABULATED DATA

REYNOLDS NUMBER 37,000 CONTROL PORT CLOSED

RUN NO.	STATION NO.	Y	U
5	3	0.57	23.84
5	3	0.60	20.65
5	3	0.62	18.47
5	3	0.65	16.86
5	3	0.67	15.99
5	3	0.70	15.99
5	4	0.03	271.83
5	4	0.05	277.00
5	4	0.07	287.08
5	4	0.10	294.41
5	4	0.12	296.81
5	4	0.15	294.41
5	4	0.17	287.08
5	4	0.20	277.00
5	4	0.22	263.87
5	4	0.25	247.19
5	4	0.27	232.37
5	4	0.30	214.90
5	4	0.32	195.87
5	4	0.35	176.81
5	4	0.37	159.93
5	4	0.40	143.54
5	4	0.42	127.83
5	4	0.45	113.09
5	4	0.47	96.84
5	4	0.50	82.59
5	4	0.52	69.51
5	4	0.55	58.40
5	4	0.57	47.68
5	4	0.60	41.29
5	4	0.62	33.72
5	4	0.65	26.65
5	4	0.67	23.84
5	4	0.70	20.65
5	4	0.72	17.68
5	4	0.75	16.86
5	4	0.77	15.08
5	4	0.80	11.92
5	4	0.82	11.92
5	5	0.03	216.54
5	5	0.05	226.17
5	5	0.07	238.41
5	5	0.10	247.19
5	5	0.12	252.87
5	5	0.15	255.66
5	5	0.17	257.88
5	5	0.20	255.66
5	5	0.22	252.87
5	5	0.25	247.19
5	5	0.27	239.89
5	5	0.30	232.37
5	5	0.32	223.01
5	5	0.35	213.24
5	5	0.37	203.00
5	5	0.40	192.21
5	5	0.42	180.78
5	5	0.45	168.58
5	5	0.47	153.12
5	5	0.50	145.99
5	5	0.52	135.91

TABULATED DATA

REYNOLDS NUMBER 37,000 CONTROL PORT CLOSED

RUN NO.	STATION NO.	Y	U
5	5	0.55	125.02
5	5	0.57	110.55
5	5	0.60	98.30
5	5	0.62	89.20
5	5	0.65	85.96
5	5	0.67	69.51
5	5	0.70	60.78
5	5	0.72	53.31
5	5	0.75	44.60
5	5	0.77	37.70
5	5	0.80	31.54
5	5	0.82	23.84
5	6	0.03	195.87
5	6	0.05	201.24
5	6	0.07	209.88
5	6	0.10	216.54
5	6	0.12	219.80
5	6	0.15	223.01
5	6	0.17	224.60
5	6	0.20	223.01
5	6	0.22	221.41
5	6	0.25	218.18
5	6	0.27	214.90
5	6	0.30	209.88
5	6	0.32	204.74
5	6	0.35	199.47
5	6	0.37	195.87
5	6	0.40	188.48
5	6	0.42	180.78
5	6	0.45	172.74
5	6	0.47	164.31
5	6	0.50	157.69
5	6	0.52	148.41
5	6	0.55	141.04
5	6	0.57	133.27
5	6	0.60	125.02
5	6	0.62	116.19
5	6	0.65	107.94
5	6	0.67	99.73
5	6	0.70	92.33
5	6	0.72	84.29
5	6	0.75	79.07
5	6	0.77	71.52
5	6	0.80	63.08
5	6	0.90	41.29
5	6	1.00	23.84
5	7	0.03	168.58
5	7	0.05	174.79
5	7	0.07	184.67
5	7	0.10	188.48
5	7	0.12	192.21
5	7	0.15	194.05
5	7	0.17	195.87
5	7	0.20	196.23
5	7	0.22	195.87
5	7	0.25	195.15
5	7	0.27	194.05
5	7	0.30	192.21
5	7	0.32	188.48
5	7	0.35	184.67

TABULATED DATA

REYNOLDS NUMBER 37,000 CONTROL PORT CLOSED

RUN NO.	STATION NO.	Y	U
5	7	0.37	182.74
5	7	0.40	178.81
5	7	0.42	172.74
5	7	0.45	168.58
5	7	0.47	164.31
5	7	0.50	159.93
5	7	0.52	153.12
5	7	0.55	148.41
5	7	0.57	143.54
5	7	0.60	138.50
5	7	0.62	133.27
5	7	0.65	127.83
5	7	0.67	122.15
5	7	0.70	116.19
5	7	0.72	109.25
5	7	0.75	105.28
5	7	0.77	99.73
5	7	0.80	92.33
5	7	0.90	73.48
5	7	1.00	55.91

TABULATED DATA

REYNOLDS NUMBER 69,000 CONTROL PORT OPEN

RUN NO.	STATION NO.	Y	U
6	1	0.03	619.40
6	1	0.05	590.03
6	1	0.07	663.70
6	1	0.10	700.16
6	1	0.12	720.17
6	1	0.15	732.89
6	1	0.17	726.07
6	1	0.20	715.22
6	1	0.22	695.07
6	1	0.25	663.70
6	1	0.27	596.02
6	1	0.30	357.61
6	1	0.32	111.82
6	1	0.35	29.20
6	1	0.37	11.92
6	1	0.13	763.28
6	2	0.03	157.69
6	2	0.05	153.12
6	2	0.07	359.59
6	2	0.10	559.12
6	2	0.12	652.91
6	2	0.15	684.77
6	2	0.17	697.11
6	2	0.20	701.18
6	2	0.22	695.07
6	2	0.25	679.57
6	2	0.27	630.77
6	2	0.30	552.73
6	2	0.32	446.02
6	2	0.35	335.05
6	2	0.37	232.37
6	2	0.40	135.91
6	2	0.42	75.39
6	2	0.45	44.60
6	2	0.47	37.70
6	2	0.50	34.13
6	2	0.52	31.54
6	2	0.55	29.20
6	2	0.57	24.43
6	2	0.60	23.84
6	3	0.03	395.35
6	3	0.05	399.82
6	3	0.07	457.81
6	3	0.10	523.00
6	3	0.12	583.98
6	3	0.15	630.77
6	3	0.17	659.40
6	3	0.20	661.55
6	3	0.22	641.93
6	3	0.25	601.95
6	3	0.27	556.57
6	3	0.30	498.67
6	3	0.32	446.02
6	3	0.35	388.10
6	3	0.37	337.16
6	3	0.40	279.56
6	3	0.42	235.41
6	3	0.45	192.21
6	3	0.47	150.78
6	3	0.50	113.09

TABULATED DATA

REYNOLDS NUMBER 69,000 CONTROL PORT OPEN

RUN NO.	STATION NO.	Y	U
6	3	0.52	83.44
6	3	0.55	60.78
6	3	0.57	44.60
6	3	0.60	37.70
6	3	0.62	33.72
6	3	0.65	29.20
6	3	0.67	26.65
6	3	0.70	23.84
6	3	0.72	23.24
6	3	0.75	20.65
6	3	0.77	20.65
6	3	0.80	17.68
6	4	0.03	450.77
6	4	0.05	453.91
6	4	0.07	488.59
6	4	0.10	508.54
6	4	0.12	526.39
6	4	0.15	541.03
6	4	0.17	546.26
6	4	0.20	546.26
6	4	0.22	538.40
6	4	0.25	527.74
6	4	0.27	505.74
6	4	0.30	476.82
6	4	0.32	449.19
6	4	0.35	416.36
6	4	0.37	386.26
6	4	0.40	353.62
6	4	0.42	319.86
6	4	0.45	287.08
6	4	0.47	255.66
6	4	0.50	224.60
6	4	0.52	195.87
6	4	0.55	187.72
6	4	0.57	141.04
6	4	0.60	119.20
6	4	0.62	96.84
6	4	0.65	79.07
6	4	0.67	63.08
6	4	0.70	51.96
6	4	0.72	41.29
6	4	0.75	34.13
6	4	0.77	29.20
6	4	0.80	23.84
6	5	0.03	436.36
6	5	0.05	441.22
6	5	0.07	469.31
6	5	0.10	479.79
6	5	0.12	487.13
6	5	0.15	488.59
6	5	0.17	488.59
6	5	0.20	484.21
6	5	0.22	476.82
6	5	0.25	461.67
6	5	0.27	449.98
6	5	0.30	437.98
6	5	0.32	418.06
6	5	0.35	400.71
6	5	0.37	382.57
6	5	0.40	359.59

TABULATED DATA

REYNOLDS NUMBER 69,000 CONTROL PORT OPEN

RUN NO.	STATION NO.	Y	U
6	5	0.42	337.16
6	5	0.45	317.18
6	5	0.47	296.81
6	5	0.50	273.91
6	5	0.52	250.04
6	5	0.55	232.37
6	5	0.57	209.88
6	5	0.60	188.85
6	5	0.62	169.42
6	5	0.65	150.78
6	5	0.67	135.91
6	5	0.70	118.01
6	5	0.72	99.73
6	5	0.75	85.96
6	5	0.77	73.48
6	5	0.80	62.17
6	5	0.82	50.57
6	5	0.90	29.20
6	5	1.00	16.86
6	6	0.03	386.26
6	6	0.05	391.74
6	6	0.07	414.65
6	6	0.10	426.48
6	6	0.12	431.45
6	6	0.15	437.98
6	6	0.17	437.98
6	6	0.20	433.91
6	6	0.22	429.80
6	6	0.25	423.13
6	6	0.27	412.93
6	6	0.30	404.24
6	6	0.32	395.35
6	6	0.35	380.71
6	6	0.37	367.41
6	6	0.40	357.61
6	6	0.42	341.35
6	6	0.45	324.27
6	6	0.47	308.55
6	6	0.50	292.96
6	6	0.52	277.00
6	6	0.55	261.16
6	6	0.57	247.19
6	6	0.60	229.29
6	6	0.62	213.24
6	6	0.65	197.68
6	6	0.67	184.67
6	6	0.70	168.58
6	6	0.72	154.51
6	6	0.75	141.04
6	6	0.77	127.27
6	6	0.80	113.09
6	6	1.00	41.29
6	7	0.03	347.54
6	7	0.05	352.61
6	7	0.07	372.21
6	7	0.10	386.26
6	7	0.12	390.84
6	7	0.15	395.35
6	7	0.17	395.35
6	7	0.20	395.35

TABULATED DATA

REYNOLDS NUMBER 69,000 CONTROL PORT OPEN

RUN NO.	STATION NO.	Y	U
6	7	0.22	393.55
6	7	0.25	387.18
6	7	0.27	384.42
6	7	0.30	376.96
6	7	0.32	369.34
6	7	0.35	365.47
6	7	0.37	357.61
6	7	0.40	347.54
6	7	0.42	337.16
6	7	0.45	324.27
6	7	0.47	313.12
6	7	0.50	306.24
6	7	0.52	294.41
6	7	0.55	282.09
6	7	0.57	271.83
6	7	0.60	258.43
6	7	0.62	247.19
6	7	0.65	235.41
6	7	0.67	223.01
6	7	0.70	209.88
6	7	0.72	199.47
6	7	0.75	188.48
6	7	0.77	180.78
6	7	0.80	168.58
6	7	0.90	130.58
6	7	1.00	99.73

TABULATED DATA

REYNOLDS NUMBER 69,000 CONTROL PORT CLOSED

RUN NO.	STATION NO.	Y	U
7	1	0.03	613.64
7	1	0.05	607.82
7	1	0.07	655.08
7	1	0.10	684.77
7	1	0.12	700.16
7	1	0.15	703.20
7	1	0.17	695.07
7	1	0.20	684.77
7	1	0.22	658.32
7	1	0.25	613.64
7	1	0.27	519.60
7	1	0.30	244.30
7	1	0.32	37.70
7	1	0.13	723.13
7	2	0.03	446.02
7	2	0.05	437.98
7	2	0.07	583.98
7	2	0.10	647.44
7	2	0.12	674.32
7	2	0.15	682.70
7	2	0.17	684.77
7	2	0.20	675.37
7	2	0.22	652.91
7	2	0.25	607.82
7	2	0.27	527.74
7	2	0.30	429.80
7	2	0.32	319.86
7	2	0.35	223.01
7	2	0.37	135.91
7	2	0.40	69.51
7	2	0.42	37.70
7	2	0.45	29.20
7	2	0.47	26.65
7	2	0.50	23.84
7	2	0.52	16.86
7	2	0.55	11.92
7	3	0.03	453.91
7	3	0.05	464.74
7	3	0.07	533.10
7	3	0.10	590.03
7	3	0.12	630.77
7	3	0.15	652.91
7	3	0.17	655.08
7	3	0.20	641.93
7	3	0.22	607.82
7	3	0.25	559.12
7	3	0.27	516.86
7	3	0.30	461.67
7	3	0.32	409.48
7	3	0.35	353.62
7	3	0.37	301.56
7	3	0.40	250.61
7	3	0.42	206.47
7	3	0.45	164.31
7	3	0.47	127.83
7	3	0.50	93.86
7	3	0.52	68.48
7	3	0.55	47.68
7	3	0.57	33.72
7	3	0.60	26.65

TABULATED DATA

REYNOLDS NUMBER 69,000 CONTROL PORT CLOSED

RUN NO.	STATION NO.	Y	U
7	3	0.62	20.65
7	3	0.65	16.86
7	3	0.67	11.92
7	4	0.03	453.91
7	4	0.05	476.82
7	4	0.07	505.74
7	4	0.10	533.10
7	4	0.12	548.86
7	4	0.15	559.12
7	4	0.17	559.12
7	4	0.20	552.73
7	4	0.22	538.40
7	4	0.25	519.60
7	4	0.27	491.49
7	4	0.30	461.67
7	4	0.32	431.45
7	4	0.35	380.71
7	4	0.37	367.41
7	4	0.40	332.92
7	4	0.42	301.56
7	4	0.45	271.83
7	4	0.47	241.37
7	4	0.50	209.88
7	4	0.52	182.74
7	4	0.55	155.42
7	4	0.57	130.58
7	4	0.60	109.25
7	4	0.62	87.60
7	4	0.65	71.52
7	4	0.67	57.17
7	4	0.70	44.60
7	4	0.72	33.72
7	4	0.75	26.65
7	4	0.77	20.65
7	4	0.80	16.86
7	5	0.03	421.45
7	5	0.05	442.02
7	5	0.07	463.21
7	5	0.10	476.82
7	5	0.12	479.79
7	5	0.15	484.21
7	5	0.17	484.21
7	5	0.20	480.53
7	5	0.22	469.31
7	5	0.25	461.67
7	5	0.27	447.61
7	5	0.30	431.45
7	5	0.32	412.93
7	5	0.35	395.35
7	5	0.37	376.96
7	5	0.40	353.62
7	5	0.42	332.92
7	5	0.45	310.85
7	5	0.47	291.99
7	5	0.50	266.55
7	5	0.52	244.30
7	5	0.55	223.01
7	5	0.57	203.00
7	5	0.60	184.67
7	5	0.62	162.13

TABULATED DATA

REYNOLDS NUMBER 69,000 CONTROL PORT CLOSED

RUN NO.	STATION NO.	Y	U
7	5	0.65	141.04
7	5	0.67	133.27
7	5	0.70	113.09
7	5	0.72	98.30
7	5	0.75	82.59
7	5	0.77	69.51
7	5	0.80	57.17
7	5	0.90	23.84
7	6	0.03	381.64
7	6	0.05	386.26
7	6	0.07	405.99
7	6	0.10	412.93
7	6	0.12	419.76
7	6	0.15	423.13
7	6	0.17	423.13
7	6	0.20	419.76
7	6	0.22	414.65
7	6	0.25	407.74
7	6	0.27	398.93
7	6	0.30	393.55
7	6	0.32	382.57
7	6	0.35	367.41
7	6	0.37	357.61
7	6	0.40	341.35
7	6	0.42	327.76
7	6	0.45	315.38
7	6	0.47	301.56
7	6	0.50	284.59
7	6	0.52	269.20
7	6	0.55	252.87
7	6	0.57	238.41
7	6	0.60	223.01
7	6	0.62	209.88
7	6	0.65	192.21
7	6	0.67	176.81
7	6	0.70	164.31
7	6	0.72	150.78
7	6	0.75	136.95
7	6	0.77	125.02
7	6	0.80	111.82
7	6	0.90	73.48
7	6	1.00	44.60
7	7	0.03	337.16
7	7	0.05	342.39
7	7	0.07	357.61
7	7	0.10	367.41
7	7	0.12	371.26
7	7	0.15	373.17
7	7	0.17	369.34
7	7	0.20	368.38
7	7	0.22	367.41
7	7	0.25	367.41
7	7	0.27	365.47
7	7	0.30	359.59
7	7	0.32	355.62
7	7	0.35	345.49
7	7	0.37	337.16
7	7	0.40	330.78
7	7	0.42	323.39
7	7	0.45	313.12

TABULATED DATA

REYNOLDS NUMBER 69,000 CONTROL PORT CLOSED

RUN NO.	STATION NO.	Y	U
7	7	0.47	301.56
7	7	0.50	293.93
7	7	0.52	282.09
7	7	0.55	271.83
7	7	0.57	261.16
7	7	0.60	250.04
7	7	0.62	238.41
7	7	0.65	226.17
7	7	0.67	219.80
7	7	0.70	206.47
7	7	0.72	195.87
7	7	0.75	188.48
7	7	0.77	176.81
7	7	0.80	168.58
7	7	0.90	130.58
7	7	1.00	99.73

TABULATED DATA

REYNOLDS NUMBER 141,000 CONTROL PORT OPEN

RUN NO.	STATION NO.	Y	U
8	1	0.03	1145.85
8	1	0.05	1082.07
8	1	0.07	1201.54
8	1	0.10	1294.88
8	1	0.12	1327.40
8	1	0.15	1348.64
8	1	0.17	1359.13
8	1	0.20	1359.13
8	1	0.22	1350.74
8	1	0.25	1327.40
8	1	0.27	1266.03
8	1	0.30	1011.48
8	1	0.32	357.61
8	1	0.35	44.60
8	1	0.13	1434.41
8	2	0.03	446.02
8	2	0.05	452.35
8	2	0.07	607.82
8	2	0.10	982.98
8	2	0.12	1238.80
8	2	0.15	1294.88
8	2	0.17	1316.65
8	2	0.20	1320.96
8	2	0.22	1320.96
8	2	0.25	1311.24
8	2	0.27	1263.78
8	2	0.30	1099.00
8	2	0.32	829.30
8	2	0.35	565.43
8	2	0.37	482.74
8	2	0.40	180.78
8	2	0.42	67.43
8	2	0.45	44.60
8	2	0.47	41.29
8	2	0.50	33.72
8	2	0.52	23.84
8	3	0.03	856.28
8	3	0.05	859.59
8	3	0.07	931.01
8	3	0.10	1066.19
8	3	0.12	1192.04
8	3	0.15	1274.98
8	3	0.17	1311.24
8	3	0.20	1300.36
8	3	0.22	1250.22
8	3	0.25	1158.18
8	3	0.27	1039.20
8	3	0.30	907.83
8	3	0.32	781.67
8	3	0.35	652.91
8	3	0.37	535.75
8	3	0.40	429.80
8	3	0.42	332.92
8	3	0.45	247.19
8	3	0.47	168.58
8	3	0.50	111.82
8	3	0.52	73.48
8	3	0.55	55.91
8	3	0.57	46.17
8	3	0.60	41.29

TABULATED DATA

REYNOLDS NUMBER 141,000 CONTROL PORT OPEN

RUN NO.	STATION NO.	Y	U
8	3	0.62	35.76
8	3	0.65	31.54
8	4	0.03	953.63
8	4	0.05	946.15
8	4	0.07	1022.66
8	4	0.10	1079.44
8	4	0.12	1123.30
8	4	0.15	1145.85
8	4	0.17	1153.26
8	4	0.20	1128.35
8	4	0.22	1079.44
8	4	0.25	1018.48
8	4	0.27	946.15
8	4	0.30	862.89
8	4	0.32	781.67
8	4	0.35	705.22
8	4	0.37	630.77
8	4	0.40	552.73
8	4	0.42	484.21
8	4	0.45	412.93
8	4	0.47	357.61
8	4	0.50	291.99
8	4	0.52	244.30
8	4	0.55	194.05
8	4	0.57	150.78
8	4	0.60	119.20
8	4	0.62	89.20
8	4	0.65	68.48
8	4	0.67	54.63
8	4	0.70	46.17
8	4	0.72	41.29
8	4	0.75	35.76
8	4	0.77	31.54
8	4	0.80	26.65
8	5	0.03	915.62
8	5	0.05	907.83
8	5	0.07	968.42
8	5	0.10	1008.66
8	5	0.12	1025.43
8	5	0.15	1028.20
8	5	0.17	1018.48
8	5	0.20	997.33
8	5	0.22	968.42
8	5	0.25	931.01
8	5	0.27	892.04
8	5	0.30	834.43
8	5	0.32	790.71
8	5	0.35	734.82
8	5	0.37	684.77
8	5	0.40	630.77
8	5	0.42	577.86
8	5	0.45	526.39
8	5	0.47	476.82
8	5	0.50	426.48
8	5	0.52	376.96
8	5	0.55	332.92
8	5	0.57	291.99
8	5	0.60	250.04
8	5	0.62	213.24
8	5	0.65	176.81

TABULATED DATA

REYNOLDS NUMBER 141,000 CONTROL PORT OPEN

RUN NO.	STATION NO.	Y	U
8	5	0.67	145.99
8	5	0.70	119.20
8	5	0.72	93.86
8	5	0.75	73.48
8	5	0.77	58.40
8	5	0.80	41.29
8	6	0.03	842.90
8	6	0.05	846.26
8	6	0.07	907.83
8	6	0.10	926.42
8	6	0.12	938.61
8	6	0.15	938.61
8	6	0.17	923.35
8	6	0.20	904.69
8	6	0.22	875.97
8	6	0.25	846.26
8	6	0.27	811.99
8	6	0.30	781.67
8	6	0.32	744.43
8	6	0.35	710.24
8	6	0.37	669.03
8	6	0.40	630.77
8	6	0.42	596.02
8	6	0.45	556.57
8	6	0.47	519.60
8	6	0.50	476.82
8	6	0.52	446.02
8	6	0.55	405.99
8	6	0.57	365.47
8	6	0.60	332.92
8	6	0.62	296.81
8	6	0.65	266.55
8	6	0.67	238.41
8	6	0.70	208.18
8	6	0.72	186.58
8	6	0.75	164.31
8	6	0.77	141.04
8	6	0.80	122.15
8	6	0.90	65.29
8	7	0.03	738.68
8	7	0.05	772.53
8	7	0.07	808.48
8	7	0.10	822.42
8	7	0.12	825.87
8	7	0.15	825.87
8	7	0.17	811.99
8	7	0.20	799.64
8	7	0.22	781.67
8	7	0.25	763.28
8	7	0.27	739.64
8	7	0.30	715.22
8	7	0.32	695.07
8	7	0.35	669.03
8	7	0.37	641.93
8	7	0.40	613.64
8	7	0.42	590.03
8	7	0.45	559.12
8	7	0.47	533.10
8	7	0.50	508.54
8	7	0.52	476.82

TABULATED DATA

REYNOLDS NUMBER 141,000 CONTROL PORT OPEN

RUN NO.	STATION NO.	Y	U
8	7	0.55	453.91
8	7	0.57	429.80
8	7	0.60	398.93
8	7	0.62	373.17
8	7	0.65	365.47
8	7	0.67	326.45
8	7	0.70	301.56
8	7	0.72	282.09
8	7	0.75	263.87
8	7	0.77	244.30
8	7	0.80	219.80
8	7	0.90	171.92
8	7	1.00	130.58

TABULATED DATA

REYNOLDS NUMBER 141,000 CONTROL PORT CLOSED

RUN NO.	STATION NO.	Y	U
9	1	0.03	1167.95
9	1	0.05	1170.38
9	1	0.07	1227.28
9	1	0.10	1281.65
9	1	0.12	1311.24
9	1	0.15	1323.11
9	1	0.17	1331.67
9	1	0.20	1327.40
9	1	0.22	1316.65
9	1	0.25	1273.86
9	1	0.27	1118.23
9	1	0.30	476.82
9	1	0.32	29.20
9	1	0.13	1369.55
9	2	0.03	990.18
9	2	0.05	968.42
9	2	0.07	1099.00
9	2	0.10	1272.75
9	2	0.12	1311.24
9	2	0.15	1322.03
9	2	0.17	1329.54
9	2	0.20	1325.25
9	2	0.22	1301.45
9	2	0.25	1209.79
9	2	0.27	982.98
9	2	0.30	707.23
9	2	0.32	446.02
9	2	0.35	247.19
9	2	0.37	101.15
9	2	0.40	50.57
9	2	0.42	41.29
9	2	0.45	36.93
9	2	0.47	29.20
9	2	0.50	20.65
9	2	0.52	11.92
9	3	0.03	997.33
9	3	0.05	1004.43
9	3	0.07	1086.00
9	3	0.10	1215.65
9	3	0.12	1294.88
9	3	0.15	1316.65
9	3	0.17	1300.36
9	3	0.20	1267.15
9	3	0.22	1184.86
9	3	0.25	1066.19
9	3	0.27	932.54
9	3	0.30	790.71
9	3	0.32	658.32
9	3	0.35	539.72
9	3	0.37	429.80
9	3	0.40	324.27
9	3	0.42	238.41
9	3	0.45	164.31
9	3	0.47	109.90
9	3	0.50	69.51
9	3	0.52	51.96
9	3	0.55	44.60
9	3	0.57	37.70
9	3	0.60	31.54
9	3	0.62	23.84

TABULATED DATA

REYNOLDS NUMBER 141,000 CONTROL PORT CLOSED

RUN NO.	STATION NO.	Y	U
9	3	0.65	16.86
9	4	0.03	1004.43
9	4	0.05	1004.43
9	4	0.07	1076.80
9	4	0.10	1143.36
9	4	0.12	1180.06
9	4	0.15	1189.65
9	4	0.17	1167.95
9	4	0.20	1118.23
9	4	0.22	1052.78
9	4	0.25	990.18
9	4	0.27	899.97
9	4	0.30	817.22
9	4	0.32	734.82
9	4	0.35	657.24
9	4	0.37	583.98
9	4	0.40	512.71
9	4	0.42	446.02
9	4	0.45	380.71
9	4	0.47	315.38
9	4	0.50	266.55
9	4	0.52	208.18
9	4	0.55	164.31
9	4	0.57	125.02
9	4	0.60	95.36
9	4	0.62	73.48
9	4	0.65	58.40
9	4	0.67	50.57
9	4	0.70	42.98
9	4	0.72	37.70
9	4	0.75	33.72
9	4	0.77	29.20
9	4	0.80	23.84
9	4	0.82	16.86
9	5	0.03	938.61
9	5	0.05	956.61
9	5	0.07	1008.66
9	5	0.10	1050.08
9	5	0.12	1063.52
9	5	0.15	1054.13
9	5	0.17	1032.34
9	5	0.20	1000.18
9	5	0.22	953.63
9	5	0.25	907.83
9	5	0.27	856.28
9	5	0.30	799.64
9	5	0.32	744.43
9	5	0.35	684.77
9	5	0.37	633.02
9	5	0.40	577.86
9	5	0.42	519.60
9	5	0.45	470.82
9	5	0.47	416.36
9	5	0.50	376.96
9	5	0.52	328.62
9	5	0.55	289.54
9	5	0.57	238.41
9	5	0.60	203.00
9	5	0.62	167.73
9	5	0.65	137.99

TABULATED DATA

REYNOLDS NUMBER 141,000 CONTROL PORT CLOSED

RUN NO.	STATION NO.	Y	U
9	5	0.67	109.90
9	5	0.70	85.96
9	5	0.72	67.43
9	5	0.75	50.57
9	5	0.77	33.72
9	5	0.80	11.92
9	6	0.03	842.90
9	6	0.05	859.59
9	6	0.07	895.22
9	6	0.10	926.42
9	6	0.12	938.61
9	6	0.15	937.10
9	6	0.17	924.89
9	6	0.20	906.26
9	6	0.22	875.97
9	6	0.25	842.90
9	6	0.27	808.48
9	6	0.30	772.53
9	6	0.32	732.89
9	6	0.35	695.07
9	6	0.37	652.91
9	6	0.40	610.16
9	6	0.42	577.86
9	6	0.45	530.42
9	6	0.47	491.49
9	6	0.50	449.19
9	6	0.52	412.93
9	6	0.55	376.96
9	6	0.57	337.16
9	6	0.60	306.24
9	6	0.62	271.83
9	6	0.65	241.37
9	6	0.67	213.24
9	6	0.70	190.35
9	6	0.72	168.58
9	6	0.75	145.99
9	6	0.77	119.20
9	6	0.80	109.25
9	6	0.90	58.40
9	6	1.00	23.84
9	7	0.03	750.13
9	7	0.05	787.11
9	7	0.07	813.74
9	7	0.10	825.87
9	7	0.12	829.30
9	7	0.15	829.30
9	7	0.17	822.42
9	7	0.20	799.64
9	7	0.22	781.67
9	7	0.25	757.67
9	7	0.27	734.82
9	7	0.30	715.22
9	7	0.32	684.77
9	7	0.35	658.32
9	7	0.37	630.77
9	7	0.40	601.95
9	7	0.42	571.68
9	7	0.45	546.26
9	7	0.47	512.71
9	7	0.50	482.74

TABULATED DATA

REYNOLDS NUMBER 141,000 CONTROL PORT CLOSED

RUN NO.	STATION NO.	Y	U
9	7	0.52	455.48
9	7	0.55	429.80
9	7	0.57	398.93
9	7	0.60	376.96
9	7	0.62	347.54
9	7	0.65	317.63
9	7	0.67	294.41
9	7	0.70	279.56
9	7	0.72	258.43
9	7	0.75	241.37
9	7	0.77	226.17
9	7	0.80	209.88
9	7	0.90	156.33
9	7	1.00	122.15

TABULATED DATA

REYNOLDS NUMBER 100,000 CONTROL PORT OPEN

RUN NO.	STATION NO.	Y	U
10	1	0.03	875.97
10	1	0.05	842.90
10	1	0.07	910.95
10	1	0.10	969.88
10	1	0.12	998.75
10	1	0.15	1011.48
10	1	0.17	1008.66
10	1	0.20	997.33
10	1	0.22	975.73
10	1	0.25	931.01
10	1	0.27	859.59
10	1	0.30	636.37
10	1	0.32	199.47
10	1	0.35	20.65
10	1	0.13	1052.78
10	2	0.03	206.47
10	2	0.05	199.47
10	2	0.07	476.82
10	2	0.10	842.90
10	2	0.12	907.83
10	2	0.15	950.65
10	2	0.17	962.53
10	2	0.20	965.48
10	2	0.22	961.05
10	2	0.25	938.61
10	2	0.27	892.04
10	2	0.30	794.29
10	2	0.32	647.44
10	2	0.35	476.82
10	2	0.37	319.86
10	2	0.40	178.81
10	2	0.42	82.59
10	2	0.45	44.60
10	2	0.47	33.72
10	2	0.50	29.20
10	2	0.52	23.84
10	2	0.55	16.86
10	3	0.03	583.98
10	3	0.05	588.82
10	3	0.07	661.55
10	3	0.10	753.91
10	3	0.12	849.61
10	3	0.15	915.62
10	3	0.17	940.12
10	3	0.20	931.01
10	3	0.22	892.04
10	3	0.25	829.30
10	3	0.27	753.91
10	3	0.30	672.21
10	3	0.32	583.98
10	3	0.35	498.67
10	3	0.37	412.93
10	3	0.40	347.54
10	3	0.42	282.09
10	3	0.45	208.18
10	3	0.47	154.51
10	3	0.50	101.15
10	3	0.52	67.43
10	3	0.55	46.17
10	3	0.57	35.76

TABULATED DATA

REYNOLDS NUMBER 100,000 CONTROL PORT OPEN

RUN NO.	STATION NO.	Y	U
10	3	0.60	29.20
10	3	0.62	23.84
10	3	0.65	16.86
10	4	0.03	678.52
10	4	0.05	682.70
10	4	0.07	725.09
10	4	0.10	761.41
10	4	0.12	787.11
10	4	0.15	799.64
10	4	0.17	804.96
10	4	0.20	794.29
10	4	0.22	772.53
10	4	0.25	734.82
10	4	0.27	695.07
10	4	0.30	641.93
10	4	0.32	596.02
10	4	0.35	546.26
10	4	0.37	491.49
10	4	0.40	437.98
10	4	0.42	395.35
10	4	0.45	347.54
10	4	0.47	303.91
10	4	0.50	159.93
10	4	0.52	209.88
10	4	0.55	174.79
10	4	0.57	143.54
10	4	0.60	113.09
10	4	0.62	73.48
10	4	0.65	69.51
10	4	0.67	55.91
10	4	0.70	44.60
10	4	0.72	37.70
10	4	0.75	31.54
10	4	0.77	29.20
10	4	0.80	23.84
10	5	0.03	652.91
10	5	0.05	657.24
10	5	0.07	695.07
10	5	0.10	713.23
10	5	0.12	715.22
10	5	0.15	719.19
10	5	0.17	713.23
10	5	0.20	695.07
10	5	0.22	678.52
10	5	0.25	653.99
10	5	0.27	630.77
10	5	0.30	601.95
10	5	0.32	571.68
10	5	0.35	539.72
10	5	0.37	505.74
10	5	0.40	476.82
10	5	0.42	437.98
10	5	0.45	404.24
10	5	0.47	367.41
10	5	0.50	339.26
10	5	0.52	310.85
10	5	0.55	279.56
10	5	0.57	244.30
10	5	0.60	213.24
10	5	0.62	184.67

TABULATED DATA

REYNOLDS NUMBER 100,000 CONTROL PORT OPEN

RUN NO.	STATION NO.	Y	U
10	5	0.65	159.93
10	5	0.67	135.91
10	5	0.70	113.09
10	5	0.72	92.33
10	5	0.75	75.39
10	5	0.77	58.40
10	5	0.80	47.68
10	6	0.03	577.86
10	6	0.05	601.95
10	6	0.07	628.51
10	6	0.10	636.37
10	6	0.12	641.93
10	6	0.15	641.93
10	6	0.17	633.02
10	6	0.20	625.11
10	6	0.22	607.82
10	6	0.25	590.03
10	6	0.27	571.68
10	6	0.30	552.73
10	6	0.32	533.10
10	6	0.35	511.33
10	6	0.37	484.21
10	6	0.40	461.67
10	6	0.42	437.98
10	6	0.45	412.93
10	6	0.47	395.35
10	6	0.50	361.56
10	6	0.52	337.16
10	6	0.55	315.38
10	6	0.57	291.99
10	6	0.60	266.55
10	6	0.62	244.30
10	6	0.65	223.01
10	6	0.67	203.00
10	6	0.70	184.67
10	6	0.72	168.58
10	6	0.75	145.99
10	6	0.77	130.58
10	6	0.80	119.20
10	6	0.90	71.52
10	6	1.00	37.70
10	7	0.03	508.54
10	7	0.05	526.39
10	7	0.07	552.73
10	7	0.10	560.38
10	7	0.12	570.44
10	7	0.15	571.68
10	7	0.17	570.44
10	7	0.20	564.18
10	7	0.22	556.57
10	7	0.25	546.26
10	7	0.27	533.10
10	7	0.30	522.32
10	7	0.32	508.54
10	7	0.35	491.49
10	7	0.37	476.82
10	7	0.40	461.67
10	7	0.42	446.02
10	7	0.45	429.80
10	7	0.47	412.93

TABULATED DATA

REYNOLDS NUMBER 100,000 CONTROL PORT OPEN

RUN NO.	STATION NO.	Y	U
10	7	0.50	395.35
10	7	0.52	376.96
10	7	0.55	357.61
10	7	0.57	337.16
10	7	0.60	319.86
10	7	0.62	310.85
10	7	0.65	291.99
10	7	0.67	277.00
10	7	0.70	261.16
10	7	0.72	241.37
10	7	0.75	226.17
10	7	0.77	213.24
10	7	0.80	199.47
10	7	0.90	153.12
10	7	1.00	119.20

TABULATED DATA

RUN NO.	2	3	4	5	6	7	8	9	10
REYNOLDS NO.	20,000	20,000	37,000	37,000	69,000	69,000	141,000	141,000	100,000
CONTROL PORT CONDITION	OPEN	CLOSED	OPEN	CLOSED	OPEN	CLOSED	OPEN	CLOSED	OPEN
X= 0.25	-44.80	-17.92	-98.44	-49.22	-171.51	-83.41	-306.27	-109.74	-223.19
X= 0.75	-3.14	0.90	-8.37	1.48	-15.85	7.30	-3.06	30.12	-23.40
X= 1.25	1.79	0.90	5.91	3.45	17.15	9.64	34.45	21.69	25.65
X= 1.75	1.79	0.90	4.92	3.74	13.51	8.60	23.23	21.69	18.00
X= 2.25	1.79	0.90	4.13	3.54	11.43	9.12	20.42	20.42	16.20
X= 2.75	1.79	0.90	3.94	3.05	10.13	8.34	18.38	19.14	14.40
X= 3.25	1.34	0.90	3.64	3.05	10.39	8.76	20.42	21.44	13.50
X= 3.75	0.90	0.90	3.45	2.95	9.87	7.82	19.14	19.78	13.32
X= 4.25	0.90	0.90	3.15	2.95	9.36	7.35	17.61	18.89	12.15
X= 4.75	0.90	0.90	2.95	2.76	8.32	6.26	16.59	17.36	11.70
X= 5.25	0.90	0.90	2.76	2.36	8.06	6.15	17.23	17.99	11.70
X= 5.75	0.90	0.36	2.36	1.97	6.76	5.06	15.31	15.82	10.80
X= 6.25	0.45	0.36	1.97	1.77	6.24	4.69	12.51	13.53	9.00
X= 6.75	0.45	0.36	1.77	1.58	5.20	3.65	12.12	12.12	7.20
X= 7.25	0.45	0.36	1.18	1.08	4.42	2.35	10.97	9.95	7.20

TABULATED VALUES OF CFP AT DIFFERENT DISTANCES (IN INCHES) FROM THE JET EXIT.

INITIAL DISTRIBUTION LIST

		No. Copies
1.	Defense Documentation Center Cameron Station Alexandria, Virginia 22314	20
2.	Library Naval Postgraduate School Monterey, California 93940	2
3.	Naval Ship Systems Command (Code 2052) Navy Department Washington, D. C. 20360	1
4.	Mechanical Engineering Department Naval Postgraduate School Monterey, California 93940	2
5.	Professor T. Sarpkaya Chairman, Mechanical Engineering Department Naval Postgraduate School Monterey, California 92940	10
6.	LCDR D. C. Richardson, USN COMSUBPAC FPO San Francisco 96610	3

DOCUMENT CONTROL DATA - R & D

(Security classification of title, body of abstract and indexing annotation must be entered when the overall report is classified)

1. ORIGINATING ACTIVITY *(Corporate author)*
Naval Postgraduate School
Monterey, California 93940

2a. REPORT SECURITY CLASSIFICATION
Unclassified

2b. GROUP

3. REPORT TITLE
Jet Attachment to Coanda Walls in Bistable Amplifiers

4. DESCRIPTIVE NOTES *(Type of report and inclusive dates)*
Thesis for Master of Science Degree, April 1969

5. AUTHOR(S) *(First name, middle initial, last name)*
Daniel Charles Richardson

6. REPORT DATE	7a. TOTAL NO. OF PAGES	7b. NO. OF REFS
April 1969	128	25

8a. CONTRACT OR GRANT NO.	9a. ORIGINATOR'S REPORT NUMBER(S)
United States Army Materiel Command, Washington, D. C.	N/A
b. PROJECT NO.	
c.	9b. OTHER REPORT NO(S) *(Any other numbers that may be assigned this report)*
d.	N/A

10. DISTRIBUTION STATEMENT
Distribution of this document is unlimited.

11. SUPPLEMENTARY NOTES	12. SPONSORING MILITARY ACTIVITY
	Naval Postgraduate School Monterey, California 93940

13. ABSTRACT

The flow in a two-dimensional plane wall jet with a control port and setback between the nozzle exit and the leading edge of the wall was probed at various stations along the jet. The nozzle dimensions, the width of the control port, the slope of the side wall, and the setback were kept constant. The Reynolds number, defined in terms of the nozzle width, was varied from 20,000 to 141,000. It was found that the region close to the leading edge of the wall behaved like a transition region where the characteristics of flow changed from those of a free jet to those of a wall jet. In addition, it was found that while the outer region of the velocity profile obeyed a similarity law beyond the transition region, the inner region of the profile followed neither the classic one-seventh power law nor any other power law with a constant exponent. In fact the results have shown that the exponent in the power-law model has to be varied from one-seventh to one-fifteenth to represent the majority of the inner velocity profiles for the range of Reynolds numbers tested. The reasons leading to this result are discussed in terms of the equation of momentum and of the pressure distribution along the wall.

14 KEY WORDS	LINK A		LINK B		LINK C	
	ROLE	WT	ROLE	WT	ROLE	WT
Fluidics						
Coanda Effect						
Fluid Amplifiers						